Willmore Surfaces of Revolution Satisfying Dirichlet Data

Dissertation

Zur Erlangung des akademischen Grades

doctor rerum naturalium

(Dr. rer. nat.)

von	Dipl.-Math. Sascha Eichmann
geb. am	01.12.1987 in Wolfenbüttel

genehmigt durch die Fakultät für Mathematik

der Otto-von-Guericke-Universität Magdeburg

Gutachter:	Prof. Dr. Hans-Christoph Grunau
	Prof. Dr. Heiko von der Mosel

eingereicht am:	30.11.2016
Verteidigung am:	02.03.2017

Abstract

This thesis deals with the Willmore equation under Dirichlet boundary conditions, which can be seen as a frame invariant clamped plate equation. We restrict ourselves to surfaces of revolution, which are constructed by rotating a curve around the x-axis. Therefore the Dirichlet condition consists of prescribing two concentric boundary circles, at which the surface will be clamped horizontically.

By working strictly below a Willmore energy threshold of 4π, we can employ a variational approach to show existence of a smooth minimiser for non-symmetric boundary data. We also present some numerical results, which are obtained by a shooting method.

If we impose more restrictive but still explicit smallness conditions on the boundary, the profile curve of our minimiser is a graph over the x-axis. To prove this result we combine an order reduction argument by Langer & Singer with a modification method for minimising sequences by Dall'Acqua, Deckelnick & Grunau.

If we only consider symmetric boundary conditions, we can show non-uniqueness by constructing additional solutions via the above mentioned order reduction method by Langer & Singer. In this setting the same method can be employed to show symmetry with respect to the y-axis of the profile graph of a minimiser.

With the same technique we will also prove a Bernstein-type result for Willmore surfaces of revolution with a profile graph over the whole x-axis.

Zusammenfassung

Diese Arbeit befasst sich mit der Willmore Gleichung unter Dirichlet Randdaten, welche als ein koordinateninvariantes Modell für eine eingespannte Platte gesehen werden kann. Dabei schränken wir uns auf axialsymmetrische Flächen ein, welche durch Rotieren einer Kurve um die x-Achse konstruiert werden. Also bestehen unsere Dirichlet Bedingungen aus zwei konzentrischen Kreisen, an denen wir die Fläche horizontal einspannen.

Indem wir unter einer Schranke von 4π für die Willmore Energie arbeiten, können wir Existenz eines glatten Minimierers für nicht-symmetrische Randdaten zeigen. Für dieses Problem geben wir außerdem einige numerische Resultate, welche durch eine Schießmethode erstellt wurden.

Wenn wir restriktivere aber immer noch explizite Kleinheitsbedingungen an die Randdaten stellen, können wir sogar zeigen, dass die Profilkurve eines Minimierers ein Graph über der x-Achse ist. Der Beweis kombiniert ein Ordnungsreduktionsargument von Langer & Singer mit einer Modifikationsmethode für Minimalfolgen von Dall'Acqua, Deckelnick & Grunau.

Unter symmetrischen Randdaten zeigen wir ein Nichteindeutigkeitsresultat, indem wir die oben genannten Methode von Langer & Singer nutzen. In derselben Problemklasse mit denselben Methoden können wir auch zeigen, dass der Profilgraph eines Minimierers symmetrisch bezüglich der y-Achse sein muss.

Auf dieselbe Art finden wir sogar ein Bernsteinartiges Resultat für den Profilgraph einer axialsymmetrischen Willmorefläche.

Editorial notes

Most of the results of this thesis have been published in the series of papers [24–26] and extend the findings of the present authors diploma thesis [23]. Here the material is rearranged for a more coherent approach.
The results of [26] are in Chapter 9. Amos Koeller's contribution (i.e. [26, Section 2]) is not included in this thesis, since in [25] a stronger result was proven later (cf. Theorem 1.3). Nevertheless the present author would not have been able to show this result without the experience gained by the joint work with Amos Koeller. The contributions of Hans-Christoph Grunau to [25] will be highlighted throughout the exposition. The results of [25] can be found in the Sections 3, 5.3 and 7. The findings of [24] are in the Sections 5.1, 5.2 and 8.
The results of the present author given in Chapter 6 and the appendix have not been published yet.
For the reader's convenience the parts of the present authors diploma thesis [23], which are needed here, are summarized in the Chapters 2 and 4.

Acknowledgements:
Zuerst danke an Sie, dafür dass Sie diese Arbeit lesen. Allerdings wäre Ihnen dieses Vergnügen wahrscheinlich nicht möglich gewesen, gäbe es da nicht ein paar besondere Menschen, die mich auf die eine oder andere Art und Weise sehr unterstützt haben:
Professor Hans-Christoph Grunau begleitete mich auf dem gesamten Weg, war immer zur Stelle, sollte ich einen Rat benötigen oder einfach nur Diskussionsbedarf haben. Und er sorgte dafür, dass mir Vorzeichenfehler nicht die Beine brechen. Er ist außerdem verantwortlich für den Kontakt zu Amos Koeller, dem ich hier danken möchten. Ohne seine Vorarbeit wären mir einige Beweise vielleicht nicht gelungen.
Natürlich sollte ich meine anderen Kollegen an der FMA in Magdeburg erwähnen, z.B. meine Arbeitsgruppe und alle anderen, die so gerne Kuchen spenden. Mit euch zusammenzuarbeiten ist großartig.

Ganz besonders ist natürlich meine Familie. Meine Mutter und mein Vater waren immer da, danke dass ihr stolz auf mich seid, es bedeutet mir sehr viel. Meine Großeltern, die sich immer Sorgen um mich machen und dem gesamten restlichen Clan möchte ich hier danken. Man sagt, man könne sich seine Familie nicht aussuchen, aber ich denke, der Zufall hat mir hier sehr gut zugespielt.
Diejenigen, die man sich aussuchen kann, sind seine Freunde. Da muss ich meiner Introviertheit danken, die dafür sorgt, dass nur besondere Menschen mir nahe stehen. Danke, die Zeit in Magdeburg hätte nicht im Ansatz so viel Spaß gemacht ohne euch.
Zum Schluss: Ich möchte meiner Ente danken, die sich ohne Widerspruch meine wirren mathematischen Gedanken anhörte und ohne Antwort half, das Knäuel im Kopf zu entwirren.

Contents

1. Introduction

1.1. The Willmore equation

This thesis deals with certain critical points of the Willmore energy of a smooth regular 2-dimensional surface $S \subset \mathbb{R}^3$, which is defined by

$$W_e(S) = \int_S H^2 \, dA. \tag{1.1}$$

H denotes the mean curvature of the surface S, i.e. the mean of the principal curvatures. It describes a kind of bending energy for thin plates, which was already studied by Poisson in [47], but technical difficulties prevented a deeper analysis at the time. This energy was picked up by Thomsen in [53], in which he discussed the Möbius invariance of the integral and found the Euler-Lagrange equation

$$\Delta_S H + 2H(H^2 - G) = 0. \tag{1.2}$$

Here Δ_S denotes the Laplace-Beltrami and G the Gauss curvature of S with respect to the first fundamental form. Every surface satisfying this equation is called a Willmore surface. This naming goes back to Willmore in [55], in which he revived the discussion about Willmore surfaces. In [11] Bryant was able to classify Willmore surfaces under an additional constraint, which gives a deep connection to minimal surfaces.

The Willmore energy can be seen as a natural modification of the area functional, which greatly motivated the development of nonlinear partial differential equations of second order in the last century. It is the present author's opinion that the Willmore energy will play a similar role for higher order equations.

Apart from pure mathematical interest the Willmore energy already plays an important role in physical applications, e.g. Helfrich modeled the elastic energy of thin shells in [30] or Ou-Yang described thin biomembranes in [45]. Other possible applications are e.g. in image inpainting (see e.g. [14]).

Many beautiful results concerning closed Willmore surfaces have been proven. Existence for minimisers with prescribed genus are established in [5, 52] and an analysis of branch points and singularities was carried out in [35,36]. By working below an energy threshold compactness results for sequences of Willmore surfaces have been proven in e.g. [9, 49]. Under additional symmetry assumptions closed Willmore surfaces were constructed in [32]. Finally Marques & Neves proved the famous Willmore conjecture

in [42] and therefore found the 'optimal' doughnut.
Recently constrained minimisation of the Willmore energy has been considered as well. For example prescribing the conformal class (see e.g. [51]), the isoperimetric ratio (see e.g. [34]) or using Lagrangian and Hamiltonian deformations (see e.g. [40]).
In contrast this thesis deals with a Dirichlet boundary problem for the Willmore equation. A discussion of suitable boundary problems was done by Nitsche in [44]. Since the Willmore equation is of fourth order, maximum principles, de Giorgi-Nash-Moser-Stampacchia-type arguments or Schwarz reflection principles cannot be applied. Furthermore the Laplace-Beltrami operator depends on the unkown surface and therefore the equation is highly nonlinear. Variational approaches are difficult as well, since the Willmore energy is invariant under Möbius transformations (see [53]) and minimising sequences do not have to be bounded in the Sobolev space H^2. Nevertheless a general existence result for branched Willmore immersions was shown by Schätzle in [50]. He worked in the sphere $\mathbb{S}^3$ to overcome certain compactness problems and therefore it is not clear, whether the point ∞ can be excluded, when the surface is pulled back to $\mathbb{R}^3$ by the stereographic projection. Also it seems very little topological or geometrical information about a solution can be be extracted of the proof. To obtain such solutions Deckelnick & Grunau started examining elastic rods in [19, 21] under Dirichlet and Navier boundary conditions, which were later extended to a full discussion in [41] by Mandel. Later surfaces of revolution were considered by Dall'Acqua, Deckelnick & Grunau in [17], to obtain 2-dimensional Willmore surfaces, where explicit geometric properties can be proven. We like to pursue a similar approach and consider Willmore surfaces of revolution as well. Here such a surface of revolution $S(c)$ is defined by a sufficiently smooth regular curve $c : [0,1] \to \mathbb{R} \times (0,\infty)$ via the following parameterisation

$$[0,1] \times [0,2\pi] \ni (t,\varphi) \mapsto f(t,\varphi) = (c^1(t), c^2(t)\cos\varphi, c^2(t)\sin\varphi). \tag{1.3}$$

These surfaces of revolution in conjunction with the Willmore energy have applications in e.g. modelling of lipid bilayers (see e.g. [27] and references therein). The corresponding Dirichlet problem, with which this thesis is mainly concerned, can be stated as

$$\begin{cases} \Delta_{S(c)} H + 2H(H^2 - G) = 0, \quad \text{in } (0,1) \\ c(0) = (-1, \alpha_-),\ c(1) = (1, \alpha_+),\ \dot{c}^2(0) = \dot{c}^2(1) = 0, \\ \dot{c}^1(0), \dot{c}^1(1) > 0, \end{cases} \tag{1.4}$$

with $\alpha_-, \alpha_+ > 0$. This thesis gives an existence result for *non-symmetric* Dirichlet data and qualitative properties are shown. In the symmetric case (i.e. $\alpha_- = \alpha_+$) additional problems, like uniqueness and symmetry of a profile curve, are adressed. These results are discussed more closely in Section 1.2.

1.2. Main results

Our first main result is concerned with existence of a solution of the Dirichlet problem (1.4), with non-symmetric data. In case of symmetric boundary conditions (i.e. $\alpha = \alpha_- = \alpha_+$) Dall'Acqua, Deckelnick & Grunau showed existence in [17] by a variational approach in the class of graphs. This existence result was later extended to arbitrary boundary angles in [18], but the data still had to be symmetric. Under natural boundary conditions existence was shown with symmetric boundary data in [6, 20] and later extended to arbitrary $\alpha_-, \alpha_+ > 0$ in [7], also by a variational approach. In this setting c can be parameterised as a graph over the x-axis. The authors of these papers inserted catenoids into a minimising sequence to obtain a priori bounds. The resulting curve would automatically satisfy $H = 0$ at the boundary. In our setting we have to respect the prescribed boundary angle, which is not necessarily preserved, if a catenoid is inserted. Therefore our reasoning is more involved than in [7].
We also proceed by a variational approach. Hence the following objects will come in handy. The class of admissible curves is denoted by

$$\begin{aligned} M_{\alpha_-,\alpha_+} := \{c \in H^2([0,1], \mathbb{R} \times (0,\infty)) :\ & c(0) = (-1, \alpha_-),\ c(1) = (1, \alpha_+), \\ & \dot{c}^2(0) = \dot{c}^2(1) = 0, \dot{c}^1(0), \dot{c}^1(1) > 0,\ |\dot{c}| \neq 0\}. \end{aligned} \tag{1.5}$$

The infimum of the Willmore energy is called

$$W^e_{\alpha_-,\alpha_+} := \inf\{W_e(S(c)) :\ c \in M_{\alpha_-,\alpha_+}\}. \tag{1.6}$$

In contrast to [7] we are not able to show existence for every $\alpha_-, \alpha_+ > 0$, hence we impose an explicit smallness condition on $W^e_{\alpha_-,\alpha_+}$. This theorem is joint work with Hans-Christoph Grunau.

Theorem 1.1 (see [25] Theorem 1.1). *Let $\alpha_-, \alpha_+ > 0$ and satisfy $W^e_{\alpha_-,\alpha_+} < 4\pi$. Then there exists a $c \in M_{\alpha_-,\alpha_+} \cap C^\infty([0,1], \mathbb{R} \times (0,\infty))$ with*

$$W_e(S(c)) = W^e_{\alpha_-,\alpha_+}.$$

This minimiser does not intersect itself.

Our reasoning consists of four major steps: First we reformulate the problem in the upper half plane (see (2.12)). Then we reparameterise a minimising sequence proportionally to hyperbolic arclength. This allows us to show boundedness in H^2, iff the hyperbolic arclength of the sequence is bounded (see Theorem 3.1). In Section 3.2 we establish these bounds by working below the energy threshold of 4π. Section 3.3 is dedicated to proving regularity of a solution. Injectivity of the minimiser can only be shown later (see Remark 5.20), after an order reduction argument of the underlying differential equation by Langer & Singer is established and analysed (see Chapters 4 and 5). Numerical examples of solutions c can be found in the Appendix A.2.

Imposing smallness conditions for boundary value problems to show existence of Willmore surfaces has already been done by Nitsche in [44], although these are very severe and by no means explicit. Recently existence of Willmore immersions without symmetry assumptions satisfying free boundary conditions and prescribed surface area were established in [2]. Also in this paper smallness assumptions had to be imposed on the surface area. Compactness under an energy threshold was also observed for closed Willmore immersions in [3], in which a bubbling phenomenon was discovered, which leads to a loss of compactness.
Unfortunately existence for arbitrary α_-, α_+ for (1.4) in contrast to Theorem 1.1 was not established in this thesis. Theorem 6.1 gives a partial answer and in Chapter B an idea on how to proceed further is presented. The idea mainly consists in employing a shooting method, which is similar to the proof of Theorem 1.4.

In [17] and [18] the profile curve of a Willmore surface of revolution, satisfying symmetric Dirichlet data, is also a graph. This observation simplifies the description of such surfaces a lot. Under natural boundary conditions this holds true for every set of boundary values (see [7]), since these solutions are close to catenoids. In our case this cannot be expected (see Lemmas 7.6 and 7.7). Nevertheless we are able to prove a similar result under more restrictive but remarkably explicit smallness conditions on the boundary data. Please note that this question is still widely open for two-dimensional Willmore graphs (cf. [22]) and we hope that our reasoning here gives some insight in this case as well.

The idea for the following smallness condition is due to Hans-Christoph Grunau and is sketched in Figure 1.1.

Assumption 1.2 (see [25] Assumption 1.2)**.** A pair $(\alpha_-, \alpha_+) \in \mathbb{R}_+ \times \mathbb{R}_+$ satisfies the Assumption 1.2, iff the following is true:

- If $\alpha_- \leq \alpha_+$, then for all $x \in \mathbb{R}$
$$p_{1,\alpha_+}(x) < \alpha_- \cosh\left(\frac{1+x}{\alpha_-}\right).$$
- If $\alpha_- > \alpha_+$, then for all $x \in \mathbb{R}$
$$p_{-1,\alpha_-}(x) < \alpha_+ \cosh\left(\frac{1-x}{\alpha_+}\right).$$

Here $p_{x_0,r}$ denotes the upper half circle with centre $(x_0, 0)$, radius r and is given by

$$p_{x_0,r}(x) = \begin{cases} \sqrt{r^2 - (x-x_0)^2}, & x \in (x_0 - r, x_0 + r) \\ 0, & \text{else.} \end{cases}$$

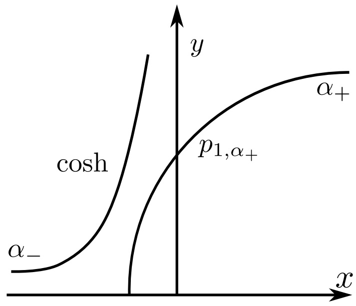

Figure 1.1.: Smallness assumption for boundary data.

Under these assumptions the following theorem holds, which is joint work with Hans-Christoph Grunau.

Theorem 1.3 (see [25] Theorem 1.3)**.** *If the pair $(\alpha_-, \alpha_+) \in \mathbb{R}_+ \times \mathbb{R}_+$ satisfies Assumption 1.2 the following Dirichlet problem possesses a graph $u : [-1, 1] \to (0, \infty)$ as solution:*

$$\begin{cases} \Delta_{S(u)} H + 2H(H^2 - G) = 0, \quad \text{in } (-1,1) \\ u(\pm 1) = \alpha_\pm, \ u'(\pm 1) = 0. \end{cases} \tag{1.7}$$

Moreover u satisfies

$$W_e(S(u)) = W^e_{\alpha_-,\alpha_+} < 4\pi.$$

For the proof (see Theorem 7.5) we use two main ingredients: First we analyse the Euler-Lagrange equation by an order reduction argument by Langer & Singer (see [37]) in Chapters 4 and 5. Then we proceed by inserting suitable parts of catenoids and half circles, if necessary. This insertion idea was first developed by Dall'Acqua, Deckelnick & Grunau in [17] and developed further by the present author and Amos Koeller in [26, Section 2]. He showed existence of a graphical minimiser for symmetric boundary data this way. Since Theorem 1.3 gives a stronger result, his contribution is not included in this thesis, although it inspired in parts the present author's reasoning for Theorem 1.3.

A similar but more general order reduction argument was also developed by Bryant & Griffiths in [12] shortly before [37], but the more ad-hoc and geometric nature of [37] enables us to reach our results more directly. These arguments were also recently picked up and extended in [31] to analyse Willmore tori restricted to conformal classes. On the other hand compactness results were also obtained in [43] for a constrained minimisation problem for the Willmore energy by also inserting suitable comparison functions into a minimising sequence.

From this point on all results on Dirichlet boundary value problems for Willmore surfaces of revolution are restricted to the symmetric case, i.e. $\alpha := \alpha_- = \alpha_+$.

Uniqueness for Willmore graphs with natural boundary data has been proven in [8]. For Dirichlet data more restrictions seem to be necessary to show a similar result. For disk type Willmore surfaces with constant boundary angle such a result was obtained in [46] and later extended to star-shaped domains in [16]. For Willmore surfaces of revolution nonuniquness was only proven under natural boundary conditions (see e.g. [7]) but for symmetric Dirichlet data numerical evidence was found in [18]. Here we give a nonuniqueness result:

Theorem 1.4 (see [24] Theorem 1.1)**.** *There exists an $\alpha^* \geq 0$ such that the following Dirichlet Problem possesses at least two different solutions $\forall \alpha > \alpha^*$.*

$$\begin{cases} \Delta_{S(u)} H + 2H(H^2 - G) = 0, & \text{in } (-1,1) \\ u(\pm 1) = \alpha, \ u'(\pm 1) = 0. \end{cases} \tag{1.8}$$

One solution was already constructed in [17] by a variational approach. We obtain another solution by a shooting method in Theorem 8.5. Again a Langer & Singer order reduction method (see [37]) is employed (see chapters 4 and 5) to analyse a solution of an initial value problem (see (4.8)) with suitable initial data. A similar kind of shooting method is explained in Section A.1 to numerically obtain a set of solutions of (1.4) in Section A.2.

Whether a minimiser of a variational problem inherits the symmetry of the boundary data is interesting, since e.g. solutions can be obtained in a simpler manner. For example the answer for the Newton problem of minimal aerodynamical resistance is 'no' (see e.g. [13, Section 1.3]), but Palmer was able to prove the opposite for Willmore graphs under zero boundary conditions in [46]. Here we show, that an energy minimising profile graph of the Willmore energy under symmetric Dirichlet boundary data has to be symmetric as well.

Theorem 1.5 (see [26] Theorem 1.1)**.** *Every energy minimising solution $u : [-1,1] \to (0,\infty)$ of (1.8) is symmetric with respect to the y-axis.*

This result is joint work with Amos Koeller, but his contribution is not integrated into this thesis. He proved existence of an energy minimising graph under symmetric Dirichlet data, but we can use Theorem 1.3 to replace this result. The present author's contribution is an a priori energy estimate (see Lemma 9.5) for non-even solutions of (1.8), which is again shown by the order reduction argument provided by Langer & Singer (see [37]). This estimate directly contradicts the energy estimate for a minimiser in Theorem 1.3. This result has another consequence: The a priori estimates obtained in [17] (they are cited in this thesis in Theorem 8.6), which were achieved in a class of of even functions, can directly be applied to a minimiser in $M_{\alpha,\alpha}$.

Since for minimal surfaces Bernstein's result holds and the Willmore energy and the area functional are related, a similar result is to be expected. For Willmore graphs such results under additional constraints (e.g. L^2 bounds) were found in [8,15]. In our situation the topological class differs, but we are able to provide a similar result with catenoids instead of planes:

Theorem 1.6 (see [24] Theorem 1.2)**.** *Let* $u : \mathbb{R} \to (0, \infty)$ *be smooth and let* $S(u)$ *satisfy the Willmore equation* (1.2)*. Then there exists a Möbius transformation* $T : \mathbb{R} \times (0, \infty) \to \mathbb{R} \times (0, \infty)$ *such that*

$$\{(x, u(x)) : \ x \in \mathbb{R}\} = \{T(x, \cosh(x)) : \ x \in \mathbb{R}\}.$$

This theorem quickly drops out of the order reduction argument by Langer & Singer (see [37]) by analysing every possible solution of the underlying differential equation (see Theorem 5.4). This result especially means, that there are no surfaces of revolution with periodic profile graphs satisfying the Willmore equation (cf. [23]).

2. Geometric background

This chapter does not contain any new results, but collects basic knowledge for the reader's convenience. These facts will be needed to prove the main results and have already been gathered in the present author's diploma thesis [23].

2.1. Surfaces of revolution and the upper half plane

In this section we derive the basic formulae we need for our calculations. These are based on [4].

For a surface of revolution $S(c)$, given by a curve $c \in M_{\alpha_-,\alpha_+}$ (see (1.5)), the metric tensor is

$$(g_{ij})_{i,j=t,\varphi} = \begin{pmatrix} (\dot{c}^1)^2 + (\dot{c}^2)^2 & 0 \\ 0 & (c^2)^2 \end{pmatrix}. \tag{2.1}$$

The second fundamental form can then be calculated as

$$(h_{ij})_{i,j=t,\varphi} = \frac{1}{|\dot{c}|} \begin{pmatrix} \ddot{c}^1 \dot{c}^2 - \ddot{c}^2 \dot{c}^1 & 0 \\ 0 & \dot{c}^1 c^2 \end{pmatrix}. \tag{2.2}$$

with respect to the 'interior' normal

$$\nu(t,\varphi) = \frac{1}{|\dot{c}|}(\dot{c}^2(t), -\dot{c}^1(t)\cos\varphi, -\dot{c}^1(t)\sin\varphi). \tag{2.3}$$

Here we use $|\dot{c}| = \sqrt{(\dot{c}^1)^2 + (\dot{c}^2)^2}$ to denote the euclidean length of a vector. Now we can write down the mean curvature H. For this we use the sign convention, that H is positive if the surface is mean convex and negative if it is mean concave with respect to the interior normal ν.

$$H = \frac{1}{2} \frac{c^2 \ddot{c}^1 \dot{c}^2 - c^2 \ddot{c}^2 \dot{c}^1 + |\dot{c}|^2 \dot{c}^1}{|\dot{c}|^3 c^2}, \tag{2.4}$$

and finally the Willmore energy is

$$W_e(S(c)) = \frac{\pi}{2} \int_0^1 \frac{(c^2 \ddot{c}^1 \dot{c}^2 - c^2 \ddot{c}^2 \dot{c}^1 + |\dot{c}|^2 \dot{c}^1)^2}{|\dot{c}|^5 c^2}\, dt. \tag{2.5}$$

Now we reformulate the problem by introducing the elastic energy for curves on the upper half plane $\mathbb{H}^2 = \{(x,y) : \ y > 0\}$, equipped with the hyperbolic metric

$$ds^2 = \frac{dx^2 + dy^2}{y^2}, \tag{2.6}$$

which will also be denoted by $g(\cdot,\cdot)$. The Christoffel symbols are given by

$$\Gamma^1_{11} = \Gamma^1_{22} = \Gamma^2_{12} = \Gamma^2_{21} = 0,\ \Gamma^1_{21} = \Gamma^1_{12} = \Gamma^2_{22} = -\frac{1}{y},\ \Gamma^2_{11} = \frac{1}{y}. \tag{2.7}$$

The covariant derivative of a curve c can then be calculated as

$$\nabla_{\dot c}\dot c = \left(\ddot c^1 - 2\frac{\dot c^1 \dot c^2}{c^2}\right)\begin{pmatrix} 1 \\ 0 \end{pmatrix} + \left(\ddot c^2 - \frac{(\dot c^2)^2}{c^2} + \frac{(\dot c^1)^2}{c^2}\right)\begin{pmatrix} 0 \\ 1 \end{pmatrix}. \tag{2.8}$$

Since the hyperbolic metric is conformal to the euclidean metric, the unit normal can be choosen as

$$N = \frac{1}{\sqrt{g_c(\dot c, \dot c)}}\begin{pmatrix} -\dot c^2 \\ \dot c^1 \end{pmatrix}. \tag{2.9}$$

We use this sign convention, because $\left(\frac{\dot c}{\sqrt{g_c(\dot c,\dot c)}}, N\right)$ becomes positively oriented. With this we obtain the geodesic curvature (please keep in mind, that $|\dot c| = \sqrt{(\dot c^1)^2 + (\dot c^2)^2}$ denotes the usual euclidean length)

$$\kappa[c] = \frac{g_c(\nabla_{\dot c}\dot c, N)}{g_c(\dot c, \dot c)} = \frac{\ddot c^2 \dot c^1 c^2 - \ddot c^1 \dot c^2 c^2 + \dot c^1 (\dot c^2)^2 + (\dot c^1)^3}{|\dot c|^3}. \tag{2.10}$$

and in turn can introduce the hyperbolic elastic energy of a curve c by

$$W_h(c) := \int_0^1 (\kappa[c](t))^2\, ds(t) = \int_0^1 \frac{(\ddot c^2 \dot c^1 c^2 - \ddot c^1 \dot c^2 c^2 + \dot c^1 (\dot c^2)^2 + (\dot c^1)^3)^2}{|\dot c|^5 c^2}\, dt. \tag{2.11}$$

The next observation goes back to Bryant & Griffiths in [12] and connects the Willmore energy with the hyperbolic elastic energy

$$\frac{2}{\pi} W_e(S(c)) = W_h(c) - 4\left[\frac{\dot c^2}{\sqrt{(\dot c^1)^2 + (\dot c^2)^2}}\right]_0^1. \tag{2.12}$$

This and [28, Lemma 8.2] shows, that the associated surface of revolution of a critical point of W_h satisfies the Willmore equation (1.2). Finally we state three equations which will be useful on several occasions: The Frenet equations for a curve c parameterised by hyperbolic arclength with geodesic curvature $\kappa[c]$ are (see (2.8))

$$\ddot{c}^1 - 2\frac{1}{c^2}\dot{c}^1\dot{c}^2 = -\kappa[c]\dot{c}^2, \tag{2.13}$$

$$\ddot{c}^2 - \frac{1}{c^2}(\dot{c}^2)^2 + \frac{1}{c^2}(\dot{c}^1)^2 = \kappa[c]\dot{c}^1. \tag{2.14}$$

If on the other hand c can be reparameterised as a smooth graph $u : [-1, 1] \to (0, \infty)$, the hyperbolic elastic energy becomes

$$W_h(u) = \int_{-1}^{1} \frac{u''(x)^2 u(x)}{(1 + u'(x)^2)^{\frac{5}{2}}} + \frac{1}{u(x)\sqrt{1 + u'(x)^2}}\, dx. \tag{2.15}$$

2.2. Möbius transformations

This section provides some lemmas and definitions concerning Möbius transformations and their connection to the Willmore energy. We start with inversions, which will be needed to define Möbius transformations. Additional information concerning these special kind of maps can be found in [48, chapter 4].

Definition 2.1 (see [48] Equations (4.1.1) and (4.1.2))**.**

1. A map $\rho : \mathbb{R}^n \to \mathbb{R}^n$ is called an inversion at a hyperplane, iff there is an $a \in \mathbb{R}^n$ with $|a| = 1$ and a $t \in \mathbb{R}$ exist, such that

   $$\forall x \in \mathbb{R}^n \quad \rho(x) = x + 2(t - \langle a, x\rangle)a.$$

   Here $\langle \cdot, \cdot \rangle$ denotes the euclidean scalar product.

2. A map $\sigma : \mathbb{R}^n \cup \{\infty\} \to \mathbb{R}^n \cup \{\infty\}$ is called an inversion at a sphere, iff there is an $a \in \mathbb{R}^n$ and an $r > 0$ exist, such that

   $$\sigma(x) = \begin{cases} a + \left(\frac{r}{|x-a|}\right)^2 (x - a), & x \in \mathbb{R}^n \setminus \{a\}, \\ a, & x = \infty, \\ \infty, & x = a. \end{cases}$$

Without loss of generality we can assume, that an inversion at a hyperplane maps ∞ to ∞. A Möbius transformation is now defined as follows.

Definition 2.2 (see [48] p. 116)**.** A map $T : \mathbb{R}^n \cup \{\infty\} \to \mathbb{R}^n \cup \{\infty\}$ is called a Möbius transformation, iff it can be expressed as a finite composition of inversions at spheres and/or hyperplanes.

Examples of Möbius transformations are translations and dilations (see e.g. [23, Example 2.31] or [48, chapter 4]). Thomsen showed in [53] the following invariance for the conformal Willmore energy $W_k(S) := \int_S (H^2 - G)\, dA$ under a Möbius transformation T which are regular on S:

$$W_k(S) = W_k(T(S)). \tag{2.16}$$

Here $S \subset \mathbb{R}^3$ denotes a smooth, regular, two dimensional surface.

With this equation and (2.12), or by direct calculations, we have on the upper half plane $\mathbb{H}^2$ the following lemmas.

Lemma 2.3 (see e.g. [23] Corollary 3.11)**.** *Let $T : \mathbb{R}^2 \cup \{\infty\} \to \mathbb{R}^2 \cup \{\infty\}$ be a Möbius transformation of the upper half plane, i.e. $T(\mathbb{H}^2) = \mathbb{H}^2$. Then W_h (cf.* (2.11)*) is invariant under T.*

We also have some pointwise properties.

Lemma 2.4 (see e.g. [23] Theorem 6.6)**.** *A Möbius transformation of the upper half plane is an isometry of $\mathbb{H}^2$ with respect to the hyperbolic metric* (2.6)*.*

Lemma 2.5 (see e.g. [23] Theorem 6.8)**.** *Let $L > 0$ and $c : [0, L] \to \mathbb{H}^2$ be a regular curve with geodesic curvature $\kappa[c]$. Let additionally $T : \mathbb{H}^2 \to \mathbb{H}^2$ be a Möbius transformation of the upper half plane and $\kappa[T(c)]$ be the geodesic curvature of $T(c)$. Then*

$$\forall t \in [0, L] \quad |\kappa[c](t)| = |\kappa[T(c)](t)|.$$

Lemma 2.6 (see e.g. [23] Theorem 6.7)**.** *Let $p \in \mathbb{H}^2$ and $V \in T_p\mathbb{H}^2$ with $|V|_g = 1$. Then there exists a Möbius transformation T with $T(\mathbb{H}^2) = \mathbb{H}^2$ and $z > 0$ such that*

$$T(p) = (0, z), \ dT(p)V = (z, 0).$$

2.3. Killing vector fields and curves with constant hyperbolic curvature

This section introduces Killing vector fields and studies their integral curves in $\mathbb{H}^2$.

Definition 2.7 (see e.g. [39] Exercise 13.13)**.** Let (M, g) be a regular Riemannian surface. Then a vector field V on M is called a Killing vector field, iff the flow $\Phi_V : M \times \mathbb{R} \to M$ of V satisfies the following condition: For every $t \in \mathbb{R}$ the map $\Phi_V(\cdot, t) : M \to M$ is an isometry with respect to g.

Remark 2.8 (see e.g. [23] Remark 5.3)**.** Every integral curve of a Killing vector field is parameterised proportionally to arclength.

Lemma 2.9 (see e.g. [33] 1.6.7)**.** *V is a Killing vector field on a regular Riemannian surface (M,g), iff in local coordinates*

$$\forall i,j=1,\dots,\dim(M):\ \sum_k\left(V^k\frac{\partial g_{ij}}{\partial x^k}+g_{jk}\frac{\partial V^k}{\partial x^i}+g_{ik}\frac{\partial V^k}{\partial x^j}\right)=0.$$

Example 2.10 (see e.g. [23] Example 5.8)**.** *V is a Killing vector field on $\mathbb{H}^2$, iff*

$$V(x,y)=a\begin{pmatrix}\frac{x^2-y^2}{2}\\ xy\end{pmatrix}+b\begin{pmatrix}x\\ y\end{pmatrix}+c\begin{pmatrix}1\\ 0\end{pmatrix},$$

with real parameters $a,b,c\in\mathbb{R}$.

Theorem 2.11 (see e.g. [23] Theorem 5.14)**.** *Let (M,g) be a two dimensional regular Riemannian surface with a Killing vector field V and the corresponding flow Φ_V. Then every integral curve $t\mapsto\Phi_V(\cdot,t)$ of V possesses constant geodesic curvature.*

The following lemma was not part of the present author's diploma thesis, but deals with Killing fields and helps to find special integral curves.

Lemma 2.12 (see e.g. [24] Lemma A.5)**.** *Let V be a Killing vector field on a regular Riemannian surface (M,g). Let $p\in M$ be critical for $|V(\cdot)|_g$. Then the integral curve of V starting in p is a geodesic.*

Proof. Using normal coordinates in p and the differential equation in Lemma 2.9 we obtain $\nabla_{V(p)}V(p)=0$. Together with Theorem 2.11 this yields the desired result. □

With Theorem 2.11 in mind we look for curves in $\mathbb{H}^2$ with constant geodesic curvature.

Example 2.13 (see e.g. [23] Example 6.9)**.** *Let $a,b,c,d\in\mathbb{R}$ and*

$$C_L:\mathbb{R}\to\mathbb{R}^2,\ t\mapsto(a,b)+t(c,d)$$

be a straight line with $C_L(\mathbb{R})\cap\mathbb{H}^2\neq\emptyset$. Then the geodesic curvature in $\mathbb{H}^2$ can be calculated by

$$\kappa[C_L]=\frac{c}{\sqrt{c^2+d^2}}.$$

Example 2.14 (see e.g. [23] Example 6.10)**.** *Let $r>0$ and $M=(M^1,M^2)\in\mathbb{R}^2$ define an euclidean circle by*

$$C_{r,M}(t):=r(\sin t,\cos t)+(M^1,M^2),\quad t\in[0,2\pi).$$

If we further assume $C_{r,M}(\mathbb{R})\cap\mathbb{H}^2\neq\emptyset$, we can compute the geodesic curvature in the intersection:

$$\kappa[C_{r,M}]=-\frac{M^2}{r}.$$

The following lemma classifies every curve with constant geodesic curvature in $\mathbb{H}^2$.

Lemma 2.15 (see e.g. [10] chapter 3 or [23] Remark 6.12)**.** *Let $\kappa[c] \in \mathbb{R}$ be the constant geodesic curvature of a regular curve c in $\mathbb{H}^2$. Then, if*

1. $|\kappa[c]| \in [0, 1)$*: c is a circle, meeting the x-axis in two different points, or c is a straight line, which is not parallel to the x-axis.*
2. $|\kappa[c]| = 1$*: c is a circle, meeting the x-axis in exactly one point, or c is a straight line parallel to the x-axis.*
3. $|\kappa[c]| > 1$*: c is a circle, which does not intersect the x-axis.*

3. Existence for curves

This chapter is dedicated to proving Theorem 1.1 except the injectivity (embeddedness) of the solution, which is shown in Chapter 5, see Remark 5.20. It consists of the Sections 3,4 and 5 of [25] and applies a variational method. In Section 3.1 we examine a special kind of parameterisation to eliminate the inner invariance of W_h (cf. (2.11)). To apply these results, a priori estimates on the hyperbolic arclength are required, which are being deduced in Section 3.2. This will give us a weak solution of (1.4), while in Section 3.3 C^∞ regularity is shown.

3.1. A suitable parameterisation

This section is taken directly out of [25, Section 3]. Here we introduce a special form of the elastic energy by reparameterising an admissible curve. Let $c \in M_{\alpha_-,\alpha_+}$ be parameterised proportionally by hyperbolic arclength and let L be the hyperbolic arclength of c. The idea to employ this special kind of parameterisation was already used by Langer & Singer in [38], but on compact manifolds in combination with the L^2-flow of $W_h(\cdot)$. By using this parameterisation we obtain

$$L^2 = g(\dot{c}, \dot{c}) = \frac{(\dot{c}^1)^2 + (\dot{c}^2)^2}{(c^2)^2}, \tag{3.1}$$

and the geodesic curvature $\kappa[c]$ satisfies

$$\kappa[c]^2 = g\left(\nabla_{\frac{\dot{c}}{L}} \frac{\dot{c}}{L}, \nabla_{\frac{\dot{c}}{L}} \frac{\dot{c}}{L}\right) = \frac{1}{L^4} g(\nabla_{\dot{c}}\dot{c}, \nabla_{\dot{c}}\dot{c}). \tag{3.2}$$

Differentiating (3.1) yields

$$\dot{c}^1\ddot{c}^1 + \dot{c}^2\ddot{c}^2 = L^2 c^2 \dot{c}^2. \tag{3.3}$$

Let us now turn to the elastic energy itself:

$$\begin{aligned}
&\int_0^1 \kappa[c]^2 \, ds = \frac{1}{L^3} \int_0^1 g(\nabla_{\dot{c}}\dot{c}, \nabla_{\dot{c}}\dot{c}) \, dt \\
=&\frac{1}{L^3} \int_0^1 \frac{1}{(c^2)^2} \left(\left(\ddot{c}^1 - 2\frac{\dot{c}^1\dot{c}^2}{c^2} \right)^2 + \left(\ddot{c}^2 - \frac{(\dot{c}^2)^2}{c^2} + \frac{(\dot{c}^1)^2}{c^2} \right)^2 \right) dt
\end{aligned}$$

$$
\begin{aligned}
=&\frac{1}{L^3}\int_0^1 \frac{1}{(c^2)^2}\Bigg((\ddot{c}^1)^2 - 4\frac{\ddot{c}^1\dot{c}^1\dot{c}^2}{c^2} + 4\left(\frac{\dot{c}^1\dot{c}^2}{c^2}\right)^2 \\
&+ (\ddot{c}^2)^2 - 2\frac{\ddot{c}^2(\dot{c}^2)^2}{c^2} + 2\frac{\ddot{c}^2(\dot{c}^1)^2}{c^2} + \frac{(\dot{c}^2)^4}{(c^2)^2} - 2\left(\frac{\dot{c}^1\dot{c}^2}{c^2}\right)^2 + \frac{(\dot{c}^1)^4}{(c^2)^2}\Bigg)\,dt \\
=&\frac{1}{L^3}\int_0^1 \frac{1}{(c^2)^2}\Bigg((\ddot{c}^1)^2 + (\ddot{c}^2)^2 - 4\frac{\ddot{c}^1\dot{c}^1\dot{c}^2}{c^2} + 2\left(\frac{\dot{c}^1\dot{c}^2}{c^2}\right)^2 \\
&- 2\frac{\ddot{c}^2(\dot{c}^2)^2}{c^2} + 2\frac{\ddot{c}^2(\dot{c}^1)^2}{c^2} + \frac{(\dot{c}^2)^4}{(c^2)^2} + \frac{(\dot{c}^1)^4}{(c^2)^2}\Bigg)\,dt \\
\overset{(3.1)}{\underset{(3.3)}{=}}&\frac{1}{L^3}\int_0^1 \frac{1}{(c^2)^2}\Bigg((\ddot{c}^1)^2 + (\ddot{c}^2)^2 - 4\frac{\ddot{c}^1\dot{c}^1\dot{c}^2}{c^2} + 2\left(\frac{\dot{c}^1\dot{c}^2}{c^2}\right)^2 \\
&+ 2\frac{\ddot{c}^1\dot{c}^2\dot{c}^1}{c^2} - 2\frac{L^2(\dot{c}^2)^2c^2}{c^2} + 2\frac{\ddot{c}^2}{c^2}(L^2(c^2)^2 - (\dot{c}^2)^2) + \frac{(\dot{c}^2)^4}{(c^2)^2} + \frac{(\dot{c}^1)^4}{(c^2)^2}\Bigg)\,dt \\
\overset{(3.3)}{=}&\frac{1}{L^3}\int_0^1 \frac{1}{(c^2)^2}\Bigg((\ddot{c}^1)^2 + (\ddot{c}^2)^2 - 2\frac{\ddot{c}^1\dot{c}^1\dot{c}^2}{c^2} + 2\left(\frac{\dot{c}^1\dot{c}^2}{c^2}\right)^2 \\
&- 2L^2(\dot{c}^2)^2 + 2\ddot{c}^2c^2L^2 + 2\frac{\ddot{c}^1\dot{c}^1\dot{c}^2}{c^2} - 2L^2(\dot{c}^2)^2 + \frac{(\dot{c}^2)^4}{(c^2)^2} + \frac{(\dot{c}^1)^4}{(c^2)^2}\Bigg)\,dt \\
=&\frac{1}{L^3}\int_0^1 \frac{1}{(c^2)^2}\Bigg((\ddot{c}^1)^2 + (\ddot{c}^2)^2 + 2\left(\frac{\dot{c}^1\dot{c}^2}{c^2}\right)^2 \\
&+ 2\ddot{c}^2c^2L^2 - 4L^2(\dot{c}^2)^2 + \frac{(\dot{c}^2)^4}{(c^2)^2} + \frac{(\dot{c}^1)^4}{(c^2)^2}\Bigg)\,dt \\
=&\frac{1}{L^3}\Bigg(\int_0^1 \frac{1}{(c^2)^2}\Bigg((\ddot{c}^1)^2 + (\ddot{c}^2)^2 + 2\left(\frac{\dot{c}^1\dot{c}^2}{c^2}\right)^2 - 2L^2(\dot{c}^2)^2 \\
&+ \frac{(\dot{c}^2)^4}{(c^2)^2} + \frac{(\dot{c}^1)^4}{(c^2)^2}\Bigg)\,dt + 2L^2\int_0^1 \ddot{c}^2\frac{1}{c^2} - \frac{(\dot{c}^2)^2}{(c^2)^2}\,dt\Bigg) \\
=&\frac{1}{L^3}\int_0^1 \frac{1}{(c^2)^2}\Bigg((\ddot{c}^1)^2 + (\ddot{c}^2)^2 - 2L^2(\dot{c}^2)^2 + \frac{(\dot{c}^2)^4}{(c^2)^2} + 2\left(\frac{\dot{c}^1\dot{c}^2}{c^2}\right)^2 + \frac{(\dot{c}^1)^4}{(c^2)^2}\Bigg)\,dt \\
&+ \frac{2}{L}\left[\frac{\dot{c}^2}{c^2}\right]_0^1 \\
\overset{(3.1)}{=}&\frac{1}{L^3}\int_0^1 \frac{1}{(c^2)^2}\Big((\ddot{c}^1)^2 + (\ddot{c}^2)^2 - 2L^2(\dot{c}^2)^2 + L^4(c^2)^2\Big)\,dt \\
&+ \frac{2}{L}\left[\frac{\dot{c}^2}{c^2}\right]_0^1.
\end{aligned}
$$

To summarize our findings we state the following equation

$$W_h(c) = \frac{1}{L^3}\int_0^1 \frac{1}{(c^2)^2}\left((\ddot{c}^1)^2 + (\ddot{c}^2)^2 - 2L^2(\dot{c}^2)^2\right)\, dt + L + \frac{2}{L}\left[\frac{\dot{c}^2}{c^2}\right]_0^1. \tag{3.4}$$

With this equation in mind we can prove the following theorem:

Theorem 3.1 (see [25] Theorem 3.1)**.** *Let $(c_n)_{n\in\mathbb{N}} \subset M_{\alpha_-,\alpha_+}$ be a minimising sequence for $W_h(c)$ with bounded hyperbolic arclength. Then there exists a curve $c \in M_{\alpha_-,\alpha_+}$ with*

$$W_h(c) = W^h_{\alpha_-,\alpha_+} := \inf\{W_h(v) :\ v \in M_{\alpha_-,\alpha_+}\}.$$

Proof. Reparameterise $c_n : [0,1] \to \mathbb{H}^2$ proportionally by hyperbolic arclength. Let L_n be the hyperbolic arclength of c_n. Since L_n is bounded, c_n^2 is bounded from above and below. (3.1) then gives us upper bounds on $|\dot{c}^1|$ and $|\dot{c}^2|$. With (3.4) there exists a $C > 0$ such that

$$C > \int_0^1 (\ddot{c}_n^1)^2 + (\ddot{c}_n^2)^2\, dt.$$

Hence we can extract a subsequence, which is weakly convergent in $H^2((0,1),\mathbb{H}^2)$ and strongly convergent in $C^1([0,1],\mathbb{H}^2)$ to a curve $c : [0,1] \to \mathbb{H}^2$. The boundary data are preserved, since we have convergence in C^1. This, (3.1) and the bound on L_n ensure, that c is parameterised proportionally by hyperbolic arclength. This in turn gives us $\dot{c} \neq 0$, since c^2 is bounded from above as well as from below. Hence c belongs to M_{α_-,α_+}. Since $\frac{1}{c_n^2}$ converges in $C^0([0,1])$, the fractions $\frac{\ddot{c}_n^1}{c_n^2}$ and $\frac{\ddot{c}_n^2}{c_n^2}$ converge weakly in $L^2((0,1),\mathbb{H}^2)$. Together with the lower semi-continuity of a norm and (3.4) this yields

$$W^h_{\alpha_-,\alpha_+} \le W_h(c) \le \liminf_{n\to\infty} W_h(c_n) \le W^h_{\alpha_-,\alpha_+} = \inf\{W_h(v) :\ v \in M_{\alpha_-,\alpha_+}\}.$$

□

3.2. Estimates on hyperbolic arclength

This section directly corresponds to [25, Section 4]. If we wish to apply Theorem 3.1 to obtain a solution of (1.4), we have to find an upper bound for the hyperbolic arclength of a minimising sequence. We can achieve this, if we work strictly below the threshold of 8 for the elastic energy. The main idea is contained in the following lemma, which was found by Hans-Christoph Grunau.

Lemma 3.2 (see [25] Lemma 4.1)**.** *Let $c \in M_{\alpha_-,\alpha_+}$ and $0 < t_1 < t_2 < 1$ with*

$$\dot{c}^1(t_1) = \dot{c}^1(t_2) = 0 \text{ and } \dot{c}^2(t_1)\cdot\dot{c}^2(t_2) < 0.$$

Then the elastic energy satisfies
$$W_h(c) \geq 8.$$

Proof. Let us distinguish two cases. The first one is $\dot{c}^2(t_1) < 0$. Equation (2.12) yields

$$\begin{aligned}
W_h(c) &= W_h(c)\big|_{[0,t_1]} + W_h(c)\big|_{[t_1,t_2]} + W_h(c)\big|_{[t_2,1]} \\
&\geq W_h(c)\big|_{[t_1,t_2]} = \frac{2}{\pi} W_e(S(c))\big|_{[t_1,t_2]} + 4\left[\frac{\dot{c}^2}{\sqrt{(\dot{c}^1)^2+(\dot{c}^2)^2}}\right]_{t_1}^{t_2} \\
&\geq 8
\end{aligned}$$

The other case is $\dot{c}^2(t_1) > 0$. The boundary data and again equation (2.12) yield

$$\begin{aligned}
W_h(c) &= W_h(c)\big|_{[0,t_1]} + W_h(c)\big|_{[t_1,t_2]} + W_h(c)\big|_{[t_2,1]} \\
&\geq W_h(c)\big|_{[0,t_1]} + W_h(c)\big|_{[t_2,1]} = \frac{2}{\pi} W_e(S(c))\big|_{[0,t_1]} + \frac{2}{\pi} W_e(S(c))\big|_{[t_2,1]} \\
&+ 4\left[\frac{\dot{c}^2}{\sqrt{(\dot{c}^1)^2+(\dot{c}^2)^2}}\right]_{0}^{t_1} + 4\left[\frac{\dot{c}^2}{\sqrt{(\dot{c}^1)^2+(\dot{c}^2)^2}}\right]_{t_2}^{1} \\
&\geq 8
\end{aligned}$$

□

Hans-Christoph Grunau discovered the following lemma for graphs and the present author extended it to curves. It uses the same idea as in Lemma 3.2.

Lemma 3.3 (see [25] Lemma 4.2)**.** *Let* $(c_n)_{n\in\mathbb{N}} \subset M_{\alpha_-,\alpha_+}$ *be a sequence, which satisfies* $\sup_n W_h(c_n) < 8$. *Then there exists a constant* $C > 0$ *with*

$$\forall t \in [0,1],\ \forall n \in \mathbb{N}:\ C < c_n^2(t).$$

Proof. We proceed by contradiction. Let us assume that no such bound exists. Hence after possibly passing to a subsequence, we can find $(t_n)_{n\in\mathbb{N}} \subset [0,1]$ with

$$c_n^2(t_n) = \min_{t\in[0,1]} c_n^2(t) \to 0,\ (n \to \infty).$$

Because of the boundary data we have $\dot{c}_n^2(t_n) = 0$ for n large enough. Let us for now assume the existence of another two sequences $0 < t_n^- < t_n < t_n^+ < 1$ with

$$\left|\frac{\dot{c}_n^2}{\sqrt{(\dot{c}_n^1)^2+(\dot{c}_n^2)^2}}(t_n^-)\right| \to 1 \ \text{ and } \left|\frac{\dot{c}_n^2}{\sqrt{(\dot{c}_n^1)^2+(\dot{c}_n^2)^2}}(t_n^+)\right| \to 1.$$

We will show the existence of these sequences later. For now we can use the idea from Lemma 3.2: Let us assume for the first case that $\dot{c}_n^2(t_n^-) < 0$ with n large enough. Then with (2.12) we obtain for n large enough

$$\begin{aligned} W_h(c_n)\big|_{[0,t_n]} &= W_h(c_n)\big|_{[0,t_n^-]} + W_h(c_n)\big|_{[t_n^-,t_n]} \geq W_h(c_n)\big|_{[t_n^-,t_n]} \\ &= \frac{2}{\pi} W_e(S(c_n))\big|_{[t_n^-,t_n]} + 4\left[\frac{\dot{c}_n^2}{\sqrt{(\dot{c}_n^1)^2 + (\dot{c}_n^2)^2}}\right]_{t_n^-}^{t_n} \\ &\geq 4 + o(1). \end{aligned}$$

If we assume on the other hand that $\dot{c}_n^2(t_n^-) > 0$ for large n, then

$$\begin{aligned} W_h(c_n)\big|_{[0,t_n]} &= W_h(c_n)\big|_{[0,t_n^-]} + W_h(c_n)\big|_{[t_n^-,t_n]} \geq W_h(c_n)\big|_{[0,t_n^-]} \\ &= \frac{2}{\pi} W_e(S(c_n))\big|_{[0,t_n^-]} + 4\left[\frac{\dot{c}_n^2}{\sqrt{(\dot{c}_n^1)^2 + (\dot{c}_n^2)^2}}\right]_{0}^{t_n^-} \\ &\geq 4 + o(1). \end{aligned}$$

We can work completely analogously in the interval $[t_n, 1]$ and obtain

$$W_h(c_n) = W_h(c_n)\big|_{[0,t_n]} + W_h(c_n)\big|_{[t_n,1]} \geq 8 + o(1),$$

which would be a contradiction. Now we have to show the existence of t_n^- and t_n^+: Again we proceed by contradiction and assume, that such sequences t_n^-, t_n^+ do not exist. After passing to a further subsequence we can find a $\delta > 0$ such that

$$\forall n \in \mathbb{N}, \forall t \in [0,1]: \ \left|\frac{\dot{c}_n^2}{\sqrt{(\dot{c}_n^1)^2 + (\dot{c}_n^2)^2}}(t)\right| \leq 1 - \delta. \tag{3.5}$$

Squaring the inequality gives us for all $t \in [0,1]$

$$\begin{aligned} &\Rightarrow (\dot{c}_n^2)^2 \leq (1-\delta)^2 \cdot ((\dot{c}_n^1)^2 + (\dot{c}_n^2)^2) \\ &\Rightarrow 0 \leq (\dot{c}_n^2)^2 (1 - (1-\delta)^2) \leq (1-\delta)^2 (\dot{c}_n^1)^2. \end{aligned}$$

Since the curves are regular ($\dot{c} \neq 0$), we obtain

$$\forall t \in [0,1]: \ \dot{c}_n^1 \neq 0.$$

Hence the curve c_n can be reparameterised as a graph on $[0,1]$. This way we obtain a sequence of functions $u_n \in H^2([-1,1],(0,\infty))$ representing the curves on $[0,1]$. To obtain a contradiction we first have to show that $|x_n| := |c_n^1(t_n)| \nrightarrow 1$. Thanks to (3.5) there exists a $C > 0$, such that $\forall x \in [-1, 1]$ we have $|u_n'(x)| \leq C$. The mean value theorem yields

$$|x_n \pm 1| \geq \frac{\min\{\alpha_-, \alpha_+\}}{C} + o(1) > 0$$

for n large enough. Since the elastic energy is a geometric functional, it is invariant under reparameterisation. This yields together with (2.15) and (2.6)

$$\begin{aligned} 8 \geq W_h(c_n)\big|_{[0,t_n]} &= W_h(u_n)\big|_{[-1,x_n]} \\ &= \int_{-1}^{x_n} \frac{u_n''(x)^2 u_n(x)}{(1+u_n'(x)^2)^{\frac{5}{2}}}\, dx + \int_{-1}^{x_n} \frac{1}{u_n(x)\sqrt{1+u_n'(x)^2}}\, dx \\ &\geq \int_{-1}^{x_n} \frac{1}{u_n(x)\sqrt{1+u_n'(x)^2}}\, dx. \\ &= \int_{-1}^{x_n} \frac{1}{1+u_n'(x)^2}\, ds(x) \\ &\geq \frac{1}{1+C^2} \int_{-1}^{x_n} ds(x) \to \infty, \end{aligned}$$

since the hyperbolic arclength tends to infinity. This is the case, because $u_n(x_n) \to 0$. The proof for t_n^+ is analogous to t_n^- by working on $[t_n, 1]$. □

The proof of the next lemma is based on the previous one and provides an upper bound.

Lemma 3.4 (see [25] Lemma 4.3)**.** *Let $(c_n)_{n\in\mathbb{N}} \subset M_{\alpha_-,\alpha_+}$ be a sequence, which satisfies $\sup_n W_h(c_n) < 8$. Then there exists a constant $C > 0$ with*

$$\forall t \in [0,1],\ \forall n \in \mathbb{N}:\ C > |c_n(t)|.$$

Proof. As in Lemma 3.3 we will proceed by contradiction. After possibly passing to a subsequence we may assume the existence of a sequence $(\xi_n)_{n\in\mathbb{N}} \subset [0,1]$ with

$$\max\{|c_n(t)|,\ t \in [0,1]\} = |c_n(\xi_n)| \to \infty,\ (n \to \infty).$$

We transform this problem in such a way, that we can directly apply our approach from Lemma 3.3. To do this we need the Cayley transformation $Q : \mathbb{H}^2 \to \{(x,y) \in \mathbb{R}^2 :\ |(x,y)| < 1\} =: \mathbb{D}^2$ given by $Q(x,y) = \frac{1}{x^2+(1+y)^2}\left(x^2 - 1 + y^2, -2x\right)$. Since it is an isometry between the Poincaré disk $\mathbb{D}^2$ and $\mathbb{H}^2$, the elastic energy remains invariant under this transformation. Now we need a rotation around $(0,0) \in \mathbb{R}^2$ with angle $\varphi > 0$. Let us denote this function by $R_\varphi : \mathbb{R}^2 \to \mathbb{R}^2$. Please keep in mind that R_φ does not change the elastic energy in $\mathbb{D}^2$, since it is an isometry of this manifold. Let us now define the transformed curves:

$$c_{n,\varphi} : [0,1] \to \mathbb{H}^2 \text{ with } c_{n,\varphi}(t) := Q^{-1}(R_\varphi(Q(c_n(t)))).$$

Figure 3.1 explains the transformation. Since $\varphi > 0$ we can find a sequence $(t_n^\varphi)_{n\in\mathbb{N}} \subset$

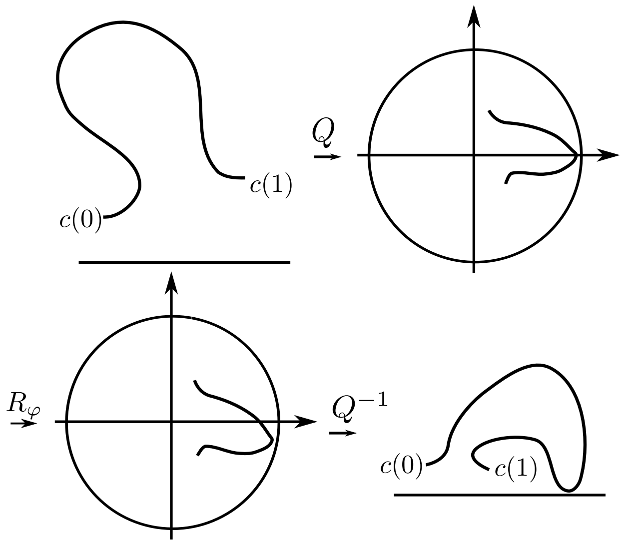

Figure 3.1.: Transformation of curves, such that an extremum tends to zero.

$(0,1)$ for n large enough with

$$c^2_{n,\varphi}(t_n^\varphi) = \min_{t\in[0,1]} c^2_{n,\varphi}(t) \to 0.$$

Let $\varepsilon > 0$ be fixated but arbitrary. Since R_φ, Q and Q^{-1} are smooth and c_n satisfies the boundary data, we can find a small angle $\varphi > 0$ with

$$\left|\frac{\dot{c}^2_{n,\varphi}(0)}{\dot{c}^1_{n,\varphi}(0)}\right| < \varepsilon \text{ and } \left|\frac{\dot{c}^2_{n,\varphi}(1)}{\dot{c}^1_{n,\varphi}(1)}\right| < \varepsilon.$$

This also yields

$$\left|\frac{\dot{c}^2_{n,\varphi}(0)}{\sqrt{(\dot{c}^1_{n,\varphi}(0))^2 + (\dot{c}^2_{n,\varphi}(0))^2}}\right| \le \left|\frac{\dot{c}^2_{n,\varphi}(0)}{\dot{c}^1_{n,\varphi}(0)}\right| < \varepsilon,$$

and the same result for $t = 1$. As in in the proof of Lemma 3.3 we can find two sequences $0 < t_n^{\varphi,-} < t_n^{\varphi} < t_n^{\varphi,+} < 1$ for n large enough, which satisfy

$$\left| \frac{\dot{c}^2_{n,\varphi}}{\sqrt{(\dot{c}^1_{n,\varphi})^2 + (\dot{c}^2_{n,\varphi})^2}}(t_n^{\varphi,\pm}) \right| \to 1, \ (n \to \infty).$$

Let us assume for large n, that we have $\dot{c}^2_{n,\varphi}(t_n^{\varphi,-}) > 0$ and $\dot{c}^2_{n,\varphi}(t_n^{\varphi,+}) > 0$. Then the elastic energy can be estimated with (2.12) as follows

$$\begin{aligned}
W_h(c_n) &= W_h(c_{n,\varphi}) \geq W_h(c_{n,\varphi})\big|_{[0,t_n^{\varphi,-}]} + W_h(c_{n,\varphi})\big|_{[t_n^{\varphi},t_n^{\varphi,+}]} \\
&= \frac{2}{\pi} W_e(S(c_{n,\varphi}))\big|_{[0,t_n^{\varphi,-}]} + \frac{2}{\pi} W_e(S(c_{n,\varphi}))\big|_{[t_n^{\varphi},t_n^{\varphi,+}]} \\
&+ 4 \left[\frac{\dot{c}^2_{n,\varphi}}{\sqrt{(\dot{c}^1_{n,\varphi})^2 + (\dot{c}^2_{n,\varphi})^2}} \right]_0^{t_n^{\varphi,-}} + 4 \left[\frac{\dot{c}^2_{n,\varphi}}{\sqrt{(\dot{c}^1_{n,\varphi})^2 + (\dot{c}^2_{n,\varphi})^2}} \right]_{t_n^{\varphi}}^{t_n^{\varphi,+}} \\
&\geq 8 + o(1) - \varepsilon > 8 - 2\varepsilon,
\end{aligned}$$

for n large enough. The remaining cases can be dealt with in the same way. By choosing $\varepsilon < \frac{1}{2}(8 - \sup_n W_h(c_n))$, we finally reach a contradiction. $\square$

Now we can tackle our main estimate for the hyperbolic arclength:

Theorem 3.5 (see [25] Theorem 4.4)**.** *Let $(c_n)_{n\in\mathbb{N}} \subset M_{\alpha_-,\alpha_+}$ be a sequence with $\sup_n W_h(c_n) < 8$. Let L_n be the hyperbolic arclength of c_n. Then there exists a constant $C > 0$ with*

$$\forall n \in \mathbb{N}: \ L_n \leq C.$$

Proof. Again we proceed by contradiction. So let us assume, that after passing to a subsequence we obtain $L_n \to \infty$ for $n \to \infty$. By reparameterising the curves proportionally by hyperbolic arclength, we achieve with Lemma 3.3 and (3.1) the following uniform convergence on $[0,1]$ for $(n \to \infty)$

$$(\dot{c}^1_n)^2 + (\dot{c}^2_n)^2 = (c^2_n)^2 L_n^2 \to \infty. \tag{3.6}$$

With Lemma 3.4 and the mean value theorem we obtain three sequences:

$$\begin{aligned}
\infty > C > \left| c^1_n\left(\frac{2}{6}\right) - c^1_n\left(\frac{1}{6}\right) \right| &= |\dot{c}^1_n(t_{n,1})| \frac{1}{6}, \ \frac{1}{6} < t_{n,1} < \frac{2}{6}, \\
\infty > C > \left| c^2_n\left(\frac{4}{6}\right) - c^2_n\left(\frac{3}{6}\right) \right| &= |\dot{c}^2_n(t_{n,2})| \frac{1}{6}, \ \frac{3}{6} < t_{n,2} < \frac{4}{6}, \\
\infty > C > \left| c^1_n\left(\frac{6}{6}\right) - c^1_n\left(\frac{5}{6}\right) \right| &= |\dot{c}^1_n(t_{n,3})| \frac{1}{6}, \ \frac{5}{6} < t_{n,3} < \frac{6}{6}.
\end{aligned}$$

(3.6) then yields for $n \to \infty$

$$
\begin{aligned}
|\dot{c}_n^2(t_{n,1})| &\to \infty, \\
|\dot{c}_n^1(t_{n,2})| &\to \infty, \\
|\dot{c}_n^2(t_{n,3})| &\to \infty.
\end{aligned}
$$

This yields

$$
\begin{aligned}
\left| \frac{\dot{c}_n^2}{\sqrt{(\dot{c}_n^1)^2 + (\dot{c}_n^2)^2}} \right| (t_{n,1}) &\to 1, \\
\left| \frac{\dot{c}_n^2}{\sqrt{(\dot{c}_n^1)^2 + (\dot{c}_n^2)^2}} \right| (t_{n,2}) &\to 0, \\
\left| \frac{\dot{c}_n^2}{\sqrt{(\dot{c}_n^1)^2 + (\dot{c}_n^2)^2}} \right| (t_{n,3}) &\to 1.
\end{aligned}
$$

As before we would need to distinguish some cases, but we will just demonstrate the case $\dot{c}_n^2(t_{n,1}) < 0$ and $\dot{c}_n^2(t_{n,3}) < 0$.

$$
\begin{aligned}
W_h(c_n) &\geq W_h(c_n)\big|_{[t_{n,1},t_{n,2}]} + W_h(c_n)\big|_{[t_{n,3},1]} \\
&= \frac{2}{\pi} W_e(S(c_n))\big|_{[t_{n,1},t_{n,2}]} + \frac{2}{\pi} W_e(S(c_n))\big|_{[t_{n,3},1]} \\
&\quad + 4 \left[\frac{\dot{c}_n^2}{\sqrt{(\dot{c}_n^1)^2 + (\dot{c}_n^2)^2}} \right]_{t_{n,1}}^{t_{n,2}} + 4 \left[\frac{\dot{c}_n^2}{\sqrt{(\dot{c}_n^1)^2 + (\dot{c}_n^2)^2}} \right]_{t_{n,3}}^{1} \\
&\geq 8 + o(1).
\end{aligned}
$$

For the other cases one just needs to adjust the intervals of integration and then the desired contradiction follows. $\square$

3.3. Regularity of a solution

This section is taken from [25, Section 5]. To show regularity of a weak solution of (1.4), we will proceed similarly to [17, Theorem 4, step 2]. First we calculate an Euler-Lagrange equation for the elastic energy $W_h(\cdot)$. Let $c \in M_{\alpha_-,\alpha_+}$ be a critical point of the hyperbolic elastic energy. We may parameterise this c proportionally by its hyperbolic arclength L. With the help of (2.10) we obtain for any testing function $\varphi \in H_0^2([0,1], \mathbb{R}^2)$:

$$
\begin{aligned}
\frac{d}{d\varepsilon}\kappa[c+\varepsilon\varphi]\bigg|_{\varepsilon=0} =& \frac{1}{|\dot{c}|^3}\big(\ddot{\varphi}^2\dot{c}^1c^2+\dot{\varphi}^1\ddot{c}^2c^2+\ddot{c}^2\dot{c}^1\varphi^2-\ddot{\varphi}^1\dot{c}^2c^2 \\
&-\ddot{c}^1\dot{\varphi}^2c^2-\ddot{c}^1\dot{c}^2\varphi^2+\dot{\varphi}^1(\dot{c}^2)^2+2\dot{c}^1\dot{\varphi}^2\dot{c}^2+3\dot{\varphi}^1(\dot{c}^1)^2\big) \\
&-3\frac{\dot{\varphi}^1\dot{c}^1+\dot{\varphi}^2\dot{c}^2}{|\dot{c}|^5}\big(\ddot{c}^2\dot{c}^1c^2-\ddot{c}^1\dot{c}^2c^2+\dot{c}^1(\dot{c}^2)^2+(\dot{c}^1)^3\big) \\
=& \frac{1}{|\dot{c}|^3}\big(\ddot{\varphi}^2\dot{c}^1c^2+\dot{\varphi}^1\ddot{c}^2c^2+\ddot{c}^2\dot{c}^1\varphi^2-\ddot{\varphi}^1\dot{c}^2c^2 \\
&-\ddot{c}^1\dot{\varphi}^2c^2-\ddot{c}^1\dot{c}^2\varphi^2+\dot{\varphi}^1(\dot{c}^2)^2+2\dot{c}^1\dot{\varphi}^2\dot{c}^2+3\dot{\varphi}^1(\dot{c}^1)^2\big) \\
&-3\frac{\dot{\varphi}^1\dot{c}^1+\dot{\varphi}^2\dot{c}^2}{|\dot{c}|^2}\kappa[c].
\end{aligned}
$$

The derivative of $W_h(\cdot)$ in $c(\cdot)$ is

$$
\begin{aligned}
0 =& \frac{d}{d\varepsilon}\int_0^1 \kappa[c+\varepsilon\varphi]^2\,ds\bigg|_{\varepsilon=0} \\
=& \int_0^1 \left(2\kappa[c]\frac{d}{d\varepsilon}\kappa[c+\varepsilon\varphi]\bigg|_{\varepsilon=0}\frac{|\dot{c}|}{c^2}+\kappa[c]^2\left(\frac{\dot{c}^1\dot{\varphi}^1+\dot{c}^2\dot{\varphi}^2}{c^2|\dot{c}|}-\frac{|\dot{c}|}{(c^2)^2}\varphi^2\right)\right)dt \\
=& \int_0^1 \Bigg(2\frac{|\dot{c}|}{c^2}\kappa[c]\Bigg(\frac{1}{|\dot{c}|^3}\Big(\dot{\varphi}^1\ddot{c}^2c^2-\ddot{\varphi}^1\dot{c}^2c^2+\dot{\varphi}^1(\dot{c}^2)^2+3\dot{\varphi}^1(\dot{c}^1)^2 \\
&+\ddot{\varphi}^2\dot{c}^1c^2+\ddot{c}^2\dot{c}^1\varphi^2-\ddot{c}^1\dot{\varphi}^2c^2-\ddot{c}^1\dot{c}^2\varphi^2+2\dot{c}^1\dot{\varphi}^2\dot{c}^2\Big) \\
&-3\kappa[c]\frac{1}{|\dot{c}|^2}(\dot{\varphi}^1\dot{c}^1+\dot{\varphi}^2\dot{c}^2)\Bigg)+\kappa[c]^2\left(\frac{\dot{c}^1\dot{\varphi}^1+\dot{c}^2\dot{\varphi}^2}{c^2|\dot{c}|}-\frac{|\dot{c}|}{(c^2)^2}\varphi^2\right)\Bigg)dt. \qquad (3.7)
\end{aligned}
$$

Let $\eta\in C_c^\infty([0,1],\mathbb{R})$ be arbitrary. We define

$$
\begin{aligned}
\mu(t) &= \int_0^t\int_0^y \eta(s)\,ds\,dy+\beta t^2+\gamma t^3 \\
\beta &= \int_0^1 \eta(s)\,ds-3\int_0^1\int_0^y \eta(s)\,ds\,dy \\
\gamma &= 2\int_0^1\int_0^y \eta(s)\,ds\,dy-\int_0^1 \eta(s)\,ds.
\end{aligned}
$$

The idea for this comparison function stems from [17, Theorem 4, step 2]. Thanks to the choice of γ and β, we have $\mu(0)=\mu(1)=\dot{\mu}(0)=\dot{\mu}(1)=0$. We also observe the following estimates

$$\beta,\ \gamma,\ \|\mu\|_{C^1} \le C\|\eta\|_{L^1}.$$

If we set $\varphi(t) = (\mu(t), 0)$, we get $\varphi \in H_0^2([0,1], \mathbb{R}^2)$. By inserting this into (3.7), we obtain for every $\eta \in C_c^\infty(0,1)$

$$\left| \int_0^1 \kappa[c](t)\eta(t)\frac{\dot{c}^2}{|\dot{c}|^2}\,dt \right| \le C(c)\|\eta\|_{L^1}, \tag{3.8}$$

since every term in (3.7) with the exception of the one with $\ddot{\varphi}^1$ (which gives us the left hand side of (3.8)) can be estimated with the help of $c \in H^2([0,1], \mathbb{R}^2)$ and $\kappa[c] \in L^2([0,1])$. Because the hyperbolic arclength is fixed, $\frac{1}{|\dot{c}|^2}$ is bounded from below as well (see (3.1)). This and $(L^1)^* = L^\infty$ ensure that $\kappa[c]\dot{c}^2 \in L^\infty([0,1])$.
We have to repeat this process for $\varphi(t) = (0, \mu(t))$, to obtain a bound for $\kappa[c]$. With the same arguments as above, we get

$$\left| \int_0^1 \kappa[c](t)\eta(t)\frac{\dot{c}^1}{|\dot{c}|^2}\,dt \right| \le C(c)\|\eta\|_{L^1}, \tag{3.9}$$

for every $\eta \in C_c^\infty([0,1])$. Hence $\kappa[c]\dot{c}^1 \in L^\infty([0,1])$. If we combine this with the bound on $\kappa[c]\dot{c}^2$ and (3.1), we finally get $\kappa[c] \in L^\infty([0,1])$. The Frenet equations (2.13) and (2.14) yield $c \in W^{2,\infty}([0,1], \mathbb{R}^2)$.
Now we can show higher differentiability: For arbitrary $\eta \in C_c^\infty([0,1])$ we define

$$\nu(t) = \int_0^t \eta(s)\,ds - 3t^2\int_0^1 \eta(s)\,ds + 2t^3\int_0^1 \eta(s)\,ds. \tag{3.10}$$

and get

$$\nu(0) = \nu(1) = \dot{\nu}(0) = \dot{\nu}(1) = 0,\ \|\nu\|_{C^0} \le C\|\eta\|_{L^1} \text{ and } \|\dot{\nu}\|_{L^1} \le C\|\eta\|_{L^1}.$$

If we now choose $\varphi(t) = (\nu(t), 0)$, insert it into (3.7) and combine it with the already established L^∞-bounds on κ and $\ddot{c}$, we obtain

$$\left| \int_0^1 \kappa[c](t)\dot{\eta}(t)\frac{\dot{c}^2}{|\dot{c}|^2}\,dt \right| \le C(c)\|\eta\|_{L^1}. \tag{3.11}$$

The functional $F(\eta) := \int_0^1 \kappa[c](t)\dot{\eta}(t)\frac{\dot{c}^2}{|\dot{c}|^2}\,dt$ is defined on $W^{1,1}([0,1])$, since $\kappa[c] \in L^\infty([0,1])$. (3.11) now allows us to extend it to a functional $\tilde{F}$ on $L^1([0,1])$, since $W^{1,1}([0,1])$ is dense in $L^1([0,1])$ and F is bounded w.r.t. to $\|\cdot\|_{L^1}$. The Riesz representation theorem (see e.g. [54, Thm. II.2.4]) then yields a $g \in L^\infty([0,1])$ with

$$\forall f \in L^1([0,1])\ \tilde{F}(f) = \int_0^1 g(t)f(t)\,dt.$$

If we go back to $C_c^\infty([0,1])$ as a domain of definition for $\tilde{F}$, we obtain

$$\forall \eta \in C_c^\infty([0,1])\ \int_0^1 g(t)\eta(t)\,dt = \int_0^1 \kappa[c](t)\dot{\eta}(t)\frac{\dot{c}^2}{|\dot{c}|^2}\,dt.$$

Since $\frac{1}{|\dot{c}|^2} \neq 0$ the curvature satisfies $\kappa[c]\dot{c}^2 \in W^{1,\infty}([0,1])$.
Repeating this argument with $\varphi = (0, \nu(t))$, we also obtain $\kappa[c]\dot{c}^1 \in W^{1,\infty}([0,1])$. Since $\dot{c} \neq 0$ and $\dot{c}$ is continous, we finally achieve $\kappa[c] \in W^{1,\infty}([0,1])$. Then the Frenet equations (2.13) and (2.14) yield that $c \in W^{3,\infty}([0,1], \mathbb{R}^2)$.
For higher regularity another form of the Euler-Lagrange equation is more appropriate. Langer & Singer deduced it in [37, p. 3]. By reparameterising c proportionally by hyperbolic arclength and denoting L as the hyperbolic arclength of c, it can be stated as follows

$$\frac{2}{L^2}\ddot{\kappa}[c](t) = -\kappa[c](t)^3 + 2\kappa[c](t). \tag{3.12}$$

So $\ddot{\kappa}[c]$ satisfies an equation with right-hand side in $W^{1,\infty}([0,1])$, which in return gives us $\kappa[c] \in W^{3,\infty}([0,1]) = C^{2,1}([0,1])$. Hence the Frenet equations (2.13) and (2.14) yield $c \in C^4([0,1])$. By straightforward bootstrapping we finally obtain $c \in C^\infty([0,1])$.

4. Order reduction for the Euler-Lagrange Equation

This chapter does not provide any new results. It instead collects very important knowledge, concerning the analysis of the Euler-Lagrange equation of W_h. It was conducted by Langer & Singer in [37] and picked up by the present author in his diploma thesis [23], in which the following results are gathered as well.

4.1. Analysis of the curvature equation

Reparameterising a critical point of W_h by hyperbolic arclength yields with (3.12) (see [37, Equation (1.2)])

$$\ddot{K} = K - \frac{1}{2}K^3. \tag{4.1}$$

K denotes the geodesic curvature of such a critical point parameterised by hyperbolic arclength. Every curve in $\mathbb{H}^2$ with geodesic curvature satisfying this equation is called an elastica (see [37, p. 3 bottom]). Multiplying it with $\dot{K}$ and integrating yields (see [37, Equation (2.1)])

$$\left(\dot{K}(s)\right)^2 = K^2(s) - \frac{1}{4}K^4(s) - K_0^2 + \frac{1}{4}K_0^4 + (\dot{K}_0)^2, \tag{4.2}$$

with constants $K_0, \dot{K}_0 \in \mathbb{R}$. Since the left hand side is always non-negativ and the right hand side would tend to $-\infty$, if $|K| \to \infty$, every solution and its derivative are bounded. Hence it can be extended on the whole real numbers (see e.g. [23, Corollary 4.2 and Remark 4.3]). The following lemma helps us to classify solutions of (4.1) (also cf. [37, p. 6]).

Lemma 4.1 (see [23] Theorem 4.15). *Let $K : \mathbb{R} \to \mathbb{R}$ be a smooth solution to (4.1). Then there exists a point $s \in \mathbb{R}$ with $\dot{K}(s) = 0$.*

Solutions of (4.1) can be expressed with the help of Jacobian elliptic functions (see [37, table 2.7]). The following definitions and properties of these functions are taken from [1, Section 16.1]: Let $0 < k < 1$ and

$$F_k(\varphi) = \int_0^{\varphi} \frac{1}{\sqrt{1 - k^2 \sin^2 \psi}}\, d\psi. \tag{4.3}$$

Since $F_k' > 0$ we can invert it and define

$$\mathrm{AM}(s,k) = F_k^{-1}(s). \tag{4.4}$$

The Jacobian elliptic functions can then be expressed as

$$\begin{gathered}\mathrm{sn}(s,k) = \sin(\mathrm{AM}(s,k)),\ \mathrm{cn}(s,k) = \cos(\mathrm{AM}(s,k)),\\ \mathrm{dn}(s,k) = \sqrt{1-k^2\,\mathrm{sn}^2(s,k)}.\end{gathered} \tag{4.5}$$

The non-trivial solutions of (4.1) are classified by the following three lemmas, since if K is a solution of (4.1), then $-K$ is as well. Therefore we also employ the following classification even if the initial curvature K_0 is negativ.

Lemma 4.2 (see [37] table 2.7c)**.** *Let $K \in C^2(\mathbb{R})$ be a solution of (4.1) with $K(0) = K_0 \in (0,2)$ and $\dot{K}(0) = 0$, then*

$$K(s) = \begin{cases} 2r\,\mathrm{dn}(r(s+s_0),k), & \text{if } K_0 \neq \sqrt{2},\\ \sqrt{2}, & \text{if } K_0 = \sqrt{2},\end{cases}$$

with

$$\begin{aligned} r &= \left\{\begin{array}{ll} \frac{K_0}{2}, & \text{if } K_0 \in (\sqrt{2},2),\\ \frac{\sqrt{4-K_0^2}}{2}, & \text{if } K_0 \in (0,\sqrt{2}),\end{array}\right\} \in \left(\frac{1}{2}\sqrt{2},1\right),\\ k &= \frac{\sqrt{2r^2-1}}{r} \in (0,1),\\ s_0 &= \begin{cases} 0, & \text{if } K_0 \in (\sqrt{2},2),\\ \frac{1}{r}F_k(\frac{\pi}{2}), & \text{if } K_0 \in (0,\sqrt{2}).\end{cases}\end{aligned}$$

These solutions are called orbitlike, or in the constant case, circular.

Lemma 4.3 (see [37] table 2.7c)**.** *Let $K \in C^2(\mathbb{R})$ be a solution of (4.1) with $K(0) = 2$ and $\dot{K}(0) = 0$, then*

$$K(s) = \frac{2}{\cosh(s)}.$$

This solution is called asymptotically geodesic.

Lemma 4.4 (see [37] table 2.7c)**.** *Let $K \in C^2(\mathbb{R})$ be a solution of (4.1) with $K(0) = K_0 > 2$ and $\dot{K}(0) = 0$, then*

$$K(s) = K_0\,\mathrm{cn}(rs,k)$$

with

$$r = \sqrt{-1+\frac{1}{2}K_0^2},\ k = \frac{K_0}{2r}.$$

These solutions are called wavelike.

4.2. A Killing field for an elastica

The next natural step to understand the shape of a possible elastica would be to integrate the Frenet equations (2.13) and (2.14). Langer & Singer instead found a different way and were able to reduce the order of the underlying differential equation with the following lemma.

Lemma 4.5 (see [37] Proposition 2.1)**.** *Let* $-\infty \leq a < b \leq \infty$ *and* $\gamma : (a,b) \to \mathbb{H}^2$ *be an elastica parameterised by hyperbolic arclength with curvature* $K : (a,b) \to \mathbb{R}$ *satisfying* (4.1)*. Then the vector field*

$$J_\gamma = K^2\dot{\gamma} + 2\dot{K}\begin{pmatrix} -\dot{\gamma}^2 \\ \dot{\gamma}^1 \end{pmatrix}$$

has a unique extension to a Killing vector field J *on the whole upper half plane* $\mathbb{H}^2$*.*

Remark 4.6 (see [23] p. 49 bottom)**.** If we combine Lemma 4.5 with Example 2.10, we find parameters $a, b, c \in \mathbb{R}$, such that an elastica γ with curvature K satisfies

$$K^2\dot{\gamma}^1 - 2\dot{K}\dot{\gamma}^2 = a\frac{(\gamma^1)^2 - (\gamma^2)^2}{2} + b\gamma^1 + c \tag{4.6}$$

$$K^2\dot{\gamma}^2 + 2\dot{K}\dot{\gamma}^1 = a\gamma^1\gamma^2 + b\gamma^2. \tag{4.7}$$

Lemma 4.7 (see [37] Proposition 2.2)**.** *Let* $-\infty \leq a < b \leq \infty$ *and* $\gamma : (a,b) \to \mathbb{H}^2$ *be an elastica parameterised by hyperbolic arclength with curvature* $K : (a,b) \to \mathbb{R}$ *satisfying* (4.1)*. Let* $s_0 \in (a,b)$ *be critical for* K*. Let also* J *be the extension of* J_γ *given by Lemma 4.5. Then the integral curve* I *of* J *starting in* $\gamma(s_0)$ *is tangent to* $\gamma(s_0)$*. The geodesic curvature* $\kappa[I]$ *of* I *is as follows:*

$$\kappa[I] = \frac{2}{K(s_0)}.$$

4.3. A suitable initial value problem and bounding circles

This section summarizes Paragraph 7 of [23], in which explicit bounds for an elastica are given in means of initial data. These bounds have already been mentioned in [37, p. 8 and Figure 2]. For this let $\gamma : \mathbb{R} \to \mathbb{H}^2$ be a smooth elastica parameterised by hyperbolic arclength with curvature K. Lemma 4.1 yields an $s_0 \in \mathbb{R}$ with $\dot{K}(s_0) = 0$. Since (4.1) is autonomous and because of the Lemmas 2.3, 2.6 and the Frenet equations (2.13), (2.14), γ satisfies without loss of generality the following initial value problem (see [23, (AWP), p. 49]).

$$\begin{cases} \nabla_{\dot{\gamma}}\dot{\gamma} = KN, \ \nabla_{\dot{\gamma}}N = -K\dot{\gamma}, & \ddot{K} = K - \frac{1}{2}K^3 \\ \gamma(0) = (0,z)\,, \ \dot{\gamma}(0) = (z,0)\,, & K(0) = K_0, \ \dot{K}(0) = 0. \end{cases} \tag{4.8}$$

Here $K_0 \in \mathbb{R}$ and $z > 0$. N is a unit normal of γ defined by $N = (-\dot{\gamma}^2, \dot{\gamma}^1)$.
The Killing field J of Lemma 4.5 can be expressed with Example 2.10 and the initial conditions to (see [23, p. 49 bottom])

$$J(x, y) = a \begin{pmatrix} \frac{x^2-y^2}{2} \\ xy \end{pmatrix} + c \begin{pmatrix} 1 \\ 0 \end{pmatrix}. \tag{4.9}$$

We are especially interested in wavelike elastica, since we need those to construct additional solutions in chapter 8. Hence let $|K_0| > 2$. Then the following lemma holds.

Lemma 4.8 (see [37] p. 8 and [23] Chapter 7)**.** *Let γ be a solution of* (4.8) *with $|K_0| > 2$. Then two euclidean circles $B_+, B_- \subset \mathbb{R}^2$ exist, which are the only integral curves of J (cf. Lemma 4.5), that are tangent to γ. Moreover γ touches B_+, iff the geodesic curvature K has a maximum and it touches B_-, iff K has a minimum.*

Let us call $B_{r_+}(x_+) = B_+$ and $B_{r_-}(x_-) = B_-$. Let $K_0 > 2$, then with Lemma 4.7 and Example 2.14 r_+ and x_+ can be calculated to (see [23, p. 52]):

$$r_+ = \frac{z}{1 - \frac{2}{K_0}}, \; x_+ = (0, m_+), \; m_+ = -z\frac{\frac{2}{K_0}}{1 - \frac{2}{K_0}}. \tag{4.10}$$

B_+ crosses the x-axis at two points $x_s > 0$ and $-x_s < 0$. The Pythagorean theorem yields (see [23, p. 52])

$$x_s = \sqrt{r_+^2 - m_+^2} = z\sqrt{\frac{K_0 + 2}{K_0 - 2}}. \tag{4.11}$$

This in turn gives us (see [23, p. 53])

$$r_- = \frac{x_s}{\sqrt{1 - \left(\frac{2}{K_0}\right)^2}} = r_+, \; x_- = (0, m_-), \; m_- = x_s \frac{\frac{2}{K_0}}{\sqrt{1 - \left(\frac{2}{K_0}\right)^2}} = -m_+. \tag{4.12}$$

The formulae for $K_0 < -2$ are completely analogous. Especially the formula for x_s does not change at all.

In the orbitlike case we could also derive such formulae, but we only need the existence of bounding circles, which can be expressed in more general terms (see also Figure 4.1):

Lemma 4.9 (see [37] Figure 2 and Section 7.3 in [23])**.** *Let $\gamma : \mathbb{R} \to \mathbb{H}^2$ be an arbitrary orbitlike elastica (cf. Lemma 4.2). Then there exists a point $p \in \mathbb{H}^2$ and two open Balls $B_1 \subset B_2 \subset \mathbb{H}^2$ with centre at p w.r.t. the hyperbolic metric, such that $\overline{B_{1,2}} \subset \mathbb{H}^2$ and*

$$\gamma(\mathbb{R}) \subset \overline{B_2} \setminus B_1.$$

Furthermore the boundaries of B_1 and B_2 are integral curves of the extended Killing vectorfield J (cf. Lemma 4.5) and one of them always touches γ, when the geodesic curvature K has an extremum.

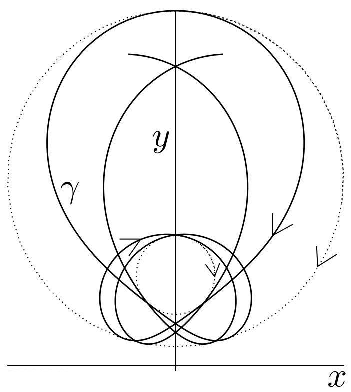

Figure 4.1.: An orbitlike elastica with bounding circles.

In the circular case γ is a circle (see Lemma 2.15 or [23, Section 7.1]). If on the other hand the curvature of γ equals zero, Lemma 2.15 yields γ to be a straight line parallel to the y-axis or a half circle centered on the x-axis.

The last cases are $K_0 = \pm 2$. These correspond to catenoids and Möbius transforms thereof:

Lemma 4.10 (see [23] Theorem 7.5)**.** *Let γ be a solution of* (4.8) *with $K_0 = 2$. Then*

$$\gamma(t) = (zt, z\cosh t).$$

Reflecting this solution at the circle of radius z and centre $(0, 0)$ yields with the help of Lemma 2.5:

Lemma 4.11 (see [23] Theorem 7.6)**.** *Let γ be a solution of* (4.8) *with $K_0 = -2$. Then*

$$\gamma(t) = \frac{z}{t^2 + \cosh^2 t}(t, \cosh t).$$

A sketch of this solution can be found in Figure 6.3.

5. Wavelike elastica

This chapter is dedicated to an analysis of wavelike elastica (cf. Lemma 4.4). These curves play a crucial role in the chapters 6, 7 and 8. It mainly consists of the sections 6 and 7 of [24] as well as the second part of section 6 of [25].

5.1. A perpendicular geodesic and a Bernstein type result

This section is a modified version of [24, Section 6]. We start with a special property of wavelike elastica, which orbitlike elastica do not possess. This was already observed by Langer & Singer in [37]. For the reader's convenience we give a proof, which is taylored to our situation here.

Lemma 5.1 (see [37] Proposition 2.3, [24] Lemma 6.1)**.** *Let $\gamma : \mathbb{R} \to \mathbb{H}^2$ be a wavelike elastica parameterised by hyperbolic arclength. Then there exists a unique integral geodesic Σ of the Killing field J (c.f. Lemma 4.5). Moreover it crosses γ perpendicularly and if and only if the geodesic curvature of γ is zero.*

Proof. Let us first show existence of such an integral curve: Let $p = \gamma(s^*) \in \mathbb{H}^2$ with $K(s^*) = 0$. The goal is to show, that the hyperbolic length of J is critical at p (see Lemma 2.12). $\dot\gamma(s^*)$ is perpendicular to $J_\gamma(s^*)$ (see Lemma 4.5). Hence these two vectors are linearly independent. Since integral curves of Killing fields are parameterised proportional to arclength, we obtain $d|J(p)|_g^2(J(p)) = 0$. (4.2) yields

$$d|J(p)|_g^2(\dot\gamma(s^*)) = \frac{d}{dt}|J_\gamma(t)|_g^2\bigg|_{t=s^*} = 8K(s^*)\dot K(s^*) = 0$$

Now we prove uniqueness: Without loss of generality γ satisfies the initial value problem (4.8) (see the beginning of section 4.3) with $|K_0| > 2$. J is of the form as in (4.9) and therefore has at most two zeros on the x-axis. The bounding circles found in section 4.3 after Lemma 4.8 are integral curves of J and cross the x-axis twice at the zeros of J. Hence Σ is an upper half circle also crossing these points and is therefore unique. Sketches of the situation can be found in the Figures 6.1 and 8.1. $\square$

Remark 5.2. The uniqueness part of the proof of Lemma 5.1 also shows the following: If the extended Killing vectorfield J (see Lemma 4.5) of a wavelike solution has only one zero on the x-axis, then the geodesic Σ has to be a straight line parallel to the y-axis.

A sketch of the situation of the following lemma can be found in Figure 6.1.

Lemma 5.3 (see [24] Corollary 6.2)**.** *Let $\gamma : \mathbb{R} \to \mathbb{H}^2$ be a wavelike solution of* (4.8)*. Let Σ be the geodesic circle found in Lemma 5.1, let Σ_+ be the open domain bounded by Σ and the x-axis. Then Σ meets the x-axis at the exact same points as the bounding circles found in Lemma 4.8. Furthermore the geodesic curvature $K(s)$ is positive, iff $\gamma(s) \in \Sigma_+$ for every $s \in \mathbb{R}$. On the other hand we have for $\Sigma_- := \mathbb{H}^2 \setminus (\Sigma_+ \cup \Sigma)$, that $K(s)$ is negative, whenever $\gamma(s) \in \Sigma_-$.*

Proof. Σ being a circle and crossing the x-axis, where B_+ and B_- do, follows from the proof of Lemma 5.1. The initial values (4.8) combined with Lemma 4.7, Example 2.14 and γ being perpendicular to Σ yield the curvature conditions. $\square$

Although the following Bernstein-type result (cf. Theorem 1.6) does not concern wavelike solutions exclusively, these have to be ruled out in a more elaborate manner.

Theorem 5.4 (see [24] Theorem 1.2)**.** *Let $u : \mathbb{R} \to (0, \infty)$ be a smooth function and let $S(u)$ be the corresponding surface of revolution given by (1.3). Let $S(u)$ additionally solve the Willmore equation (1.2). Then there exists a Möbius transformation T of the upper half plane with*

$$\{(x, u(x)),\ x \in \mathbb{R}\} = \{T((x, \cosh(x)),\ x \in \mathbb{R}\}.$$

Proof. Let $\tilde{\gamma}$ be the reparameterisation of $(\cdot, u(\cdot))$ to arclength. The Lemmas 4.9 and 2.15 rule out the possibility of $\tilde{\gamma}$ being orbitlike or of constant curvature, since it would mean, that $\tilde{\gamma}$ is bounded in the direction of the x-coordinate.
Let us now denote with γ the Möbius transformed $\tilde{\gamma}$ according to Lemma 2.6 satisfying (4.8). Now we have to rule out the possibility of $\tilde{\gamma}$ being wavelike. The only way a Möbius transformation of the upper half plane can map γ in such a way, that it becomes unbounded in the x direction, is consisting of an inflection at a sphere (see Figure 5.1), such that the bounding circles B_- and B_+ of $\tilde{\gamma}$ become straight lines. These lines cross the x-axis once and therefore the geodesic Σ found in Lemma 5.1 of $\tilde{\gamma}$ has to be a straight line parallel to the y-axis (see Remark 5.2). $\tilde{\gamma}$ still crosses this line perpendicularly and infinitely often. This contradicts $\tilde{\gamma}$ being a graph. $\square$

5.2. Flow coordinates

This part is taken from [24, section 7]. For the remainder of this section, γ satisfies the initial value problem (4.8) with $|K_0| > 2$ and $z > 0$. Our first main goal is to establish coordinates of $\mathbb{H}^2$, in which the Killing field J (see Theorem 4.5) becomes one of the

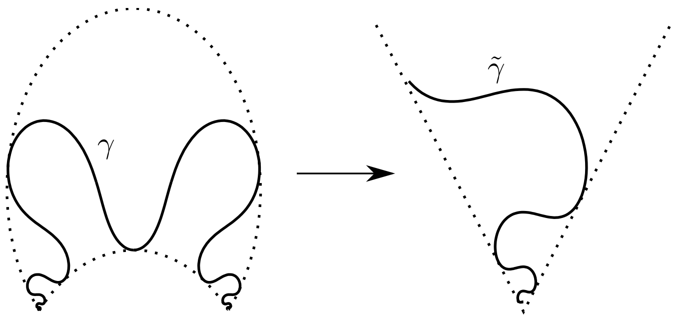

Figure 5.1.: A bounded and an unbounded wavelike elastica.

basis vectors in the tangent bundle. Langer & Singer used similar coordinates in the sphere (see [37, p. 8]) to deduce the same kind of formulae we will find later. The construction is analogous to the proof of [39, Theorem 9.22]. The idea is to follow integral curves of J, which start at the y-axis. Hence we will need the flow of J, denoted by $\Phi_J : \mathbb{H}^2 \times \mathbb{R} \to \mathbb{H}^2$.

Lemma 5.5 (see [24] Lemma 7.1)**.** *The Killing field J can be written with $a = -\frac{K_0(K_0-2)}{z}$ and $c = \frac{zK_0(K_0+2)}{2}$ as*

$$J(x,y) = a \begin{pmatrix} \frac{x^2-y^2}{2} \\ xy \end{pmatrix} + c \begin{pmatrix} 1 \\ 0 \end{pmatrix}.$$

Proof. The initial condition (4.8) and the two zeros $\pm x_s = \pm z\sqrt{\frac{K_0+2}{K_0-2}}$ of J on the x-axis (see (4.11)) combined with (4.9) yield

$$\begin{aligned} J^1(0,z) &= -a\frac{1}{2}z^2 + c = K_0^2 z \\ J^1(x_s,0) &= a\frac{1}{2}x_s^2 + c = 0. \end{aligned}$$

Please keep in mind, that (4.11) is independent of the sign of K_0. Subtracting these two equations gives us

$$\begin{aligned} &\frac{a}{2}\left(z^2 + x_s^2\right) = -K_0^2 z \\ \Rightarrow a = -&\frac{2K_0^2 z}{z^2 + z^2\frac{K_0+2}{K_0-2}} = -\frac{K_0(K_0-2)}{z}. \end{aligned}$$

By inserting this into $c = K_0^2 z + \frac{a}{2}z^2$, we obtain the desired result. $\square$

Lemma 5.6 (see [24] Lemma 7.2). *Let I_y be the integral curve of J, which starts at $(0,y) \in \mathbb{H}^2$. Let also $\kappa[I_y]$ be the geodesic curvature of I_y. Then*

$$\kappa[I_y] = 1 - \frac{2}{1 + z^2 \frac{K_0+2}{K_0-2} \frac{1}{y^2}} \in (-1,1).$$

Proof. The formulae from Lemma 5.5, combined with the Christoffel symbols (2.7) are used to calculate the covariant derivative $\nabla_J J(0,y)$:

$$\begin{aligned} \nabla_J J(0,y) &= \left(\begin{array}{c} ax(a\frac{x^2-y^2}{2} + c) + (-ay)(axy) - \frac{2}{y}(axy(a\frac{x^2-y^2}{2} + c)) \\ ay(a\frac{x^2-y^2}{2} + c) + ax(axy) + \frac{1}{y}(a\frac{x^2-y^2}{2} + c)^2 - \frac{1}{y}(axy)^2 \end{array} \right) \Bigg|_{x=0} \\ &= \left(\begin{array}{c} 0 \\ ay(c - a\frac{y^2}{2}) + \frac{1}{y}(c - a\frac{y^2}{2})^2 \end{array} \right). \end{aligned}$$

The needed unit normal vector is given by $\nu = (0,y)$. The curvature of an integral curve of a Killing field is constant (see Lemma 2.11), which yields:

$$\begin{aligned} \kappa[I_y] &= \frac{g(\nabla_J J, \nu)}{g(J,J)}(0,y) = \frac{1}{y^2}(ay^2(c - a\frac{y^2}{2}) + (c - a\frac{y^2}{2})^2)\frac{y^2}{(-a\frac{y^2}{2} + c)^2} \\ &= 1 + ay^2 \frac{1}{c - \frac{ay^2}{2}} = 1 + 2\frac{1}{\frac{2c}{ay^2} - 1}. \end{aligned}$$

Lemma 5.5 finishes the proof. □

Lemma 5.7 (see [24] Lemma 7.3). *Let $(y,t) \in \mathbb{R}^+ \times \mathbb{R}$ be arbitrary, then*

$$g_{\Phi_J((0,y),t)}\left(\frac{\partial \Phi_J}{\partial y}((0,y),t), \frac{\partial \Phi_J}{\partial t}((0,y),t)\right) = 0.$$

Proof. Please note, that

$$\frac{\partial}{\partial y}\Phi_J((0,y),t) = d\Phi_J((0,y),t)\left(\begin{array}{c} 0 \\ 1 \end{array}\right).$$

Since J is invariant under its own flow (see [39, Corollary 9.43]), we have

$$\begin{aligned} \frac{\partial}{\partial t}\Phi_J((0,y),t) &= J(\Phi_J((0,y),t)) = d\Phi_J((0,y),t)J((0,y)) \\ &= d\Phi_J((0,y),t)\left(\begin{array}{c} |J((0,y))|_g \\ 0 \end{array}\right). \end{aligned}$$

The result then follows from Φ_J being an isometry. □

The following theorem introduces the flow coordinates .

Theorem 5.8 (see [24] Theorem 7.4)**.** *The map* $F : \mathbb{R}^+ \times \mathbb{R} \to \mathbb{H}^2$ *given by* $F(y,t) = \Phi_J((0,y),t)$ *is a diffeomorphism.*

Proof. Let us first prove surjectivity of F: The Lemmas 5.6, 4.8 and 2.15 imply, that every integral curve of J is a circle crossing the x-axis at exactly two points $(0, \pm x_s)$ (cf. (4.11)). Let $p \in \mathbb{H}^2$ be arbitrary. Then the centre $(0, m_p)$ of a circle meeting p and $(0, \pm x_s)$ is given by the following geometrical construction: Connect p and $(0, x_s)$ by a straight line and find the perpendicular bisector of this line. It will cross the y-axis somewhere and this point is $(0, m_p)$. Using the north pole of this circle as a starting point for an integral curve of J yields surjectivity. This construction is explained by Figure 5.2.

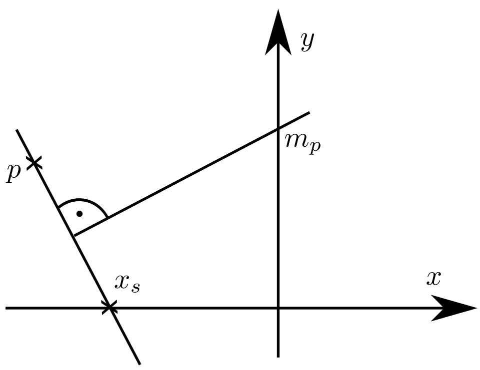

Figure 5.2.: Surjectivity of F.

Injectivity follows easily from Φ_J being a flow of a smooth vector field, with integral curves crossing the y-axis exactly once.
Finally the regularity of F and F^{-1} is due to Lemma 5.7 in combination with the inverse function theorem. $\square$

Remark 5.9 (see [24] Remark 7.5)**.** The metric tensor of $\mathbb{H}^2$ in flow coordinates (see Theorem 5.8) is given by

$$(F^*g)(y,t) = \begin{pmatrix} |\partial_y \Phi_J|_g^2 & 0 \\ 0 & |J|_g^2 \end{pmatrix}.$$

Definition 5.10 (see [24] Definition 7.6)**.** With Theorem 5.8 we find smooth functions $t_\gamma : \mathbb{H}^2 \to \mathbb{R}$ and $Y_\gamma : \mathbb{H}^2 \to \mathbb{R}^+$ satisfying

$$\forall p \in \mathbb{H}^2 : \quad F(Y_\gamma(p), t_\gamma(p)) = p.$$

Now we analyse these function and give some explicit formulae.

Lemma 5.11 (see [24] Lemma 7.7)**.** *Let a and c be given as in Lemma 5.5. Then* $\forall s \in \mathbb{R}$

$$Y_\gamma(\gamma(s)) = -\frac{|J_\gamma(s)|_g}{a} - \operatorname{sign}(K(s))\sqrt{\frac{|J_\gamma(s)|_g^2}{a^2} + 2\frac{c}{a}}.$$

Proof. $\gamma(s)$ lies on an integral curve of J. If we follow this curve back to the y-axis, we will find $Y_\gamma(\gamma(s))$. Integral curves of Killing fields are parameterised proportionally by arclength. Hence the hyperbolic length $|J_\gamma(s)|_g$ of the tangent of this curve is the same when it meets the y-axis. By Lemma 5.5 we obtain a quadratic polynomial for Y_γ, which yields two possible solutions. Lemma 5.3 then eliminates the wrong solution:

$$\begin{aligned} & |J(0, Y_\gamma(\gamma(s)))|_g^2 = \frac{(-a\frac{1}{2}Y_\gamma^2 + c)^2}{Y_\gamma^2} = |J_\gamma(s)|_g^2 \\ \overset{a<0,\ c>0}{\Rightarrow} \quad & Y_\gamma^2 + 2\frac{|J_\gamma(s)|_g}{a}Y_\gamma - 2\frac{c}{a} = 0 \\ \overset{5.3}{\Rightarrow} \quad & Y_\gamma(\gamma(s)) = -\frac{|J_\gamma(s)|_g}{a} - \operatorname{sign}(K(s))\sqrt{\frac{|J_\gamma(s)|_g^2}{a^2} + 2\frac{c}{a}}. \end{aligned}$$

$\square$

Remark 5.12 (see [24] Equation (5.4))**.** The hyperbolic length of $J(\gamma(s))$ can be expressed with Lemma 4.5, (4.8) and (4.2):

$$|J_\gamma(s)|_g^2 = K^4(s) + 4(\dot{K}(s))^2 = 4K^2(s) - 4K_0^2 + K_0^4.$$

Bryant & Griffiths already found the following formula (see [12, p. 569]). Langer & Singer used it to obtain quantitative information on the wavelength of elastica (see [37, Proposition 5.1]) and deduced it similar to our reasoning (see [37, p. 8]). For the reader's convenience we give a proof of the statement.

Lemma 5.13 (see [37] p. 8 bottom)**.** *Let γ be a wavelike solution of* (4.8) *with geodesic curvature K. Then* $\forall s \in \mathbb{R}$

$$t_\gamma(\gamma(s)) = \int_0^s \frac{K(l)^2}{K(l)^4 + 4K'(l)^2}\, dl = \int_0^s \frac{K(l)^2}{4K(l)^2 - 4K_0^2 + K_0^4}\, dl.$$

Proof. The goal is to derive $t_\gamma(\gamma(\cdot))$. We proceed by analysing the covariant gradient $\nabla t_\gamma = \sum_j g^{ij}\partial_j t_\gamma$. In flow coordinates (see Theorem 5.8) we obtain $\partial_j(t_\gamma(F(y,t))) = \delta_{2j}$, because $t_\gamma(F(y,t)) = t$. But this derivative is the second basis vector, which by construction is $J(F(y,t))$. By Remark 5.9 we get $\nabla t_\gamma = \frac{J}{|J|_g^2}$. By combining this with

Theorem 4.5 we obtain

$$\frac{d}{ds}t_\gamma(\gamma(s)) = dt_\gamma(\gamma(s))\dot{\gamma}(s) = g(\nabla t_\gamma, \dot{\gamma}) = g\left(\frac{J_\gamma}{|J_\gamma|_g^2}, \dot{\gamma}\right) = \frac{K^2}{|J_\gamma|_g^2}.$$

Remark 5.12 finally yields the desired result. □

To solve the initial value problem (4.8) for wavelike elastica, we have to find an explicit expression for the flow coordinates, which were introduced in Theorem 5.8. The idea is to parameterise an arbitrary circle proportionally to hyperbolic arclength, because these are the integral curves of J.
Let us consider a circle $C_{r,(0,m)}$ (see Example 2.14). Let it additionally cross the x-axis at $(x_s, 0)$ with $x_s > 0$ (cf. (4.11)). Let also $(0, y)$ be the north pole of $C_{r,(0,m)}$. Then the Pythagorean theorem yields

$$m = y - r, \quad m^2 + x_s^2 = r^2, \tag{5.1}$$

which in turn gives us

$$m = m(y) = y - \frac{x_s^2 + y^2}{2y}, \; r = r(y) = \frac{x_s^2 + y^2}{2y}. \tag{5.2}$$

$C_{r,(0,m)}$ can be parameterised by standard trigonometrical functions (see Example 2.14):

$$C_{r,(0,m)}(t) = \begin{pmatrix} 0 \\ m \end{pmatrix} + r \begin{pmatrix} \sin t \\ \cos t \end{pmatrix}. \tag{5.3}$$

We have $|m| < r$, because the circle meets the x-axis. This ensures $\omega = \arccos(\frac{m}{r})$ to be well defined. With this in mind we can calculate the arclength of $C_{r,(0,m)}$ by standard trigonometric functions:

$$\begin{aligned}
\int_0^t \frac{r}{m + r\cos\ell}\, d\ell = \int_0^t \frac{1}{\frac{m}{r} + \cos\ell}\, d\ell &= \int_0^t \frac{1}{\cos\omega + \cos\ell}\, d\ell \\
&= \int_0^t \frac{1}{2\cos(\frac{\omega+\ell}{2})\cos(\frac{\omega-\ell}{2})}\, d\ell \\
&= \frac{1}{2}\int_0^t \frac{\sin(\frac{\omega+\ell}{2} + \frac{\omega-\ell}{2})}{\cos(\frac{\omega+\ell}{2})\cos(\frac{\omega-\ell}{2})}\frac{1}{\sin\omega}\, d\ell \\
&= \frac{1}{2\sin\omega}\int_0^t \tan\left(\frac{\omega+\ell}{2}\right) + \tan\left(\frac{\omega-\ell}{2}\right) d\ell \\
&= -\frac{1}{\sin\omega}\left[\ln|\cos\frac{\omega+\ell}{2}| - \ln|\cos\frac{\omega-\ell}{2}|\right]_0^t
\end{aligned}$$

$$= -\frac{1}{\sin\omega}\ln\left|\frac{\cos\frac{\omega+t}{2}}{\cos\frac{\omega-t}{2}}\right|.$$

Since $0 < \cos(\omega)+\cos(\ell) = 2\cos\left(\frac{\omega+\ell}{2}\right)\cos\left(\frac{\omega-\ell}{2}\right)$ (it is the second coordinate of $C_{r,(0,m)}$), we can leave out the absolute values and obtain

$$\int_0^t \frac{r}{m+r\cos\ell}\,d\ell = -\frac{1}{\sin\omega}\ln\left(\frac{\cos\frac{\omega+t}{2}}{\cos\frac{\omega-t}{2}}\right). \tag{5.4}$$

Let $s = s(t) = \int_0^t \frac{r}{m+r\cos\ell}\,d\ell$ the arclength of the circle. Rearranging the equation yields

$$\begin{aligned}
&s = -\frac{1}{\sin\omega}\ln\left(\frac{\cos\frac{\omega+t}{2}}{\cos\frac{\omega-t}{2}}\right)\\
\Leftrightarrow\ &\exp(-s\sin\omega) = \frac{\cos\frac{\omega+t}{2}}{\cos\frac{\omega-t}{2}} = \frac{\cos\frac{\omega}{2}\cos\frac{t}{2}-\sin\frac{\omega}{2}\sin\frac{t}{2}}{\cos\frac{\omega}{2}\cos\frac{t}{2}+\sin\frac{\omega}{2}\sin\frac{t}{2}}\\
\Leftrightarrow\ &(1-\exp(-s\sin\omega))\cos\frac{\omega}{2}\cos\frac{t}{2} = (1+\exp(-s\sin\omega))\sin\frac{\omega}{2}\sin\frac{t}{2}\\
\Leftrightarrow\ &t = 2\arctan\left(\frac{1-\exp(-s\sin\omega)}{1+\exp(-s\sin\omega)}\cot\frac{\omega}{2}\right),
\end{aligned}$$

which defines a new function:

$$\phi(s) = 2\arctan\left(\frac{1-\exp(-s\sin\omega)}{1+\exp(-s\sin\omega)}\cot\frac{\omega}{2}\right). \tag{5.5}$$

If we collect all these results, we obtain

$$F(y,t) = C_{r(y),(0,m(y))}\left(\phi(|J(0,y)|_g t)\right). \tag{5.6}$$

5.3. A closer analysis of the shape of a wavelike elastica

This section is the second part of [25, Section 6]. Here we like to give some additional properties of wavelike elastica, which will prepare the proof of Theorem 1.3. At first we show, that a non-projectable solution of (1.4), which was constructed in Theorem 1.1, has to be wavelike. Then we give a few lemmas, which give a closer description of the behaviour of a wavelike elastica.

The following lemma will help us in finding a zero in the curvature of a solution.

Lemma 5.14 (see [25] Lemma 6.8)**.** *Let $-\infty \le a < b \le \infty$ and $c : (a,b) \to \mathbb{H}^2$ be regular and parameterised by hyperbolic arclength with curvature $\kappa[c]$. Additionally let*

$a < t_1 \leq t_2 < b$ with

$$\dot{c}^1(t_1) = \dot{c}^1(t_2) = 0,\ \dot{c}^2(t_1) \cdot \dot{c}^2(t_2) > 0,\ \ddot{c}^1(t_1) \cdot \ddot{c}^1(t_2) \leq 0.$$

Then there exists a $t_* \in [t_1, t_2]$ satisfying $\kappa[c](t_*) = 0$.

Proof. The Frenet equation (2.13) yields

$$\begin{aligned}\ddot{c}^1(t_1) &= -\kappa(t_1)\dot{c}^2(t_1)\\ \ddot{c}^1(t_2) &= -\kappa(t_2)\dot{c}^2(t_2).\end{aligned}$$

By multiplying both equations we obtain

$$0 \geq \ddot{c}^1(t_1)\ddot{c}^1(t_2) = \kappa(t_1)\kappa(t_2)\dot{c}^2(t_1)\dot{c}^2(t_2).$$

Then the intermediate value theorem gives us the desired zero. □

The next lemma shows, that a non-projectable solution of (1.4) has to be wavelike.

Lemma 5.15 (see [25] Lemma 6.9)**.** *Let $c : [0, 1] \to \mathbb{H}^2$ be a solution of (1.4) with $W_h(c) < 8$ and let $0 < t^* < 1$ satisfy $\dot{c}^1(t^*) = 0$. Then c is wavelike (cf. Lemma 4.4) and the geodesic from Lemma 5.1 is an upper half circle centered on the x-axis.*

Proof. First we will show the existence of a zero in the curvature. Due to the discussion in Section 4.1 the solution then has to be wavelike. For this we need to distinguish three cases:

i) $\ddot{c}^1(t^*) = 0$: Equation (2.10) yields a zero in the geodesic curvature.

ii) $\ddot{c}^1(t^*) < 0$: In this case c^1 has a local maximum in t^*. Hence there exists an $\varepsilon > 0$, such that $\forall t \in (t^*, t^* + \varepsilon) : \dot{c}^1(t) < 0$. Then $\dot{c}^1(1) > 0$ yields the existence of a $t_* \in (t^*, 1)$ in which c^1 has a local minimum. Now we can distinguish two cases (since c is regular, we have $\dot{c}^2(t_*) \neq 0$ and $\dot{c}^2(t^*) \neq 0$):

   a) $\dot{c}^2(t^*) \cdot \dot{c}^2(t_*) < 0$: Lemma 3.2 gives us $W_h(c) \geq 8$, which is a contradiction.

   b) $\dot{c}^2(t^*) \cdot \dot{c}^2(t_*) > 0$: Reparameterising c by hyperbolic arclength, yields with Lemma 5.14 a zero of the geodesic curvature in $[t^*, t_*]$.

iii) $\ddot{c}^1(t^*) > 0$: This case can be treated as case ii): c^1 has a local minimum in t^*. As seen above we can find a local maximum in $(0, t^*)$. With the same distinction in subcases we also obtain a zero in the curvature.

This shows, that the solution c has to be wavelike. Let us turn to the shape of the geodesic Σ given by Lemma 5.1. Let t_0 denote our zero of the geodesic curvature $\kappa[c]$. We proceed by contradiction and assume Σ to be a parallel line to the y-axis. Since Σ is perpendicular to $\dot{c}(t)$, iff $\kappa[c](t) = 0$, Equation (2.10) yields $\ddot{c}^1(t^*) \neq 0$. The existence proof for the zero in the curvature now yields a $t_* \in (0,1) \setminus \{t^*\}$ with $\dot{c}^1(t_*) = 0$. The proof also shows, that we can assume without loss of generality $t^* < t_0 < t_*$. The perpendicularity of Σ also gives us $\dot{c}^2(t_0) = 0$. Let us now put everything together and assume for a moment that $\dot{c}^2(t^*), \dot{c}^2(t_*) > 0$. Equation (2.12) yields

$$\begin{aligned}
W_h(c) &\geq W_h(c)\big|_{[0,t^*]} + W_h(c)\big|_{[t_0,t_*]} \\
&= \frac{2}{\pi} W_e(S(c))\big|_{[0,t^*]} + \frac{2}{\pi} W_e(S(c))\big|_{[t_0,t_*]} \\
&\quad + 4\left[\frac{\dot{c}^2}{\sqrt{(\dot{c}^1)^2 + (\dot{c}^2)^2}}\right]_0^{t^*} + 4\left[\frac{\dot{c}^2}{\sqrt{(\dot{c}^1)^2 + (\dot{c}^2)^2}}\right]_{t_0}^{t_*} \\
&\geq 4\left[\frac{\dot{c}^2}{\sqrt{(\dot{c}^1)^2 + (\dot{c}^2)^2}}\right]_0^{t^*} + 4\left[\frac{\dot{c}^2}{\sqrt{(\dot{c}^1)^2 + (\dot{c}^2)^2}}\right]_{t_0}^{t_*} = 8.
\end{aligned}$$

This is a contradiction to $W_h(c) < 8$. So Σ has to be a half circle centered on the x-axis.
The other cases can be treated analogously. □

Now we collect a few lemmas, which will help us in proving Theorem 1.3 by giving us an idea of the behaviour of a wavelike elastica. We start with an estimate for the elastic energy in terms of the period of the curvature. It will also be needed to show Theorem 1.5.

Lemma 5.16 (see [25] Lemma 6.4)**.** *Let $K \in C^2(\mathbb{R})$ be wavelike with parameters $K_0 > 2$, k and r given as in Lemma 4.4. Additionally let $n \in \mathbb{N}$ be arbitrary. Then the following estimate holds*

$$\int_0^{n\frac{1}{r}F_k\left(\frac{\pi}{2}\right)} (K(s))^2\, ds \geq n\pi.$$

One may observe that $\frac{1}{r}F_k(\frac{\pi}{2})$ is a $\frac{1}{4}$-period of $K(\cdot)$.

Proof. By using $nF_k\left(\frac{\pi}{2}\right) = F_k\left(n\frac{\pi}{2}\right)$, we find

$$\begin{aligned}
\int_0^{\frac{1}{r}nF_k\left(\frac{\pi}{2}\right)} (K(s))^2\, ds &= K_0^2 \int_0^{\frac{1}{r}F_k\left(n\frac{\pi}{2}\right)} \operatorname{cn}^2(rs,k)\, ds \\
&= K_0^2 \int_0^{\frac{1}{r}F_k\left(n\frac{\pi}{2}\right)} \cos^2(F_k^{-1}(rs))\, ds \\
&= K_0^2 \int_0^{n\frac{\pi}{2}} \frac{1}{r}\cos^2(x)\frac{1}{\sqrt{1-k^2\sin^2(x)}}\, dx
\end{aligned}$$

$$\geq \frac{K_0^2}{\sqrt{\frac{1}{2}K_0^2 - 1}} \int_0^{n\frac{\pi}{2}} \cos^2(x)\, dx$$
$$= \frac{K_0^2}{\sqrt{\frac{1}{2}K_0^2 - 1}} n\frac{\pi}{4}.$$

Now we need to estimate the prefactor:

$$(K_0^2 - 4)^2 \geq 0$$
$$\Rightarrow K_0^4 \geq 8K_0^2 - 16 = 16\left(\frac{K_0^2}{2} - 1\right)$$
$$\Rightarrow \frac{K_0^2}{\sqrt{\frac{K_0^2}{2} - 1}} \geq 4.$$

□

The next lemma helps us in determining locally the sign of the geodesic curvature of a wavelike elastica. Langer & Singer already observed this in [37, Proposition 5.1] and they even gave a more precise statement. For the readers convenience we will point out how to obtain the proof by arguments, which are scattered throughout the Sections 5.1 and 5.2. Figure 5.3 explains the geometric meaning of the next lemma.

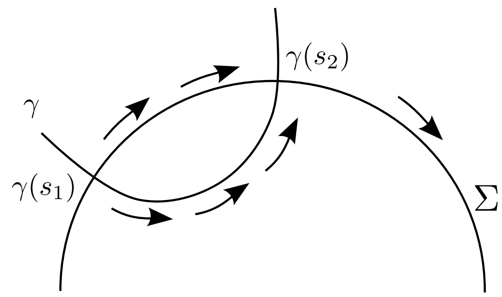

Figure 5.3.: Constant hyperbolic increment on the geodesic Σ.

Lemma 5.17 (see [37], Proposition 5.2 (iii) and [25] Lemma 6.10)**.** *Let $\gamma : \mathbb{R} \to \mathbb{H}^2$ be a wavelike (see Lemma 4.4) elastica parameterised by hyperbolic arclength with geodesic curvature K. Let J be the Killing vector field given by Theorem 4.5 and let Φ_J be the corresponding flow of J. Let Σ denote the geodesic given by Lemma 5.1 and let $p \in \Sigma$. Let further be $s_1 < s_2$, such that $K(s_1) = K(s_2) = 0$ and $|s_1 - s_2|$ is minimal. Then* *there exist parameters* $t_1 < t_2$ *with* $\Phi_J(p, t_1) = \gamma(s_1)$ *and* $\Phi_J(p, t_2) = \gamma(s_2)$*. Moreover, the hyperbolic distance of* $\gamma(s_1)$ *and* $\gamma(s_2)$ *is the same for any such pair of points. This means, if there exists another pair* $\tilde{s}_1 < \tilde{s}_2$ *satisfying the same assumptions, we have*

$$\mathrm{dist}_g(\gamma(s_1), \gamma(s_2)) = \mathrm{dist}_g(\gamma(\tilde{s}_1), \gamma(\tilde{s}_2)) > 0.$$

Proof. Theorem 5.8 in combination with Lemma 2.6 and (4.8) shows the existence of the parameters t_1, t_2.
Since J is a Killing vector field, every integral curve of J is parameterised proportionally by hyperbolic arclength: Let $t \in \mathbb{R}$, then

$$g_{\Phi(p,t)}\left(\frac{\partial}{\partial t}\Phi(p,t), \frac{\partial}{\partial t}\Phi(p,t)\right) = g_{\Phi(p,t)}(J(\Phi(p,t)), J(\Phi(p,t))) = g_p(J(p), J(p)).$$

Also every integral curve possesses constant geodesic curvature (see Theorem 2.11). Hence they have to be euclidean circles (see Lemma 2.15). Since K is periodic, Lemma 5.13 shows, that the above mentioned distance of $\gamma(s_1)$ and $\gamma(s_2)$ is constant. □

The next lemma will help us spot extrema of the geodesic curvature.

Lemma 5.18 (see [25] Lemma 6.11)**.** *Let* $\gamma : \mathbb{R} \to \mathbb{H}^2$ *be a wavelike elastica (see Lemma 4.4) parameterised by hyperbolic arclength. The corresponding Killing vector field will be denoted by* J *respectively* J_γ *(see Theorem 4.5). Let* K *denote the geodesic curvature of* γ*. Furthermore let* $s_0 \in \mathbb{R}$ *with* $K(s_0) = 0$ *and* $s_1 > s_0$ *minimal, such that* $|K(s_1)|$ *is maximal. Finally let* I *be an arbitrary integral curve of* J*. Then the number of elements in* $\gamma([s_0, s_1]) \cap I$ *is at most* 1*.*

Proof. Equation (4.2) (also see Remark 5.12) yields

$$g(J_\gamma, J_\gamma) = 4K^2 + const.$$

Since K^2 is strictly increasing on $[s_0, s_1]$, $g(J_\gamma, J_\gamma)$ has to be strictly monotone as well. Theorem 5.8 and Lemma 5.11 give us a one to one correspondence between the hyperbolic length of J_γ and the set of integral curves of J, as long as K does not change sign. Thus the lemma follows. □

By the next lemma a wavelike solution has to be injective.

Lemma 5.19 (see [25] Lemma 6.12)**.** *As before let* $\gamma : \mathbb{R} \to \mathbb{H}^2$ *be a wavelike elastica (cf. Lemma 4.4) parameterised by hyperbolic arclength and* J *the corresponding Killing vector field (cf. Theorem 4.5). We set* $J^\perp := (-J^2, J^1)$ *as the perpendicular vector field of* J*. Let now* $I \subset \mathbb{H}^2$ *be an integral curve of* $J^\perp$ *defined on its maximal interval of existence. Then* I *intersects* γ *exactly once.*

Proof. First let us fixate the notation: K is the geodesic curvature of γ, Φ_J the flow of J and J_γ the local variant of J (see Theorem 4.5). Lemma 2.6 and Lemma 5.5 (see also the discussion at the beginning of Section 4.3) allow us without loss of generality to write J as

$$J(x,y) = a\begin{pmatrix} \frac{x^2-y^2}{2} \\ xy \end{pmatrix} + c\begin{pmatrix} 1 \\ 0 \end{pmatrix},$$

with $a < 0$ and $c > 0$. Since Φ_J is an isometry and hence preserves orthogonality, we have that for all $t \in \mathbb{R}$ the curve $\Phi_J(I,t)$ is again an integral curve of $J^\perp$. Furthermore Theorem 5.8 gives us that $\Phi_J((0,\cdot),\cdot)$ is a diffeomorphism of $\mathbb{H}^2$ with $\Phi_J(\{(0,y), y > 0\}, \mathbb{R}) = \mathbb{H}^2$. If we fixate a $p \in I$, then there exists a $t \in \mathbb{R}$, such that $\Phi_J(p,t) \in \{(0,y), y > 0\}$. We have achieved, that $\Phi_J(I,t) \subset \{(0,y), y > 0\}$, because $\Phi_J(I,t)$ is an integral curve of $J^\perp$. If we assume the existence of a $q \in \{(0,y), y > 0\}$ with $q \notin \Phi_J(I,t)$, we could further extend $\Phi_J(I,t)$ as an integral curve to the whole of $\{(0,y), y > 0\}$. This would contradict I being defined on its maximal interval of existence. Hence we can assume without loss of generality that

$$I = \{(0,y),\ y > 0\}.$$

Multiplying $\dot\gamma$ and J_γ yields

$$g(J_\gamma, \dot\gamma) = (K(s))^2 \geq 0. \tag{5.7}$$

Now we proceed by contradiction and assume that $s_1 < s_2 \in \mathbb{R}$ exist and satisfy

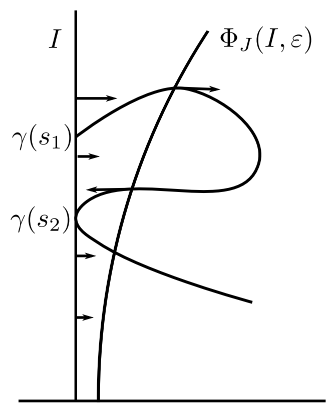

Figure 5.4.: If I meets γ at least twice, then there exists a sign change in $g(J_\gamma, \dot\gamma)$.

$\gamma(s_1), \gamma(s_2) \in I$. For every $y > 0$ the Killing vector field satisfies $J^1(0,y) > 0$ and $J^2(0,y) = 0$. In combination with (5.7) and Lemma 5.1 this yields without loss of generality $K(s_2) = 0$. Then $K(s_1) \neq 0$. Otherwise $\gamma(s_1)$ and $\gamma(s_2)$ would both lie on the unique geodesic Σ (see Lemma 5.1). Since Σ is an upper half circle (see e.g. Lemma 5.3), this would be a contradiction. Now we can find an $\varepsilon \neq 0$ such that $\Phi_J(I, \varepsilon)$ meets γ at least twice with different signs for $g(J_\gamma, \dot{\gamma})$. This contradicts (5.7). Figure 5.4 explains the situation. $\square$

Remark 5.20 (see [25] Remark 6.14)**.** Lemma 5.19 and Lemma 5.15 show, that our energy minimising solution found in Theorem 1.1 does not intersect itself. This completes the proof of Theorem 1.1.

6. A set of solutions with large difference in the boundary data

This chapter gives a partial answer to the question of existence of solutions for (1.4), if $|\alpha_- - \alpha_+|$ is large. This idea has not yet been published.

6.1. Finding a set of solutions

The following solutions will be constructed via a shooting method, which is similar to the way non-uniqueness for (1.8) is established in Section 8.2.

Theorem 6.1. *There exists a continuously differentiable curve $\alpha : (-\infty, -2) \to (0, \infty) \times (0, \infty)$, such that for every $K_0 \in (-\infty, -2)$ there exists a smooth $c_{K_0} : [0, 1] \to \mathbb{H}^2$ satisfying*

$$\begin{cases} \Delta_{S(c_{K_0})} H + 2H(H^2 - G) = 0, \quad \text{in } (0,1) \\ c_{K_0}(0) = (-1, \alpha^1(K_0)),\ c_{K_0}(1) = (1, \alpha^2(K_0)),\ \dot{c}^2_{K_0}(0) = \dot{c}^2_{K_0}(1) = 0, \\ \dot{c}^1_{K_0}(0), \dot{c}^1_{K_0}(1) > 0. \end{cases}$$

Furthermore we have

$$\lim_{K_0 \nearrow -2} |\alpha^1(K_0) - \alpha^2(K_0)| = \infty.$$

$K_0 \in (-\infty, -2)$ is the minimal geodesic curvature of c_{K_0} w.r.t. the hyperbolic metric of $\mathbb{H}^2$. The Willmore energy satisfies

$$\liminf_{K_0 \nearrow -2} W_e(S(c_{K_0})) \geq 4\pi.$$

Proof. We will employ a shooting method, which was already used in [24], but with opposite sign on K_0 (see also Section 8.2). Therefore let γ be the solution of the initial value problem (4.8) with $z = 1$ and initial curvature $K_0 < -2$. Hence γ is wavelike with curvature K given as in Lemma 4.4 (please note, that if K is a solution of (4.1), then $-K$ is as well). Let J be the Killing vector field from Lemma 4.5. The Lemmas 5.1, 5.3, 4.8 and Equation (4.11) yield a sketch of γ in Figure 6.1:

Claim 1. *There exists an $s : (-\infty, -2) \to (0, \infty)$, such that*

$$\dot{\gamma}^2(s(K_0)) = 0, \quad \dot{\gamma}^1(s(K_0)) = \gamma^2(s(K_0)), \quad K(s(K_0)) > 0.$$

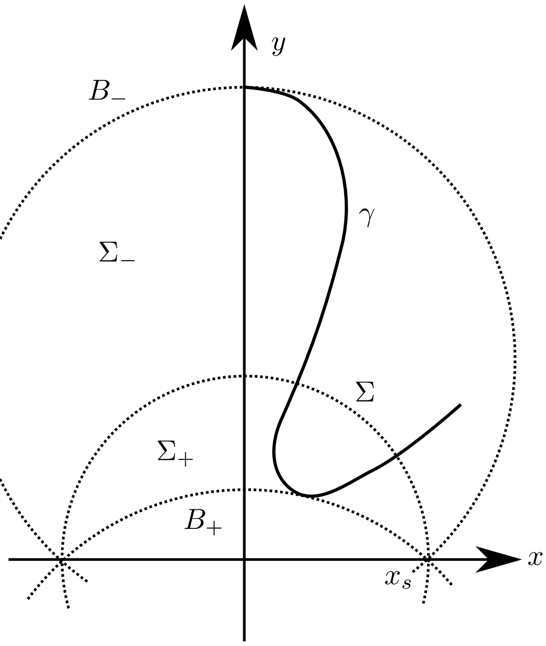

Figure 6.1.: Sketch of wavelike elastica γ with initial curvature $K_0 < -2$.

Furthermore $s(K_0)$ is a local minimum of γ^2.

Proof. Let $s_0 > 0$ be minimal, such that $K(s_0)$ is a maximum. Lemma 5.19 yields $\gamma^1(s_0) > 0$ and hence (4.7) and Lemma 4.8 give us

$$\dot{\gamma}^1(s_0) > 0, \quad \dot{\gamma}^2(s_0) < 0.$$

Let $s_1 > s_0$ minimal with $K(s_1) = 0$. With the Lemmas 5.1 and 5.3 we have

$$\dot{\gamma}^1(s_1) > 0, \quad \dot{\gamma}^2(s_1) > 0.$$

Hence s_{min}, defined by $\gamma^2(s_{min}) = \min_{s\in[s_0,s_1]} \gamma^2(s)$, satisfies

$$s_{min} \in (s_0, s_1).$$

Since it is a minimum, we have $\dot{\gamma}^2(s_{min}) = 0$. We set $s(K_0) := s_{min}$. Since γ is parameterised by hyperbolic arclength (cf. (3.1)), we have $|\dot{\gamma}^1(s(K_0))| = |\gamma^2(s(K_0))|$. Let us assume $\dot{\gamma}^1(s(K_0)) < 0$. Then (2.10) yields $K(s(K_0)) < 0$, which contradicts $\gamma(s(K_0)) \in \Sigma_+$ (see Lemma 5.3). $\square$

Claim 2. *The map $s : (-\infty, -2) \to (0, \infty)$ found in Claim 1 is continuously differentiable.*

Proof. We will apply the inverse function theorem to gain the desired regularity. We proceed by contradiction and assume

$$\ddot{\gamma}^2(s(K_0)) = 0.$$

The Frenet equation (2.13) yields

$$\ddot{\gamma}^1(s(K_0)) = 0. \tag{6.1}$$

The other Frenet equation (2.14) gives us

$$\dddot{\gamma}^2(s(K_0)) = \gamma^2(s(K_0))(K(s(K_0)) - 1), \tag{6.2}$$

since γ is parameterised by hyperbolic arclength (see also Claim 1). This yields $K(s(K_0)) = 1$. Differentiating (4.6) and (4.7) yields with $b = 0$ (This computation was already carried out in [26, Equation (3.8)] and will also be needed in Section 9.1)

$$\begin{aligned} 2K\dot{K}\begin{pmatrix} \dot{\gamma}^1 \\ \dot{\gamma}^2 \end{pmatrix} &+ K^2\begin{pmatrix} \dddot{\gamma}^1 \\ \dddot{\gamma}^2 \end{pmatrix} + 2\ddot{K}\begin{pmatrix} -\dot{\gamma}^2 \\ \dot{\gamma}^1 \end{pmatrix} + 2\dot{K}\begin{pmatrix} -\ddot{\gamma}^2 \\ \ddot{\gamma}^1 \end{pmatrix} \\ &= a\begin{pmatrix} \gamma^1\dot{\gamma}^1 - \gamma^2\dot{\gamma}^2 \\ \dot{\gamma}^1\gamma^2 + \gamma^1\dot{\gamma}^2 \end{pmatrix}. \end{aligned} \tag{6.3}$$

With the second coordinate of (6.3) combined with (4.1) and Lemma 5.5 we obtain

$$\begin{aligned} 0 = K^2(s(K_0))\dddot{\gamma}^2(s(K_0)) &= a(\gamma^2(s(K_0)))^2 - 2\ddot{K}(s(K_0))\gamma^2(s(K_0)) \\ &= \gamma^2(s(K_0))(-K_0(K_0 - 2)\gamma^2(s(K_0)) - 2K(s(K_0)) + (K(s(K_0)))^3) \\ &= \gamma^2(s(K_0))(-K_0(K_0 - 2)\gamma^2(s(K_0)) - 1). \end{aligned}$$

Since $K_0 < -2$, we have $-1 > 0$, a contradiction. ☐

Claim 3. *The map $s : (-\infty, -2) \to (0, \infty)$ from Claim 1 satisfies*

$$\lim_{K_0 \nearrow -2} \left| \frac{1}{\gamma^1(s(K_0))} - \frac{\gamma^2(s(K_0))}{\gamma^1(s(K_0))} \right| = \infty.$$

Proof. Since $K(s(K_0)) > 0$, $\gamma(s(K_0)) \in \Sigma_+$ (see Lemma 5.3). On the other hand the crossing point x_s (see (4.11)) of the geodesic Σ with the x-axis satisfies (please note, that the derivation of x_s is independent of the sign of K_0)

$$\lim_{K_0 \nearrow -2} x_s = \lim_{K_0 \nearrow -2} \sqrt{\frac{K_0 + 2}{K_0 - 2}} = 0.$$

This implies

$$\lim_{K_0 \nearrow -2} \gamma(s(K_0)) = 0,$$

which yields the claim. □

If we translate $\gamma\big|_{[0,s(K_0)]}$ to the left by $\frac{\gamma^1(s(K_0))}{2}$ and dilate it by $\frac{2}{\gamma^1(s(K_0))}$, the resulting curve satisfies (1.4) with

$$\alpha^1(K_0) := \alpha_- = \frac{2}{\gamma^1(s(K_0))}, \quad \alpha^2(K_0) := \alpha_+ = 2\frac{\gamma^2(s(K_0))}{\gamma^1(s(K_0))}.$$

Now only the asymptotic of the energy remains to be shown, for which the following claim will be useful.

Claim 4. *With the notation of Lemma 4.4 we have*

$$\lim_{K_0 \nearrow -2} \int_0^{\frac{1}{r}F_k\left(\frac{\pi}{2}\right)} (K(s))^2 \, ds = 4.$$

Proof. With $r = \sqrt{-1 + \frac{1}{2}K_0^2}$ and $k = \frac{K_0}{2r}$ we have

$$\begin{aligned}
\int_0^{\frac{1}{r}F_k\left(\frac{\pi}{2}\right)} (K(s))^2 \, ds &= K_0^2 \int_0^{\frac{1}{r}F_k\left(\frac{\pi}{2}\right)} \operatorname{cn}^2(rs, k) \, ds \\
&= K_0^2 \int_0^{\frac{1}{r}F_k\left(\frac{\pi}{2}\right)} \cos^2(F_k^{-1}(rs)) \, ds \\
&= K_0^2 \int_0^{\frac{\pi}{2}} \frac{1}{r} \cos^2(x) \frac{1}{\sqrt{1 - k^2 \sin^2(x)}} \, dx \\
&= \frac{K_0^2}{\sqrt{\frac{1}{2}K_0^2 - 1}} \int_0^{\frac{\pi}{2}} \frac{\cos^2(x)}{\sqrt{1 - \frac{K_0^2}{2K_0^2 - 4} \sin^2(x)}} \, dx. \\
&= \frac{K_0^2}{\sqrt{\frac{1}{2}K_0^2 - 1}} \int_0^{\frac{\pi}{2}} \frac{\cos^2(x)}{\sqrt{\frac{2K_0^2 - 4 - K_0^2 \sin^2(x)}{2K_0^2 - 4}}} \, dx
\end{aligned}$$

$$= \frac{K_0^2}{\sqrt{\frac{1}{2}K_0^2 - 1}} \int_0^{\frac{\pi}{2}} \sqrt{2K_0^2 - 4} \frac{\cos^2(x)}{\sqrt{2K_0^2 - 4 - K_0^2 + K_0^2 \cos^2(x)}}\, dx$$
$$= 2K_0^2 \int_0^{\frac{\pi}{2}} \frac{\cos^2(x)}{\sqrt{K_0^2 - 4 + K_0^2 \cos^2(x)}}\, dx.$$

Since $K_0^2 - 4 \geq 0$, the integrand satisfies

$$\left| \frac{\cos^2(x)}{\sqrt{K_0^2 - 4 + K_0^2 \cos^2(x)}} \right| \leq \frac{\cos^2(x)}{|K_0 \cos(x)|}$$
$$\leq \frac{1}{2}.$$

The dominated convergence theorem yields

$$\int_0^{\frac{1}{r}F_k\left(\frac{\pi}{2}\right)} (K(s))^2\, ds = 2K_0^2 \int_0^{\frac{\pi}{2}} \frac{\cos^2(x)}{\sqrt{K_0^2 - 4 + K_0^2 \cos^2(x)}}\, dx$$
$$\to 8 \int_0^{\frac{\pi}{2}} \frac{\cos^2(x)}{2|\cos(x)|}\, dx = 4.$$

□

The geodesic curvature K has at least one minimum in $s = 0$ and one maximum in $s = 2\frac{1}{r}F_k\left(\frac{\pi}{2}\right)$ (see again Lemma 4.4). Claim 4, the symmetry properties of K and (2.12) yield the desired result. □

Remark 6.2. Experiments in matlab$^{\text{TM}}$ (see Figure 6.2) conducted with the help of (5.6) and the Lemmas 5.11 and 5.13, give rise to the conjecture, that α_+ stays bounded, as K_0 approaches -2.

6.2. Asymptotic behaviour

In this section we study the behaviour of the solution γ, constructed in the proof of Theorem 6.1, at the boundary, when K_0 converges to -2. This question is similar to [29], in which the answer was gained by comparison functions. Here we use a different approach and employ the continuity for initial value problems in terms of their initial data. Let us start with the left boundary $\gamma(0)$:
Since solutions of an initial value problem are continous in their initial data, γ tends

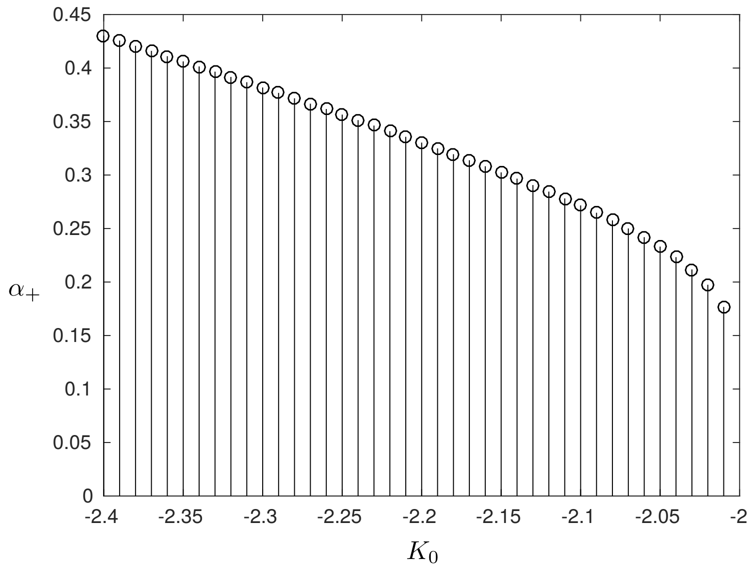

Figure 6.2.: α_+ seems to stay bounded, if K_0 is close to -2.

at $s = 0$ locally uniformly to the solution of the following problem (cf. (4.8))

$$\begin{cases} \nabla_{\dot\gamma_0}\dot\gamma_0 = \kappa[\gamma_0]N,\ \nabla_{\dot\gamma_0}N = -\kappa[\gamma_0]\dot\gamma_0, & \ddot\kappa[\gamma_0] = \kappa[\gamma_0] - \frac{1}{2}\kappa[\gamma_0]^3 \\ \gamma_0(0) = (0,1)\,,\ \dot\gamma_0(0) = (1,0)\,, & \kappa[\gamma_0](0) = -2,\ \dot\kappa[\gamma_0](0) = 0. \end{cases}$$

The solution is given by Lemma 4.11 and illustrated by Figure 6.3.

Let us study the other boundary $\gamma(s(K_0))$. Our reasoning will include formulae, which have already been used in [26, Section 3.2] by the present author (see also Section 9.1):
As in the other case we calculate the asymptotic of $K(s(K_0))$ and $\dot K(s(K_0))$. Let us start with $K(s(K_0))$:
Since $\gamma^2(s(K_0))$ is a local minimum of γ^2 (see Claim 1), (6.2) yields

$$K(s(K_0)) \geq 1. \tag{6.4}$$

By inserting (6.1) and (6.2) into the second row of (6.3) we obtain

$$\gamma^2(s(K_0))K^2(s(K_0))(K(s(K_0)) - 1) + 2\gamma^2(s(K_0))\ddot K(s(K_0)) = a(\gamma^2(s(K_0)))^2,$$

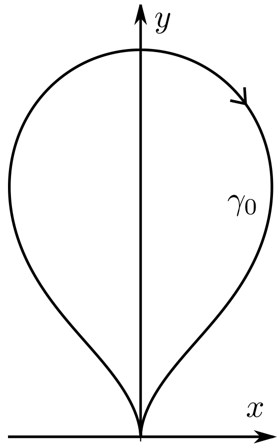

Figure 6.3.: A catenoid reflected at a sphere.

which can be further simplified by (4.1) to

$$K(s(K_0))(2 - K(s(K_0)) = a\gamma^2(s(K_0)). \tag{6.5}$$

Lemma 5.5 yields $\lim_{K_0 \nearrow -2} a = -8$, which in combination with the proof of Claim 3 gives us

$$\lim_{K_0 \nearrow -2} K(s(K_0)) = 2. \tag{6.6}$$

Let us now turn to $\dot{K}(s(K_0))$:
(4.7) yields with $b = 0$ and Claim 1

$$2\dot{K}(s(K_0)) = a\gamma^1(s(K_0)). \tag{6.7}$$

Therefore we have

$$\lim_{K_0 \nearrow -2} \dot{K}(s(K_0)) = 0. \tag{6.8}$$

We now dilate and translate γ in such a way, that $\gamma^1(s(K_0)) = 0$ and $\gamma^2(s(K_0)) = 1$. Since (4.1) is autonomous we can assume without loss of generality, that $s(K_0) = 0$. As with the other boundary γ tends locally uniformly around $s = 0$ to the solution of the following initial value problem:

$$\begin{cases} \nabla_{\dot{\gamma}_0}\dot{\gamma}_0 = \kappa[\gamma_0]N,\ \nabla_{\dot{\gamma}_0}N = -\kappa[\gamma_0]\dot{\gamma}_0, & \ddot{\kappa}[\gamma_0] = \kappa[\gamma_0] - \frac{1}{2}\kappa[\gamma_0]^3 \\ \gamma_0(0) = (0,1)\,,\ \dot{\gamma}_0(0) = (1,0)\,, & \kappa[\gamma_0](0) = 2,\ \dot{\kappa}[\gamma_0](0) = 0, \end{cases}$$

which is solved by Lemma 4.10 to be a catenoid.

7. Projectable solutions

This chapter is dedicated to Theorem 1.3. It is proven in Section 7.1 and the discussion in Section 7.2 shows, that a similar statement cannot be expected for every boundary value. These two sections are taken from [25, Section 7] and [25, Appendix A].

7.1. Existence of projectable solutions under smallness conditions

This section comes from [25, Section 7]. In it we will prove, that the solution obtained in Theorem 1.1 is a graph $(\cdot, u(\cdot))$, if we assume the smallness condition 1.2. It will be an important argument to compare the energy of our solution to special comparison functions, which we calculate now:

Example 7.1 (see [25] Example 7.1)**.** *The euclidean Willmore energy of a revolved upper half circle centered on the x-axis is*

$$W_e(S(p_{x_0,r})) = 4\pi$$

for all $x_0 \in \mathbb{R}$ and $r > 0$.

Proof. Since an upper half circle is a geodesic with respect to the hyperbolic metric, the elastic energy is zero. (2.12) yields the desired result, because this circle meets the x-axis perpendicularly. □

Example 7.2 (see [25] Example 7.2)**.** *The hyperbolic elastic energy of a catenoid c_{cat} is*

$$W_h(c_{cat}) = 8.$$

Proof. The geodesic curvature of c_{cat} parameterised by hyperbolic arclength can be expressed as (see Lemma 4.10)

$$K(s) = \frac{2}{\cosh(s)}.$$

Integration yields

$$W_h(c_{cat}) = \int_{-\infty}^{\infty} \left(\frac{2}{\cosh(s)} \right)^2 ds = 4\big[\tanh(x)\big]_{-\infty}^{\infty} = 8.$$

□

To get a grasp of the local elastic energy of a curve, we need the following lemma, which is basically the same as Lemma 3.2:

Lemma 7.3 (see [25] Lemma 7.3)**.** *Let $c : [0,1] \to \mathbb{H}^2$ be a smooth regular curve, such that there exists a $t^* \in (0,1)$ with $\dot{c}^1(t^*) = 0$. c should also satisfy $\dot{c}^2(0) = \dot{c}^2(1) = 0$. Then its hyperbolic elastic energy satisfies*

$$W_h(c) \geq 4.$$

Proof. Without loss of generality we can assume that $\dot{c}^2(t^*) > 0$. Then we have with the help of (2.12) that

$$\begin{aligned} W_h(c) &= W_h(c)\big|_{[0,t^*]} + W_h(c)\big|_{[t^*,1]} \\ &\geq \frac{2}{\pi} W_e(S(c))\big|_{[0,t^*]} + 4\left[\frac{\dot{c}^2}{\sqrt{(\dot{c}^1)^2 + (\dot{c}^2)^2}}\right]_0^{t^*} \\ &\geq 4. \end{aligned}$$

□

To apply Theorem 1.1 we need a suitable comparison function, which was found by Hans-Christoph Grunau:

Lemma 7.4 (see [25] Lemma 7.4)**.** *If the pair (α_-, α_+) satisfies Assumption 1.2, then*

$$W^h_{\alpha_-,\alpha_+} = \inf\{W_h(v) : \; v \in M_{\alpha_-,\alpha_+}\} < 8.$$

Proof. Without loss of generality we assume $\alpha_- \leq \alpha_+$. Furthermore let

$$\cosh_-(x) = \alpha_- \cosh\left(\frac{1+x}{\alpha_-}\right) \text{ and } \cosh_+(x) = \alpha_+ \cosh\left(\frac{1-x}{\alpha_+}\right).$$

Now define $t \mapsto (x(t), r(t))$ in such a way, that the upper half circle $p_{x(t),r(t)}(\cdot)$ is tangent to the graph of $\cosh_+$ at $(1-t, \cosh_+(1-t))$. Since $\cosh_+$ is smooth, $x(\cdot)$ and $r(\cdot)$ are continuous. Assumption 1.2 also ensures that $p_{x(0),r(0)} = p_{1,\alpha_+}$ and $\cosh_-$ do not meet. Since $\cosh_-$ and $\cosh_+$ do meet, we can find a first time $t_0 > 0$, such that a $\tilde{t} > t_0$ exists, for which $p_{x(t_0),r(t_0)}$ is tangent to the graph of $\cosh_-$ in $(1-\tilde{t}, \cosh_-(1-\tilde{t}))$. Figure 7.1 gives a sketch of the situation. We can define the desired comparison function by

$$v_{\alpha_-,\alpha_+}(x) = \begin{cases} \cosh_-(x), & x \in \left[-1, 1-\tilde{t}\right] \\ p_{x(t_0),r(t_0)}(x), & x \in \left(1-\tilde{t}, 1-t_0\right] \\ \cosh_+(x), & x \in (1-t_0, 1] \end{cases}$$

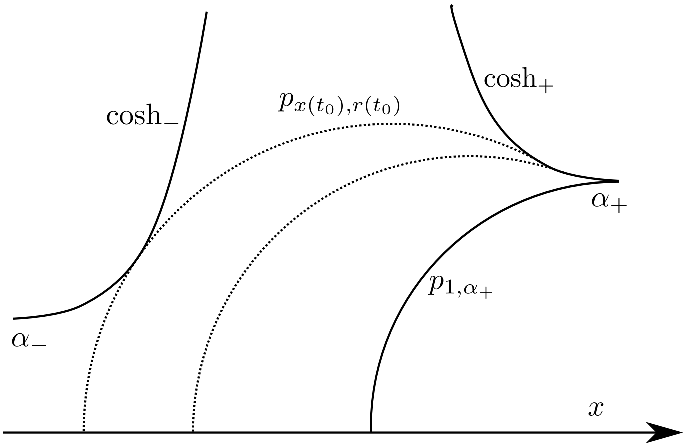

Figure 7.1.: Comparison function for the elastic energy.

Since $v_{\alpha_-,\alpha_+} \in C^{1,1}([-1,1])$, it is also an element of M_{α_-,α_+}. Since $p_{x(t_0),r(t_0)}$ is a geodesic w.r.t. to the hyperbolic metric, it does not contribute to the hyperbolic elastic energy W_h. The proof of Example 7.2 then shows

$$W^h_{\alpha_-,\alpha_+} \le W_h(v_{\alpha_-,\alpha_+}) < 8.$$

□

We are now able to tackle the main result of this section. Parts of this proof are by Hans-Christoph Grunau. These will be highlighted during the exposition.

Theorem 7.5 (see [25] Theorem 7.5)**.** *Let the pair $(\alpha_-,\alpha_+) \in \mathbb{R}_+ \times \mathbb{R}_+$ obey Assumption 1.2. Also let $c \in C^\infty([0,1],\mathbb{H}^2) \cap M_{\alpha_-,\alpha_+}$ satisfy*

$$W_e(S(c)) = W^e_{\alpha_-,\alpha_+} = \inf\{W_e(S(v)) : v \in M_{\alpha_-,\alpha_+}\}.$$

(Existence is proven by Theorem 1.1 and Lemma 7.4). Then c can be represented as a graph $(\cdot, u(\cdot))$ with $u \in C^\infty([-1,1],(0,\infty))$.

Proof. Without loss of generality we can assume

$$\alpha_- \le \alpha_+.$$

Otherwise we simply reflect c at the y-axis. Let $L > 0$ be the hyperbolic arclength of c and $\gamma : [0,L] \to \mathbb{H}^2$ the reparameterisation by hyperbolic arclength with $\dot\gamma^1(0) > 0$. Then the corresponding geodesic curvature $K : [0,L] \to \mathbb{R}$ satisfies (4.1). Lemma

4.5 gives us the Killing vector field J, which is the unique extension of $J_\gamma = K^2\dot{\gamma} + 2\dot{K}(-\dot{\gamma}^2, \dot{\gamma}^1)$. We proceed by contradiction and assume, that there exists a **minimal** $s^* \in (0, L)$ with $\dot{\gamma}^1(s^*) = 0$. Lemma 5.15 yields K to be wavelike (cf. Lemma 4.4) and the unique geodesic Σ (cf. Lemma 5.1) to be an upper half circle with centre on the x-axis.
We can now state the following observation concerning the geodesic curvature of γ:

Claim 5. *K possesses at most two zeros in $[0, L]$.*

Proof. Assume the existence of at least three zeros of K in $[0, L]$. Then $[0, L]$ contains at least one period of K. Lemma 5.16 yields $W_h(\gamma) \geq 4\pi > 8$, a contradiction to Lemma 7.4. □

For the remainder of the proof we need to distinguish two major cases. For now let

$$\dot{\gamma}^2(s^*) > 0.$$

Now we have to prove a claim concerning Σ, which is described by Figure 7.2 (cf. Lemma 5.3).

Claim 6. *From an euclidean viewpoint the geodesic Σ seperates $\mathbb{H}^2$ into an unbounded part Σ_- and a bounded part Σ_+. For all $s \in [0, L]$ we then have:*
$\gamma(s) \in \Sigma_-$, iff $K(s) < 0$. On the other hand $\gamma(s) \in \Sigma_+$, iff $K(s) > 0$.
We also have that $K(s^*) \geq 0$.

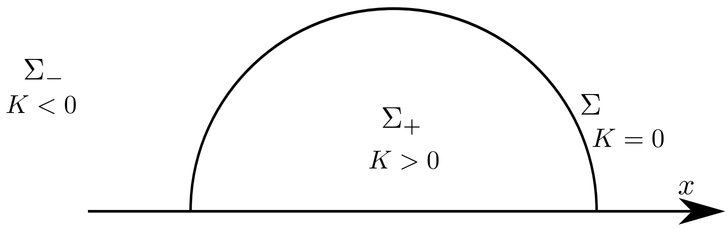

Figure 7.2.: Decomposition of $\mathbb{H}^2$ by means of the geodesic curvature K.

Proof. Unfortunately we cannot directly apply Lemma 5.3 since γ does not necessarily satisfy (4.8). So we need another distinction of cases:

1. $\ddot{\gamma}^1(s^*) \neq 0$: This means we have an extremum of γ^1 in s^*. Since s^* is minimal the boundary datum $\dot{\gamma}^1(0) > 0$ yields s^* to be a local maximum of γ^1. Please note that then $\ddot{\gamma}^1 < 0$. With $\dot{\gamma}^1(L) > 0$ we can then find an $s_* \in (s^*, L)$ minimal with $\dot{\gamma}^1(s_*) = 0$ and $\ddot{\gamma}^1(s_*) \geq 0$. The minimality ensures $\forall s \in (s^*, s_*)$ $\dot{\gamma}^1(s) < 0$. By Lemma 7.3 (cf. Lemma 3.2) we also obtain $\forall s \in [s^*, s_*]$ that $\dot{\gamma}^2(s) > 0$,

because $W_h(\gamma) < 8$. Let us take a look at the curvature K: Equation (2.10) yields

$$K(s_*^*) = -\frac{\ddot{\gamma}^1\dot{\gamma}^2\gamma^2}{|\dot{\gamma}|^3}(s_*^*).$$

Here s_*^* denotes, that the equation is satisfied for s_* and s^*. Hence $K(s^*) > 0$ and $K(s_*) \leq 0$. On the other hand the sign conditions on $\dot{\gamma}$ ($\forall s \in (s^*, s_*)$ $\dot{\gamma}^1(s) < 0$, $\dot{\gamma}^2(s) > 0$), Σ being a geodesic circle and γ crossing Σ perpendicularly in zeros of K yield $\gamma(s^*) \in \Sigma_+$ and $\gamma(s_*) \in \overline{\Sigma_-}$. Figure 7.3 explains this situation.

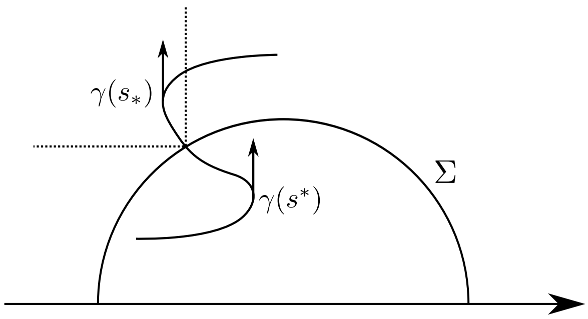

Figure 7.3.: Proof of curvature decomposition of $\mathbb{H}^2$, part 1.

2. $\ddot{\gamma}^1(s^*) = 0$: Equation (2.10) yields $K(s^*) = 0$. Lemma 5.1 then yields $\gamma(s^*) \in \Sigma$. Since Σ is a half circle, $\gamma(s^*)$ has to be the north pole of this geodesic. Since we have chosen s^* to be minimal, we can reparameterise $\gamma\big|_{[0,s^*)}$ as a smooth graph $(x, u(x))$ with $u : [-1, \gamma^1(s^*)) \to (0, \infty)$. The geodesic curvature $\kappa[u]$, which represents K in this parameterisation, can be calculated by (cf. (2.10))

$$\frac{u''(x)u(x)}{(1 + (u'(x))^2)^{\frac{3}{2}}} + \frac{1}{\sqrt{1 + (u'(x))^2}} = \kappa[u](x). \tag{7.1}$$

We also have $\lim\limits_{x \nearrow \gamma^1(s^*)} u'(x) = +\infty$. The mean value theorem yields a sequence $\xi_k \nearrow \gamma^1(s^*)$ with

$$u''(\xi_k)\left(\gamma^1(s^*) - \frac{1}{k} + 1\right) = u'\left(\gamma^1(s^*) - \frac{1}{k}\right) - u'(-1) \to \infty.$$

For $k \in \mathbb{N}$ big enough we obtain $u''(\xi_k) \geq 0$. For these k equation (7.1) then gives us $\kappa[u](\xi_k) > 0$. This yields a sequence $s_k \nearrow s^*$ with $K(s_k) > 0$. Since $\gamma^1(s^*)$ lies on the north pole of Σ and $\dot{\gamma}^2(s^*) > 0$, we have $\gamma(s_k) \in \Sigma_+$ for $k \in \mathbb{N}$ big enough.

□

As a corollary to the proof of Claim 6 we have the following:

Claim 7. *There exists an $s_0 \in (0, L)$ with $K(s_0) = 0$ and in which the geodesic curvature changes sign from positive to negative. This point also satisfies $s^* \leq s_0$ and $\forall s \in (s^*, s_0)$ we have $\dot{\gamma}^1(s) \neq 0$.*
If $K(s^*) > 0$, there exists exactly one $s_* \in [s_0, L)$ with $\dot{\gamma}^1(s_*) = 0$ and $K(s_*) \leq 0$.
If on the other hand $K(s^*) = 0$, we do not have another point $s \in [0, L] \setminus \{s^*\}$ with $\dot{\gamma}^1(s) = 0$.

Proof. The proof of Claim 6 already showed most of the statement. All that is left is the uniqueness property of s_*. The aforementioned proof yields an $s_* \in [s^*, L)$ with $\dot{\gamma}^1(s_*) = 0$, $K(s_*) \leq 0$, $\dot{\gamma}^2(s_*) > 0$ and $\forall s \in (s^*, s_*)$ $\dot{\gamma}^1(s) \neq 0$ (If $K(s^*) = 0$ we set $s_* := s^*$). Let us proceed by contradiction and assume that a minimal $\tilde{s} \in (s_*, L)$ with $\dot{\gamma}^1(\tilde{s}) = 0$ exists. Lemma 3.2 yields $\dot{\gamma}^2(\tilde{s}) > 0$.
Here we need to distinguish a few cases to demonstrate how the above mentioned arguments apply:

1. $K(s^*) > 0$: The arguments for Claim 6, case 1, show that $K(s_*) \leq 0$, since $\gamma(s_*) \in \overline{\Sigma}_-$. Figure 7.3 gives a sketch of the situation. Now two subcases need to be considered (see Figure 7.4):
   (a) $\ddot{\gamma}^1(\tilde{s}) = 0$: The proof of Claim 6, case 2, yields a $\delta > 0$, such that $\forall s \in (\tilde{s} - \delta, \tilde{s})$ we have $K(s) > 0$. $K(s_*) \leq 0$ and Lemma 4.4 (K behaves like a cosine) yield three zeros of K, which contradicts Claim 5.
   (b) $\ddot{\gamma}^1(\tilde{s}) \neq 0$: As in Claim 6, case 1, $K(\tilde{s}) > 0$ and we find an $s_1 \in (\tilde{s}, L]$ with $K(s_1) = 0$. $K(s_*) \leq 0$ and Lemma 4.4 yield a zero of K between s_* and $\tilde{s}$. Hence we found three zeros of K, contradicting Claim 5.

2. $K(s^*) = 0$: The proof of Claim 6, case 2, gives us a $\delta > 0$, such that $\forall s \in (s^*, s^* + \delta]$ we have $K(s) < 0$. Hence equation (7.1) yields γ to be a strictly concave graph on $(s^*, s^* + \delta]$. Now we need to consider two subcases (see Figure 7.5):
   (a) $\ddot{\gamma}^1(\tilde{s}) \neq 0$: Since $\dot{\gamma}^1(s^* + \delta) > 0$ we can apply the arguments of case 1 of the proof of Claim 6. Hence $K(\tilde{s}) > 0$ and we find an $s_1 \in (\tilde{s}, L]$ with $K(s_1) = 0$. $K(s^* + \delta) < 0$ yields again at least three zeros of K contradicting Claim 5.
   (b) $\ddot{\gamma}^1(\tilde{s}) = 0$: Since γ is a graph on $(s^*, \tilde{s})$ the arguments of case 2 of the proof of Claim 6 yield $K(\tilde{s}) = 0$ and the existence of a $\tilde{\delta} > 0$, such that for all $s \in [\tilde{s} - \tilde{\delta}, \tilde{s})$ we have $K(s) > 0$. In combination with $K(s^* + \delta) < 0$ we obtain at least three zeros of K, contradicting again Claim 5.

□

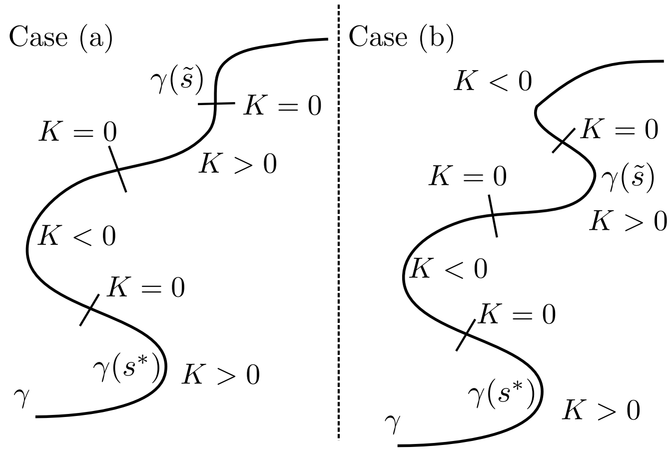

Figure 7.4.: Uniqueness of s_* and s^*, case 1.

Claim 7 also means we have at most two points $s^* \leq s_*$, such that $\dot{\gamma}^1(s^*_*) = 0$ (cf. Figure 7.6). For the sake of simplicity we set $s_* := s^*$, if we only have one such point. Claim 5 shows, that K has at most two zeros. With this in mind we distinguish the following cases to prove our main result:

1. $K(L) < 0$:
   Claim 7 and Claim 5 show, that $\forall s \in [s_*, L]$ we have $K(s) \leq 0$. Let us take a closer look at the behaviour of γ on $[s_*, L]$. For this let us reparameterise γ locally around $s = L$ as a smooth graph $(\cdot, u(\cdot))$. The geodesic curvature $\kappa[u]$ then satisfies (7.1). Since $\forall s \in (s_*, L]$: $K(s) < 0$ the function u has to be strictly concave until $\gamma^1(s_*) =: x_0 < \gamma^1(L)$ with $\lim\limits_{x \searrow x_0} u'(x) = \infty$. By comparing this to Assumption 1.2 we obtain $\forall s \in [s_*, L]$: $\gamma^2(s) \leq p_{1,\alpha_+}(\gamma^1(s))$, because the geodesic curvature of p_{1,α_+} is zero. Then the intermediate value theorem and the boundary data give us an $\hat{s} \in (0, s_*]$ with $\gamma^2(\hat{s}) = p_{1,\alpha_+}(\gamma^1(\hat{s}))$.
   To construct a suitable comparison curve for γ, let us define a family of catenoids $cat_s : [0, \infty) \to \mathbb{H}^2$ by $cat_s(0) = \gamma(s)$, $\dot{cat}_s(0) = \dot{\gamma}(s)$ and by cat_s being parameterised by hyperbolic arclength. For reasons of consistency cat_s is defined as a straight line parallel to the y-axis, whenever $\dot{\gamma}^1(s) = 0$. By the smallness condition 1.2 cat_0 cannot intersect p_{1,α_+}. The existence of $\hat{s}$ on the other hand gives us an $\bar{s} \in (0, \hat{s}]$, such that $cat_{\bar{s}}$ is tangent to p_{1,α_+}. Figure 7.6 explains the situation. Two different situations can now arise. To distinguish these subcases let us define $\bar{x} \in \mathbb{R}$ as the point, in which $p_{1,\alpha_+}(\bar{x})$ is tangent to $cat_{\bar{s}}$. The first case reflects the situation described by Figure 7.6.

   a) $\bar{x} \leq 1$:

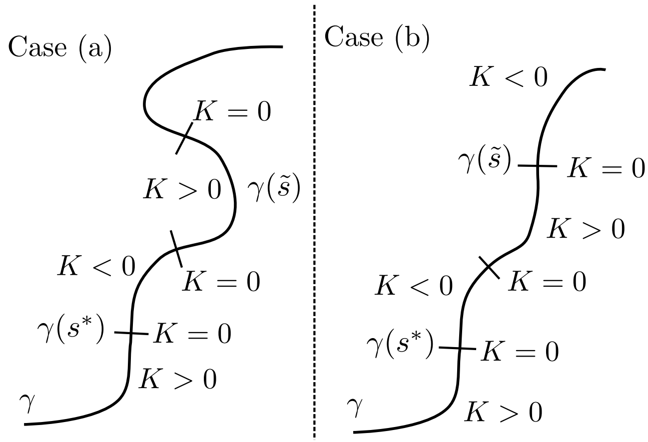

Figure 7.5.: Uniqueness of $s_* = s^*$, case 2.

For the following let $\tilde{p} : \mathbb{R} \to \mathbb{H}^2$ be the reparameterisation of p_{1,α_+} by hyperbolic arclength, satisfying $\tilde{p}^2(0) = p_{1,\alpha_+}(\bar{x})$. Let $\tilde{s} \in \mathbb{R}$ be given by $cat_{\bar{s}}(\tilde{s}) = \tilde{p}(0)$. Furthermore we need $\tilde{L} \geq 0$ defined by $\tilde{p}(\tilde{L}) = (1, \alpha_+)$. Now we can write down our comparison curve:

$$v(s) = \begin{cases} \gamma(s), & s \in [0, \bar{s}) \\ cat_{\bar{s}}(s - \bar{s}), & s \in [\bar{s}, \bar{s} + \tilde{s}) \\ \tilde{p}(s - (\bar{s} + \tilde{s})), & s \in [\bar{s} + \tilde{s}, \bar{s} + \tilde{s} + \tilde{L}]. \end{cases} \tag{7.2}$$

By construction $v \in C^{1,1}([0, \bar{s} + \tilde{s} + \tilde{L}], \mathbb{R}^2)$ and satisfies the boundary conditions. Let us compare v to $\gamma\big|_{[\bar{s},L]}$ in terms of the Willmore energy (see (2.12)):

$$\begin{aligned} W_e(S(\gamma))\big|_{[\bar{s},L]} &\geq W_e(S(\gamma))\big|_{[s_*,L]} \\ &= \frac{\pi}{2} W_h(\gamma)\big|_{[s_*,L]} - 2\pi \left[\frac{\dot{\gamma}^2}{\sqrt{(\dot{\gamma}^1)^2 + (\dot{\gamma}^2)^2}} \right]_{s_*}^{L} \geq 2\pi. \end{aligned}$$

On the other hand Example 7.1 shows $W_e(S(v))\big|_{[\bar{s},\tilde{L}]} < 2\pi$. All in all we have

$$W_e(S(\gamma)) > W_e(S(v)),$$

because catenoids are minimal surfaces. Hence γ would not have been an energy minimiser, a contradiction.

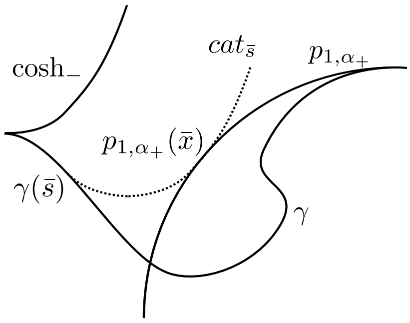

Figure 7.6.: A comparison curve for γ.

b) $\bar{x} > 1$:
This assumptions yields the existence of an $s_1 \in (0, \bar{s}]$ with $\gamma^2(s_1) > \alpha_+$. Additionally this point has to satisfy $\gamma^1(s_1) < \gamma^1(s_*)$, since we would otherwise find an $s \in (s_1, L)$ with $\dot{\gamma}^1(s) = 0$ and $\dot{\gamma}^2(s) < 0$. In combination with Lemma 3.2 this would be a contradiction. The perpendicularity condition with Σ then ensures $\gamma(s_1) \in \Sigma_-$. This in turn means $K(s_1) < 0$. Since this s_1 exists, we can find an $s_2 \in [0, s_1)$ with $K(s_2) > 0$. This is due to a concavity argument in combination with (7.1). Figure 7.7 gives a sketch of the situation. Claim 7 states that K changes sign in s_0 from

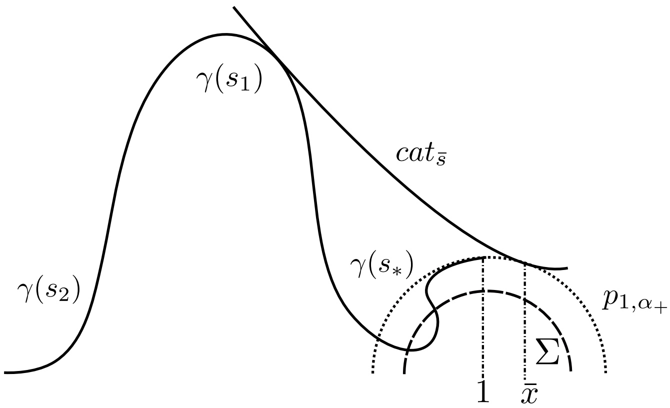

Figure 7.7.: Behaviour of γ with $\bar{x} > 1$.

positive to negative. This gives us at least three zeros in K, which is a direct contradiction to Claim 5.

2. $K(L) > 0$:
The Claims 5 and 7 imply $K(0) > 0$ and the existence of exactly two zeros of K. In turn Claim 6 yields $\gamma(0), \gamma(L) \in \Sigma_+$. Let $(x_0, 0) \in \mathbb{R}^2$ be the centre of Σ. Since every integral curve of J is an euclidean circle (c.f. Lemma 2.11 and Lemma 2.15) and J satisfies Example 2.10, every centre of it is of the form $(x_0, y) \in \mathbb{R}^2$. We discuss in detail the case $x_0 \geq -1$. Otherwise we have $x_0 < -1 < 1$ and the same arguments as below can be applied around $\gamma(L)$. Let $s_0 > 0$ be the first zero of K. Now we like to show the existence of an $\tilde{s} \in [0, s_0)$, such that $K(\tilde{s})$ is a maximum. Lemma 5.16 would then give us $W_h(\gamma) \geq 3\pi > 8$, a contradiction. Let us now assume such an $\tilde{s} \in [0, s_0)$ does not exist. We can extend γ as a solution of the differential equation (4.1) to $(-\infty, L]$ (see e.g. (4.2)). We can choose $s_1 < 0$ to be maximal with $K(s_1) = 0$. Then we can find an $\bar{s} \in (s_1, 0)$ with $K(\bar{s})$ being a maximum. Lemma 4.8 yields $\gamma(\bar{s}) \in B_+$. Let $I \subset \mathbb{H}^2$ be the integral curve of J starting at $\gamma(0) = (-1, \alpha_-)$. With $-1 \leq x_0$ and again Lemma 4.8 the derivative $\dot{\gamma}(0) = (\alpha_-, 0)$ points strictly inward with respect to I. The intermediate value theorem gives us at least two intersecting points of $\gamma|_{(\bar{s}, s_0)}$ with I. This contradicts Lemma 5.18, because the proof of this lemma shows, that therein the order of the zero of K and the extremum of K can be reversed. Thus we apply this argument in the intervall $[\bar{s}, s_0]$. Figure 7.8 describes the situation.

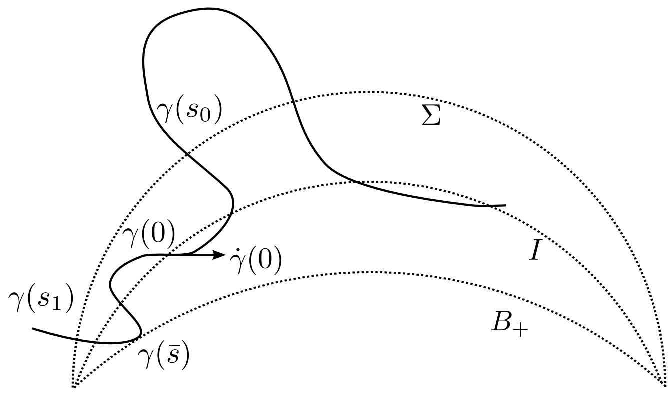

Figure 7.8.: Existence of a maximum of K by contradiction.

Now we can switch to the other major case:

$$\dot{\gamma}^2(s^*) < 0.$$

With similar arguments we can give analogous statements to the Claims 6 and 7. Let us point out the difference:

Claim 8. *From an euclidean viewpoint the geodesic* Σ *seperates* $\mathbb{H}^2$ *into an unbounded part* Σ_- *and a bounded part* Σ_+*. For all* $s \in [0, L]$ *we then have:*
$K(s) < 0$*, iff* $\gamma(s) \in \Sigma_-$*. On the other hand* $\gamma(s) \in \Sigma_+$*, iff* $K(s) > 0$*.*
We also have $K(s^*) \leq 0$*.*

Proof. Case $\ddot{\gamma}^1(s^*) \neq 0$ can be proven with precisely the same arguments as in Claim 6. Case $\ddot{\gamma}^1(s^*) = 0$ is a bit more involved:

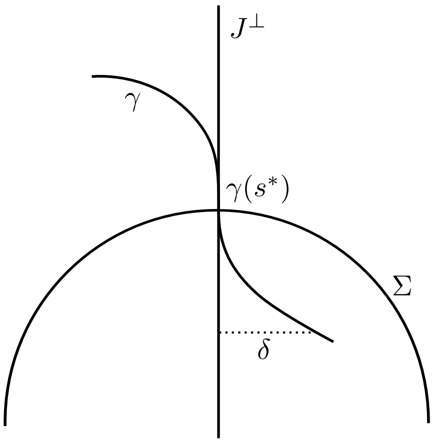

Figure 7.9.: Case $\dot{\gamma}^1(s^*) < 0$: Curvature decomposition of $\mathbb{H}^2$, case $\ddot{\gamma}^1(s^*) = 0$.

As illustrated by Figure 7.9, Lemma 5.19 gives us $\omega, \delta > 0$, such that γ can be reparameterised on $(s^*, s^* + \omega)$ as a smooth graph $u : (\gamma^1(s^*), \gamma^1(s^*) + \delta) \to (0, \infty)$ with $\lim\limits_{x \searrow \gamma^1(s^*)} u'(x) = -\infty$. The mean value theorem yields a sequence $\xi_k \searrow \gamma^1(s^*)$ with $k \in \mathbb{N}$ large enough, such that

$$u''(\xi_k) \left(\delta - \frac{1}{k} \right) = u'(\gamma^1(s^*) + \delta) - u' \left(\gamma^1(s^*) + \frac{1}{k} \right) \to \infty.$$

For k large enough we obtain $u''(\xi_k) \geq 0$. Hence (7.1) yields $\kappa[u](\xi_k) > 0$. $\square$

By using the argument as for Claim 8, the proof of the next claim is completely analogous to Claim 7.

Claim 9. *There exists an* $s_0 \in (0, L)$ *with* $K(s_0) = 0$ *and in which the geodesic curvature changes sign from negative to positive. This point also satisfies* $s^* \leq s_0$ *and* $\forall s \in (s^*, s_0)$ *we have* $\dot{\gamma}^1(s) \neq 0$*.*
If $K(s^*) < 0$*, there exists exactly one* $s_* \in [s_0, L)$ *with* $\dot{\gamma}^1(s_*) = 0$ *and* $K(s_*) \geq 0$*.*

If on the other hand $K(s^*) = 0$ we do not have another point $s \in [0, L] \setminus \{s^*\}$ with $\dot{\gamma}^1(s) = 0$.

As in the first major case we identify without loss of generality $s_* := s^*$, if $K(s^*) = 0$. Again we have to distinguish cases by the sign of the geodesic curvature:

1. $K(0) < 0$: Here we need to consider two subcases:

   a) $K(L) > 0$:
   We will show $\alpha_- > \alpha_+$, which would contradict our general assumption from the beginning of the proof. Claim 5 and Claim 9 yield exactly one zero $s_0 \in [s^*, s_*]$ of the geodesic curvature K. If we reparameterise γ as a smooth graph $(\cdot, u(\cdot))$ at $\gamma(0)$, this u would be strictly concave. This is due to $K(s) \leq 0$ for all $s \in [0, s^*]$ and equation (7.1). We then have $\gamma^2(s_0) < \gamma^2(0)$, since Lemma 7.3 yields $\forall s \in [s^*, s_*]\ \dot{\gamma}^2(s) < 0$.
   If we assume $\alpha_+ > \gamma^2(s_0)$, we would find an $\hat{s} \in (s_0, L)$ with $\dot{\gamma}^1(\hat{s}) = 0$ and $\dot{\gamma}^2(\hat{s}) > 0$, because $\gamma(L) \in \Sigma_+$ and $\dot{\gamma}^1(L) > 0$. Figure 7.10 explains the situation. Lemma 3.2 finally yields a contradiction.

   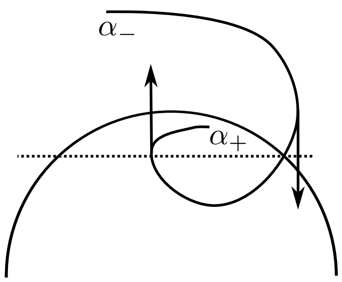

   Figure 7.10.: $\alpha_- > \alpha_+$ or $W_h(\gamma) > 8$.

   b) $K(L) < 0$:
   This case was proven by an idea of Hans-Christoph Grunau: Claim 5 and Claim 9 yield exactly two zeros $s_0 < s_1$ of K with $s_0 \in [s^*, s_*]$ and $s_* < s_1$. Our aim is to construct a suitable comparison function to show that γ cannot be a minimiser for the Willmore energy. As in case $\dot{\gamma}(s^*) > 0$, subcase $K(L) < 0$, we define a family of catenoids $cat_s : \mathbb{R} \to \mathbb{H}^2$, $s \in [0, s^*)$, such that $cat_s(0)$ is tangent to $\gamma(s)$. Additionally we parameterise every catenoid by hyperbolic arclength.
   At first we have to show that γ meets cat_0 only at $\gamma(0)$: As shown in case $\dot{\gamma}^2(s^*) < 0$, subcase $K(L) > 0$, we have for all $s \in (0, s_1]\ \gamma^2(s) < \alpha_-$. Since $cat_0^2(t)$ is monotonically increasing for $t > 0$, $\gamma|_{(0,s_1]}$ and $cat_0(\mathbb{R})$ do not meet. On the other intervall $[s_1, L]$ the curvature satisfies $K \leq 0$. Since

p_{1,α_+} is a geodesic circle, the boundary datum $\dot{\gamma}^2(L) = 0$ yields for all $s \in [s_1, L]$ $p_{1,\alpha_+}(\gamma(s)) \geq \gamma^2(s)$. With Assumption 1.2 γ meets cat_0 only in $\gamma(0)$. Figure 7.11 gives a sketch of the situation.

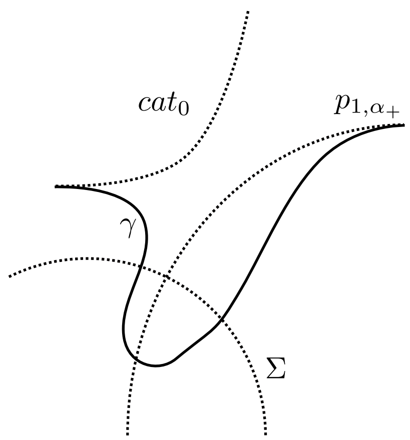

Figure 7.11.: Situation for $\dot{\gamma}^2(s_*) < 0$, $K(0) < 0$ and $K(L) < 0$.

For $s \nearrow s^*$ the vertex of cat_s approaches zero. Then the boundary data for γ yield an $\bar{s} \in (0, s^*)$ and an $\tilde{s} \in (\bar{s}, L)$, such that $cat_{\bar{s}}$ touches γ at $\gamma(\tilde{s})$. Before we can define a comparison curve, we have to show $\dot{\gamma}^1(\tilde{s}) > 0$. Since $\forall s \in [s^*, s_*]$ we have $\gamma^1(s) \leq \gamma^1(s^*)$ and $\gamma^2(s) \leq \gamma(s^*)$, the catenoid $cat_{\bar{s}}$ does not intersect $\gamma|_{[s^*,s_*]}$. Claim 9 on the other hand shows, that γ can be reparameterised as a graph on $[0, L] \setminus [s^*, s_*]$. This yields $\dot{\gamma}^1(\tilde{s}) > 0$.
The resulting situation is sketched in Figure 7.12.

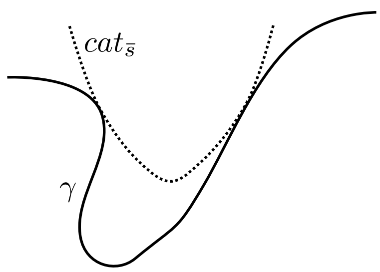

Figure 7.12.: Inserting a catenoid.

Let $\tilde{L} > 0$ be the point with $cat_{\bar{s}}(\tilde{L}) = \gamma(\tilde{s})$. We can now define the desired comparison curve:

$$v(s) = \begin{cases} \gamma(s), & s \in [0, \bar{s}) \\ cat_{\bar{s}}(s - \bar{s}), & s \in [\bar{s}, \bar{s} + \tilde{L}) \\ \gamma(s - (\bar{s} + \tilde{L}) + \tilde{s}), & s \in [\bar{s} + \tilde{L}, \bar{s} + \tilde{L} + L - \tilde{s}]. \end{cases} \tag{7.3}$$

Since catenoids are minimal surfaces, their associated mean curvature vanishes. Hence their Willmore energy is zero. This in turn yields $W_e(S(v)) < W_e(S(\gamma))$. Equality cannot arise, because it would mean, that γ would be a catenoid. This is not possible due to the boundary data.

2. $K(0) > 0$:
   Claim 9 and Claim 5 yield exactly two zeros of K. This gives $K(L) > 0$. By Claim 8 the proof is from here on out completely analogous to $\dot{\gamma}(s^*) > 0$, subcase $K(L) > 0$.

$\square$

7.2. Estimates on the infimum of the Willmore energy

This section shows, that the projectability property of a solution of (1.4) can in general not hold. It is taken from [25, Appendix A]. At first we provide an estimate, which proves, that the elastic energy is not uniformely bounded for (α_-, α_+) in the class of graphs. This lemma is by Hans-Christoph Grunau:

Lemma 7.6 (see [25] Lemma A.1)**.** *If $\alpha_+ > \alpha_- + 1$, then for every function $u \in C^{1,1}([-1,1], (0,\infty))$ satisfying $u(-1) = \alpha_-$, $u(1) = \alpha_+$ and $u'(\pm 1) = 0$ we have*

$$W_h(u) \geq \frac{\alpha_+ - 1}{10}.$$

Proof. Equation (2.15) yields

$$\begin{aligned} W_h(u) &= \int_{-1}^{1} \frac{u''(x)^2 u(x)}{(1+u'(x)^2)^{\frac{5}{2}}} + \frac{1}{u(x)\sqrt{1+u'(x)^2}}\, dx \\ &\geq \int_{-1}^{1} \frac{u''(x)^2 u(x)}{(1+u'(x)^2)^{\frac{5}{2}}}\, dx \\ &= \int_{-1}^{1} u(x)\sqrt{1+(u'(x))^2} \left(\frac{u''(x)}{(1+(u'(x))^2)^{\frac{3}{2}}} \right)^2 dx \end{aligned}$$

We may now choose $x_1 \in (-1,1)$, such that $u'(x_1) \geq \frac{1}{2}$ and $u\big|_{[x_1,1]} \geq \alpha_+ - 1$. We conclude:

$$\begin{aligned}
W_h(u) &\geq \int_{-1}^{1} u(x)\sqrt{1+(u'(x))^2}\left(\frac{u''(x)}{(1+(u'(x))^2)^{\frac{3}{2}}}\right)^2 dx \\
&\geq \int_{x_1}^{1} u(x)\sqrt{1+(u'(x))^2}\left(\frac{u''(x)}{(1+(u'(x))^2)^{\frac{3}{2}}}\right)^2 dx \\
&\geq (\alpha_+ - 1)\int_{x_1}^{1}\left(\frac{u''(x)}{(1+(u'(x))^2)^{\frac{3}{2}}}\right)^2 dx \\
&\geq \frac{\alpha_+ - 1}{|1-x_1|}\left(\int_{x_1}^{1}\frac{u''(x)}{(1+(u'(x))^2)^{\frac{3}{2}}}\,dx\right)^2 \\
&= \frac{\alpha_+ - 1}{1-x_1}\left(\frac{u'(x_1)}{\sqrt{1+(u'(x_1))^2}}\right)^2 \geq \frac{\alpha_+ - 1}{2}\left(\frac{\frac{1}{2}}{\sqrt{1+\frac{1}{4}}}\right)^2 = \frac{\alpha_+ - 1}{10}.
\end{aligned}$$

□

If α_+ tends to ∞, the elastic energy of graphs will tend to ∞ as well.

In contrast to Lemma 7.6 the following lemma shows, that in the class of curves the infimum of the elastic energy is bounded for small α_- and big α_+:

Lemma 7.7 (see [25] Lemma A.3)**.** *Let* $(\alpha_-, \alpha_+) \in (0,\infty)^2$ *satisfy*

$$\frac{\alpha_+}{\sqrt{2}+1} + \frac{\alpha_-}{\sqrt{2}-1} \geq 2 \text{ and } \alpha_+ > \alpha_-(\sqrt{2}+1)^4,$$

then

$$W^e_{\alpha_-,\alpha_+} < 2\pi^2.$$

Proof. Thanks to (2.12) it suffices to show $W^h_{\alpha_-,\alpha_+} = \inf\{W_h(v) : \; v \in M_{\alpha_-,\alpha_+}\} < 4\pi$. Let us define two circles (see Example 2.14):

$$C_{\alpha_-} := C_{\frac{\alpha_-}{\sqrt{2}-1},\left(-1,\alpha_- + \frac{\alpha_-}{\sqrt{2}-1}\right)} \text{ and } C_{\alpha_+} := C_{\frac{\alpha_+}{\sqrt{2}+1},\left(1,\alpha_+ - \frac{\alpha_+}{\sqrt{2}+1}\right)}$$

Example 2.14 yields

$$\kappa[C_{\alpha_\pm}] = -\sqrt{2}$$

and therefore the elastic energy of one half of a circle is with the help of maple™

$$\int_0^\pi (\kappa[C_{\alpha_-}])^2(t)\,ds(t) = \int_0^\pi \frac{2\frac{\alpha_-}{\sqrt{2}-1}}{\frac{\alpha_-}{\sqrt{2}-1}\cos(t) + \alpha_- + \frac{\alpha_-}{\sqrt{2}-1}}\,dt = 2\pi.$$

Analogously we obtain $\int_{-\pi}^{0}(\kappa[C_{\alpha_+}])^2(t)\,ds(t) = 2\pi$.
$\alpha_+ > \alpha_-(\sqrt{2}+1)^4$ is equivalent to

$$\alpha_+ - 2\frac{\alpha_+}{\sqrt{2}+1} > \alpha_- + 2\frac{\alpha_-}{\sqrt{2}-1}.$$

Hence C_{α_-} and C_{α_+} do not intersect. On the other hand the line $G_{\frac{\pi}{2}}$, which is parallel to the y-axis and starts at $C_{\alpha_-}(\frac{\pi}{2})$, intersects $C_{\alpha_+}\big|_{[-\pi,0]}$ because $\frac{\alpha_+}{\sqrt{2}+1} + \frac{\alpha_-}{\sqrt{2}-1} \geq 2$. We can now define a family of geodesics (upper half circles) G_t, which are tangent to C_{α_-} at $C_{\alpha_-}(t)$. Since G_0 does not intersect C_{α_+} we find a $t_0 \in (0, \frac{\pi}{2})$ such that G_{t_0} touches C_{α_+}. As in Lemma 7.4 we obtain a comparison curve v with

$$W_h(v) < 4\pi$$

Figure 7.13 sketches the situation. □

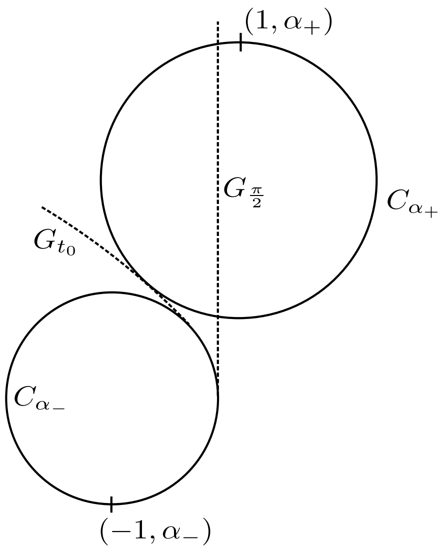

Figure 7.13.: A comparison curve for small α_- and big α_+.

Remark 7.8 (see [25] Remark A.4)**.** The choice of the circles C_{α_-} and C_{α_+} in Lemma 7.7 is not accidental. They are part of the Clifford torus and therefore minimal in the class of possible circles for the construction made above (see e.g. [37, Theorem 4.1] or the proof of the Willmore conjecture [42]).

8. Non-uniqueness results

This chapter is taken from [24, Section 8] and deals with non-uniqueness properties of the Dirichlet problem (1.4). We need to make certain restrictions for our constructions to work. Therefore we will only examine symmetric profile curves or graphs, i.e. $\alpha := \alpha_- = \alpha_+$.

8.1. Non-uniqueness with curves

In this section we will examine the following Dirichlet problem, where the angle at the boundary is prescribed with a $\beta \in \mathbb{R}$ (cf. [24, Equation (8.1)]):

$$\begin{cases} \Delta_{S(c)} H + 2H(H^2 - G) = 0, \quad \text{in } (0,1) \\ c(0) = (-1, \alpha),\ c(1) = (1, \alpha),\ -\frac{\dot{c}^2(0)}{\dot{c}^1(0)} = \frac{\dot{c}^2(1)}{\dot{c}^1(1)} = \beta, \\ \dot{c}^1(0), \dot{c}^1(1) > 0, \end{cases} \tag{8.1}$$

with $\alpha > 0$ and $\beta \in \mathbb{R}$. The positivity of the first component of the derivative at the boundary ensures c to be locally a graph. [18, Theorem 1] gives us a graphical solution for every $\alpha > 0$ and $\beta \in \mathbb{R}$. Now we will find non-graphical solutions for certain boundary data, which showcases the possibly wide variety of solutions, when no bounds on the Willmore energy are given.

Theorem 8.1 (see [24] Theorem 8.1)**.** *There exists infinitely many different pairs* $(\alpha, \beta) \in \mathbb{R}^+ \times \mathbb{R}$*, for which* (8.1) *does possess a solution, which cannot be parameterised as a graph.*

Proof. Let $\gamma : \mathbb{R} \to \mathbb{H}^2$ be a wavelike solution (see Lemma 4.4) of the initial value problem (4.8) (i.e. $|K_0| > 2$). Let B_+ be the lower bounding circle found in Lemma 4.8 and let Σ be the orthogonal geodesic found in Lemma 5.1 (see Figures 8.1 and 5.1). Let $s_n > 0$ be a sequence, such that $\gamma(s_n) \in B_+$. With Lemma 5.13 the hyperbolic progress of $\gamma(s_n)$ to $\gamma(s_{n+1})$ on B_+ can be chosen as a constant for all $n \in \mathbb{N}$, which implies the sequence s_n to be monotonically increasing. Theorem 4.7 and Example 2.14 yield $\dot{\gamma}^1(s_n) > 0$ and $0 > \frac{\dot{\gamma}^2(s_1)}{\dot{\gamma}^1(s_1)} > \frac{\dot{\gamma}^2(s_2)}{\dot{\gamma}^1(s_2)} > \ldots$. If we choose s_1 sufficently big, such that $\gamma([0, s_1])$ crosses Σ at least twice, we find a sign change in $\dot{\gamma}^1$ (see Lemma 5.1). This implies $\gamma([-s_1, s_1])$ cannot be parameterised as a graph. After a suitable dilation $\gamma^1(\pm s_1) = \pm 1$ is fulfilled. By reparameterising $\gamma([-s_1, s_1])$ we find a solution

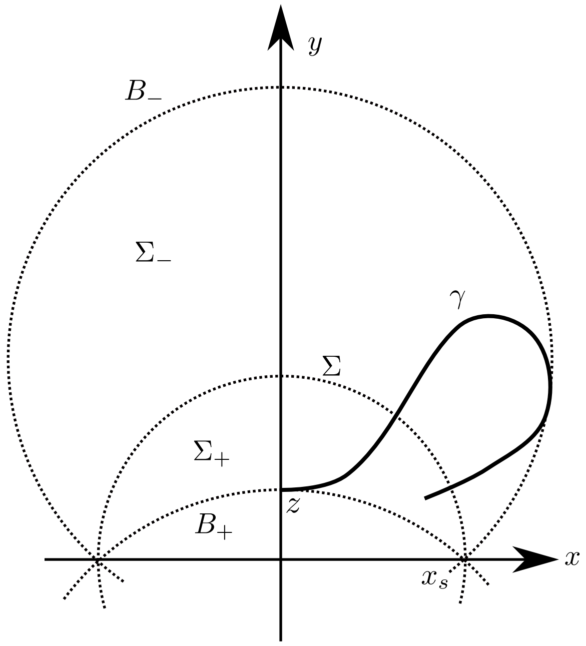

Figure 8.1.: Sketch of a wavelike elastica with initial curvature $K_0 > 2$.

of (8.1). Repeating the argument for every $n \in \mathbb{N}$ yields the desired result, because dilations preserve angles. $\square$

Remark 8.2 (see [24] Remark 8.2)**.** The sequence of solutions $\gamma([-s_n, s_n])$ constructed in Theorem 8.1 possesses unbounded Willmore energy for $n \to \infty$, because the squared hyperbolic curvature repeats itself everytime γ meets B_+. Hence the hyperbolic arclength tends to ∞ as well.

8.2. A second family of projectable solutions

This section is taken from [24, Section 8.2]. Here we will prove Theorem 1.4 by constructing a new set of solutions with a shooting method. This method is similar to the one employed in Section 6.1, but we will use the opposite sign of the initial geodesic curvature. The solutions obtained here differ from solutions found in [17], since the geodesic curvature has zeros.
For the remainder of this section we will focus on wavelike solutions γ of (4.8) with

$$K_0 > 2.$$

With Lemma 4.8 we find two bounding circles B_+, B_- of γ, which intersect the x-axis at exactly two points $x_s > 0$ and $-x_s < 0$ (see (4.11)). Let J be the unique extension of J_γ (see Lemma 4.5) as a Killing field to $\mathbb{H}^2$ with parameters $a < 0, c > 0$ given as in Lemma 5.5. Please note, that the proof of Lemma 5.5 also shows

$$x_s^2 = -2\frac{c}{a}. \tag{8.2}$$

As usual let K be the geodesic curvature of γ. Further let $s_* > 0$ denote half of the period of K. This implies $K(s_*) = -K_0$. We start with a lemma, which hints at γ being locally a graph.

Lemma 8.3 (see [24] Lemma 8.3)**.** *Let $s^* \in [0, s_*]$ be in such a way, that $\forall s \in [0, s^*]$: $\gamma^1(s) < x_s$. Then $\gamma\big|_{[-s^*,s^*]}$ can be parameterised as a graph.*

Proof. If we assume $J^1((x, y)) = 0$ at a certain point $(x, y) \in \mathbb{H}^2$, then a simple calculation based on Lemma 5.5 and (8.2) shows $x^2 \geq x_s^2$. With $J^1((0, \cdot)) > 0$ this yields $J^1(\gamma(s)) > 0$ for all $s \in [0, s^*]$.
Let us now proceed by contradiction. If we assume that $\gamma\big|_{[0,s^*]}$ cannot be parameterised as a graph, then there exists an $\tilde{s} \in [0, s^*]$ with $\dot{\gamma}^1(\tilde{s}) = 0$. Equation (4.7) then gives us $K^2(\tilde{s})\dot{\gamma}^2(\tilde{s}) = a\gamma^1(\tilde{s})\gamma^2(\tilde{s})$. This yields $\dot{\gamma}^2(\tilde{s}) < 0$. By (4.6) with $\dot{K}(\tilde{s}) \leq 0$ in mind we obtain

$$0 \geq -2\dot{K}(\tilde{s})\dot{\gamma}^2(\tilde{s}) = J^1(\gamma(\tilde{s})) > 0,$$

which is an obvious contradiction. $\square$

Now we will examine γ in case of a large K_0. For this we will estimate the wavelength of γ (see Lemma 5.13). Langer & Singer already gave a formula pointing into that direction (see [37, Proposition 5.2 (iii)]), but it is restricted to the hyperbolic distance of crossing points of γ with the perpendicular geodesic Σ (see Lemma 5.1).

Lemma 8.4 (see [24] Lemma 8.4)**.** *Let $s \in [0, s_*]$ be arbitrary, then*

$$\operatorname{dist}_g(\gamma(s), \{(0, y) \in \mathbb{R}^2 : y > 0\}) \leq \pi \frac{K_0^2}{\sqrt{K_0^2 - 4}(K_0^2 - 4)} \to 0, \text{ if } K_0 \to \infty.$$

Proof. First we will estimate t_γ (see Lemma 5.13) with the help of Lemma 4.4:

$$\begin{aligned} t_\gamma(\gamma(s)) &= \int_0^s \frac{K^2}{4K^2 - 4K_0^2 + K_0^4}\, ds \leq \int_0^{s_*} \frac{K^2}{4K^2 - 4K_0^2 + K_0^4}\, ds \\ &= \int_0^{s_*} \frac{\operatorname{cn}^2(rs, k)}{4\operatorname{cn}^2(rs, k) - 4 + K_0^2}\, ds \leq \int_0^{s_*} \frac{1}{K_0^2 - 4} \operatorname{cn}^2(rs, k)\, ds \\ &= \frac{1}{K_0^2 - 4} \int_0^{\frac{1}{r}AM^{-1}(\pi,k)} \cos^2(AM(rs, k))\, ds \end{aligned}$$

$$
\begin{aligned}
&= \frac{1}{K_0^2-4}\frac{1}{r}\int_0^\pi \cos^2(x)\frac{1}{\sqrt{1-k^2\sin^2(x)}}\,dx \\
&\le \frac{1}{K_0^2-4}\frac{1}{r}\frac{1}{\sqrt{1-k^2}}\int_0^\pi \cos^2(x)\,dx \\
&= \frac{\pi}{2}\frac{1}{K_0^2-4}\frac{1}{\sqrt{\frac{1}{2}K_0^2-1}}\frac{1}{\sqrt{1-\frac{K_0^2}{4(-1+\frac{1}{2}K_0^2)}}} \\
&= \frac{\pi}{2}\frac{1}{K_0^2-4}\frac{2}{\sqrt{2K_0^2-4}}\sqrt{\frac{-4+2K_0^2}{-4+K_0^2}} = \pi\frac{1}{\sqrt{K_0^2-4}(K_0^2-4)}.
\end{aligned}
$$

There exists a unique integral curve connecting $\gamma(s)$ and the y-axis (see Theorem 5.8). Since these curves are parameterised proportional by arclength, we can calculate the hyperbolic length of these curves by t_γ and $|J_\gamma|_g$:

$$
\begin{aligned}
\operatorname{dist}_g(\gamma(s),\{(0,y)\in\mathbb{R}^2 : y>0\}) &\le |J_\gamma(s)|_g t_\gamma(\gamma(s)) \le \max|J_\gamma|_g t_\gamma(\gamma(s_*)) \\
&\le \pi\frac{K_0^2}{\sqrt{K_0^2-4}(K_0^2-4)}.
\end{aligned}
$$

□

(4.11) yields with $K_0 > 0$

$$
x_s = z\frac{\sqrt{K_0+2}}{\sqrt{K_0-2}} = z\frac{\sqrt{1+\frac{2}{K_0}}}{\sqrt{1-\frac{2}{K_0}}} \ge z. \tag{8.3}
$$

Now we are ready to tackle our main result in this section.

Theorem 8.5 (see [24] Theorem 8.5)**.** *There exists an $\alpha^* \ge 0$, such that for every $\alpha > \alpha^*$ the Dirichlet problem*

$$
\begin{cases} \Delta_{S(u)}H + 2H(H^2-G) = 0, & \text{in } (-1,1) \\ u(\pm1) = \alpha,\ u'(\pm1) = 0. \end{cases} \tag{8.4}
$$

possesses a solution $u : [-1,1] \to \mathbb{R}^+$ with two sign changes in the geodesic curvature.

Proof. Let γ be a wavelike solution of (4.8) with $K_0 > 2$, $z = 1$ and geodesic curvature K. Let us fixate some further notations: B_- is the outer bounding circle of γ and B_+ the respective inner bounding circle (see Lemma 4.8). Let additionally be Σ the perpendicular geodesic found in Lemma 5.1 and let $x_s > 0$ be the crossing point of these circles with the x-axis (see Equation (4.11)). Figure 8.1 gives a sketch of the situation. Let $s^*, s_* > 0$ be minimal with $K(s^*) = 0$ and $K(s_*) = -K_0$.

1. $\gamma(s^*) \in \Sigma$, the minimality of s^* and Lemma 5.3 yield $\dot\gamma^2(s^*) > 0$. On the other hand we have $\dot\gamma^2(s_*) < 0$, because $\dot K(s_*) = 0$ implies $\gamma(s_*) \in B_-$ and thus $K(s_*)^2\dot\gamma^2(s_*) = J^2(\gamma(s_*)) < 0$ (see Lemmas 4.5 and 5.5). The intermediate value theorem then yields an $\tilde s \in (s^*, s_*)$ with $\dot\gamma^2(\tilde s) = 0$.

2. Now we will show, that $\gamma\big|_{[-\tilde s,\tilde s]}$ can be reparameterised as a graph u. Since for all $s \in [0, s^*]$ $\gamma(s) \in \overline{\Sigma}_+$ (see Lemma 5.3), we obtain $\gamma^1(s) < x_s$. Lemma 8.3 and the symmetry to the y-axis then yield, that $\gamma([-s^*, s^*])$ can be parameterised as a graph u. Since u solves an ordinary differential equation, it can be uniquely extended to an $x^* > \gamma^1(s^*)$. By γ being bounded, we obtain $\lim\limits_{x\nearrow x^*} u'(x) = \pm\infty$. Lemma 5.3 implies for all $s \in [s^*, s_*]$, that $K(s) \le 0$. Equation (7.1) yields u to be concave as long as the geodesic curvature is negative. Hence $u'(x^*) = -\infty$ or $x^* \ge \gamma^1(s_*)$. Either way we can choose $\tilde s$ in such a way, that $\gamma([-\tilde s, \tilde s])$ can be parameterised as a graph, since we have $u'(\gamma(s^*)) > 0$.

3. The second coordinate of the Frenet equation (see (2.14)) gives us in $\tilde s$:

$$\ddot\gamma^2(\tilde s) = K(\tilde s)\dot\gamma^1(\tilde s) - \frac{(\dot\gamma^1(\tilde s))^2}{\gamma^2(\tilde s)} < 0,$$

since $\gamma\big|_{[-\tilde s,\tilde s]}$ is graph und therefore $\dot\gamma^1(\tilde s) > 0$. The inverse function theorem in combination with the concavity argument from above yields the existence of a unique smooth function $\tilde s : (2, \infty) \to \mathbb{R}^+$ with $\dot\gamma^2(\tilde s(\cdot)) = 0$ and $s^* < \tilde s(\cdot) < s_*$.

4. Finally we can find a dilation $\Xi_{K_0} : \mathbb{H}^2 \to \mathbb{H}^2$, centered at the origin, such that $\Xi_{K_0}(\gamma(\tilde s(K_0))) = (1, \alpha(K_0))$. Lemma 8.4 and (8.3) yield

$$\alpha(K_0) = \frac{\gamma^2(\tilde s(K_0))}{\gamma^1(\tilde s(K_0))} \to \infty \text{ if } K_0 \to \infty.$$

In combination with $\tilde s(\cdot)$ being continous the desired result follows.

□

Combining Theorem 8.5 with the following existence result yields the proof of Theorem 1.4, because the solution found in this theorem possesses positive curvature.

Theorem 8.6 (see Theorem 1.1 in [17] and Proposition 6.7 in [18])**.** *For every $\alpha > 0$, there exists a smooth, even function $u \in C^\infty([-1, 1], (0, \infty))$, such that the corresponding surface of revolution solves the Dirichlet problem for the Willmore equation*

$$\begin{cases} \Delta_{S(u)} H + 2H(H^2 - G) = 0 \ \textit{in}\ (-1, 1) \\ u(\pm 1) = \alpha, u'(\pm 1) = 0. \end{cases}$$

This solution u is even and has the following additional properties:

$$\forall x \in [0,1]: \ 0 \le x + u(x)u'(x), \ u'(x) \le 0,$$
$$\forall x \in [-1,1]: \ \alpha \le u(x) \le \alpha + 1, \ |u'(x)| \le \frac{1}{\alpha},$$
$$\forall x \in (-1,1) \text{ the hyperbolic curvature satisfies } \kappa[u](x) > 0.$$

Remark 8.7. Numerical experiments conducted in matlab$^{\text{TM}}$ using (5.6) in combination with the Lemmas 5.11 and 5.13 give rise to the conjecture that the optimal α^* (see Thm. 8.5) is strictly positive (see Figure 8.2). Another topic that has to be left

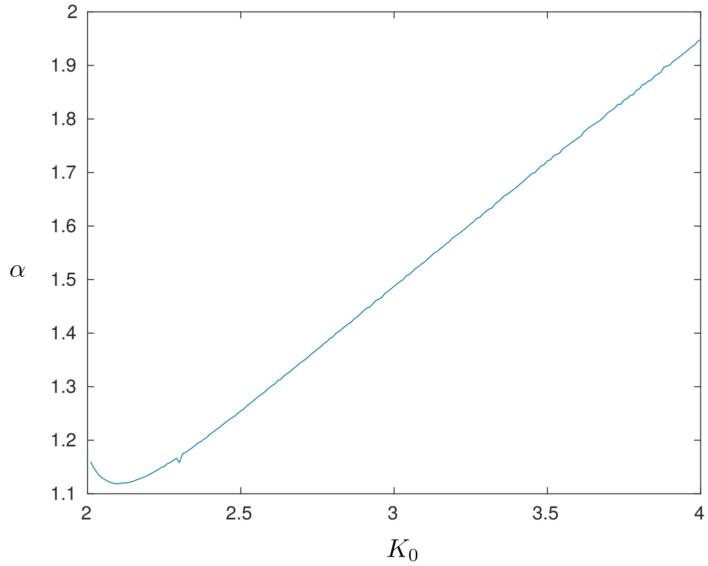

Figure 8.2.: Boundary values in comparison to the initial curvature.

open is the question of a possible convergence of the solution γ, if K_0 tends to 2. Due to the experiments mentioned above the present author conjectures γ to tend to two Möbius inverted Catenoids with negative geodesic curvature (see Lemma 4.11, Figures 6.3, B.2 and the discussion in Section 6.2), which meet at an irregular point at the origin (see Figure 8.3).

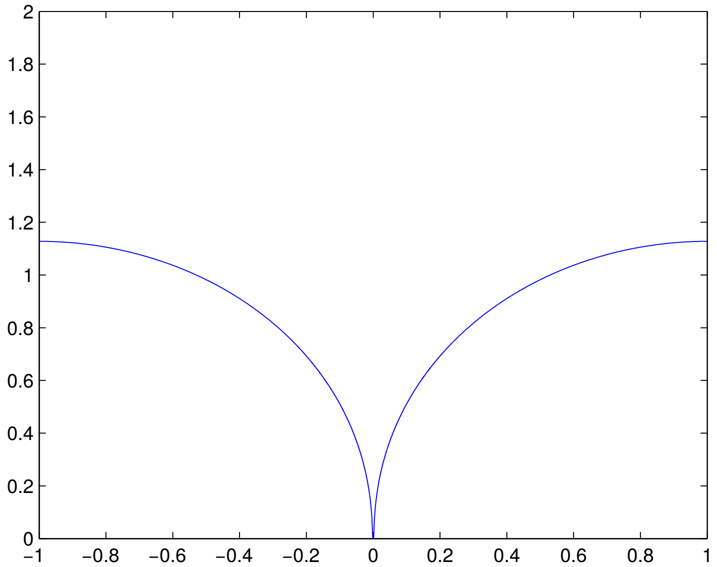

Figure 8.3.: Plot of symmetric solution with $\alpha = 1.1278$, $K_0 = 2.0001$.

9. Symmetry for energy-minimising solutions

This section is dedicated to proving Theorem 1.5. It is taken out of [26, Section 3]. Amos Koellers contribution to this article consists solely of [26, Section 2], which is not contained in this thesis. This chapter is organized as follows. First some necessary conditions for a non-even solution are derived. These conditions are used in Section 9.2 to show, that such a solution possesses high Willmore energy.
Since we are dealing with a symmetry problem, we set $\alpha := \alpha_- = \alpha_+$.

9.1. Necessary conditions for non-symmetric solutions

This section is taken from [26, Section 3.2]. Some of the following formulae have already been derived in Chapter 6 for symmetric Killing fields J (see Lemma 4.5). Since we are especially interested in the non-symmetric case, the resulting formulae are a bit more involved. Differentiating (4.6) and (4.7) by hyperbolic arclength yields (cf. (6.3) for the symmetric case)

$$\begin{aligned} 2K\dot{K}\begin{pmatrix} \dot{\gamma}^1 \\ \dot{\gamma}^2 \end{pmatrix} &+ K^2 \begin{pmatrix} \ddot{\gamma}^1 \\ \ddot{\gamma}^2 \end{pmatrix} + 2\ddot{K}\begin{pmatrix} -\dot{\gamma}^2 \\ \dot{\gamma}^1 \end{pmatrix} + 2\dot{K}\begin{pmatrix} -\ddot{\gamma}^2 \\ \ddot{\gamma}^1 \end{pmatrix} \\ &= a\begin{pmatrix} \gamma^1\dot{\gamma}^1 - \gamma^2\dot{\gamma}^2 \\ \dot{\gamma}^1\gamma^2 + \gamma^1\dot{\gamma}^2 \end{pmatrix} + b\begin{pmatrix} \dot{\gamma}^1 \\ \dot{\gamma}^2 \end{pmatrix}. \end{aligned} \tag{9.1}$$

The subscript $+$ shall now indicate that the corresponding object is evaluated at the right border, for example $K_+ = \kappa[u](1)$. The subscript $-$ represents the left border analogously. The boundary conditions with the parameterisation by hyperbolic arclength (cf. (3.1)) yield

$$\gamma^2_\pm = \alpha,\ \gamma^1_\pm = \pm 1,\ \dot{\gamma}^2_\pm = 0,\ \dot{\gamma}^1_\pm = \alpha. \tag{9.2}$$

Inserting this into (4.6) yields

$$\alpha K^2_\pm = a\frac{1-\alpha^2}{2} \pm b + c.$$

By subtracting these two equations we obtain

$$\alpha(K_+^2 - K_-^2) = 2b. \tag{9.3}$$

On the other hand (4.7) yields

$$2\dot{K}_\pm = \pm a + b. \tag{9.4}$$

By adding these two equations we obtain

$$\dot{K}_+ + \dot{K}_- = b \tag{9.5}$$

Now we make use of the Frenet equations evaluated at the boundary (see (2.13), (2.14) and cf. (6.1), (6.2))

$$\ddot{\gamma}_\pm^1 = 0,\ \ddot{\gamma}_\pm^2 = \alpha(K_\pm - 1).$$

Combining this with the second row of (9.1) yields

$$\alpha K_\pm^2(K_\pm - 1) + 2\alpha\ddot{K}_\pm = a\alpha^2,$$

which can be further simplified by (4.1) to (cf. (6.5))

$$2K_\pm - K_\pm^2 = a\alpha. \tag{9.6}$$

With these equations in mind we can prove our first lemma concerning even solutions:

Lemma 9.1 (see [26] Lemma 3.5)**.** *A smooth solution $u : [-1,1] \to (0,\infty)$ of* (1.8) *is even if and only if*

$$\kappa[u](-1) = \kappa[u](1).$$

Proof. If u is even the above equation simply follows from (7.1) and the boundary conditions.

Let us now consider a solution u of (1.8) with $\kappa[u](-1) = \kappa[u](1)$. Let γ be this solution reparameterised as a curve by hyperbolic arclength with geodesic curvature K. The equations (9.3) and (9.5) then imply

$$\dot{K}_- = -\dot{K}_+.$$

By reflecting γ at the y-axis we obtain a curve $\tilde{\gamma}$. This operation is a Möbius transformation, so $\tilde{\gamma}$ still solves (1.8) and still satisfies the ordinary differential equation in (4.8) with the following initial conditions:

$$\tilde{\gamma}(0) = (1,\alpha),\ \dot{\tilde{\gamma}}(0) = (-\alpha, 0),\ \kappa[\tilde{\gamma}](0) = -K_- = -K_+,\ \dot{\kappa}[\tilde{\gamma}](0) = -\dot{K}_- = \dot{K}_+.$$

If we now switch the orientation of $\tilde{\gamma}$ (meaning $\tilde{\gamma}(s) \mapsto \tilde{\gamma}(L-s)$) we obtain a curve which satisfies the same initial data as γ. Hence this curve has to be γ itself. □

We can now turn to conditions for non-even solutions:

Lemma 9.2 (see [26] Corollary 3.6)**.** *Let* $u : [-1, 1] \to (0, \infty)$ *be a smooth solution of* (1.8)*, which shall be* ***non****-even. Then*

$$\kappa[u](-1) + \kappa[u](1) = 2.$$

Proof. By a simple subtraction we deduce from (9.6)

$$0 = 2(K_+ - K_-) - (K_+^2 - K_-^2) = (K_+ - K_-)(2 - (K_+ + K_-)).$$

Lemma 9.1 now yields the desired result. □

Lemma 9.3 (see [26] Corollary 3.7)**.** *Let* $u : [-1, 1] \to (0, \infty)$ *be a smooth,* ***non****-even solution of* (1.8)*. Then*

$$u''(-1) = -u''(1), \quad u''(1) \neq 0.$$

Proof. Evaluating (7.1) at the boundary and adding the resulting equations yield together with Lemma 9.2 $u''(-1) = -u''(1)$. $u''(1) \neq 0$ follows from Lemma 9.1. □

The following lemma is paramount in proving the energy estimate stated in Lemma 9.5:

Lemma 9.4 (see [26] Corollary 3.8)**.** *Let* $u : [-1, 1] \to (0, \infty)$ *be a smooth,* ***non****-even solution of* (1.8)*. Then the curvature* K *reparameterised by hyperbolic arclength is periodic with fundamental period* $P > 0$*, satisfying*

$$P \leq \int_{-1}^{1} \frac{\sqrt{1 + u'(\xi)}}{u(\xi)} \, d\xi.$$

Hence the fundamental period is smaller than the hyperbolic arclength of u*.*

Proof. We show the following claim, which is sufficient by the Lemmas 4.1, 4.2, 4.3 and 4.4.

$$\text{There exist } -1 < x_1 < x_2 < x_3 < 1 \text{ and a } C \in \mathbb{R} \text{ such that}$$
$$\kappa[u](x_1) = \kappa[u](x_2) = \kappa[u](x_3) = C.$$

By Lemma 9.3 we can assume without loss of generality that $u''(-1) < 0$ and $u''(1) > 0$. Due to the boundary data u has to have a strict maximum in $x = -1$ and strict minimum in $x = 1$. With $u(-1) = u(1)$ we find $-1 < x_- < x_+ < 1$ satisfying

$$u'(x_+) = 0, \; u''(x_+) \leq 0, \quad u'(x_-) = 0, \; u''(x_-) \geq 0.$$

Equation (7.1) yields

$$\kappa[u](-1) < 1,\ \kappa[u](x_-) \geq 1,\ \kappa[u](x_+) \leq 1,\ \kappa[u](1) > 1.$$

The intermediate value theorem yields the desired result. □

9.2. A priori energy estimates

This section is taken from [26, Section 3.3] and is dedicated to proving the following energy estimate:

Lemma 9.5 (see [26], Theorem 3.9)**.** *Let $u : [-1,1] \to (0,\infty)$ be a smooth solution of* (1.8)*, which shall be **non**-even. Then*

$$W_e(S(u)) > 4\pi.$$

With Lemma 9.4 in mind, we have to estimate the elastic energy for the fundamental period of the functions given in Lemma 4.2 and Lemma 4.4. The presented proof in the orbitlike case is by Hans-Christoph Grunau, but it was already observed by Langer & Singer (see [37, page 19]):

Lemma 9.6 (see [37] p. 19, [26] Lemma 3.10)**.** *Let $K : \mathbb{R} \to \mathbb{R}$ be non constant and given as in Lemma 4.2 with parameters K_0, k, r. Then*

$$\int_0^{\frac{1}{r}F_k(\pi)} K^2(s)ds > 8.$$

Proof. Let K, K_0, r and k be given as in Lemma 4.2. Since (4.1) is autonomous, we can assume without loss of generality, that $|K_0| > \sqrt{2}$ and therefore $s_0 = 0$. Then

$$\begin{aligned}
\int_0^{\frac{1}{r}F_k(\pi)} K^2(s)\,ds &= \int_0^{\frac{1}{r}F_k(\pi)} 4r^2\,\mathrm{dn}^2(rs,k)\,ds \\
&= 4r^2 \int_0^{\frac{1}{r}F_k(\pi)} (1 - k^2\sin^2(F_k^{-1}(rs)))\,ds \\
&= 4r\int_0^{\pi} \frac{1-k^2\sin^2(x)}{\sqrt{1-k^2\sin^2(x)}}\,dx \\
&= 8\int_0^{\frac{\pi}{2}} \sqrt{r^2 - (2r^2-1)\sin^2(x)}\,dx.
\end{aligned}$$

Now we consider the function

$$(\frac{1}{2},1) \ni \rho \to \phi(\rho) = \int_0^{\frac{\pi}{2}} \sqrt{\rho - (2\rho-1)\sin^2(x)}\,dx$$

and show $\phi(\rho) > 1$. With $\phi(1) = \int_0^{\frac{\pi}{2}} \cos(x)\,dx$ it suffices to prove $\phi'(\rho) < 0$ for $\rho \in (\frac{1}{2},1)$.

$$\begin{aligned}
2\phi'(\rho) &= \int_0^{\frac{\pi}{2}} \frac{1-2\sin^2 x}{\sqrt{\rho-(2\rho-1)\sin^2 x}}\,dx = \int_0^{\frac{\pi}{2}} \frac{\cos(2x)}{\sqrt{\rho-(2\rho-1)\sin^2 x}}\,dx \\
&= \int_0^{\frac{\pi}{4}} \frac{\cos(2x)}{\sqrt{\rho-(2\rho-1)\sin^2 x}}\,dx + \int_{\frac{\pi}{4}}^{\frac{\pi}{2}} \frac{\cos(2x)}{\sqrt{\rho-(2\rho-1)\sin^2 x}}\,dx \\
&= \int_0^{\frac{\pi}{4}} \frac{\cos(2x)}{\sqrt{\rho-(2\rho-1)\sin^2 x}}\,dx + \int_0^{\frac{\pi}{4}} \frac{\cos(\pi-2x)}{\sqrt{\rho-(2\rho-1)\cos^2 x}}\,dx \\
&= \int_0^{\frac{\pi}{4}} \cos(2x)\left(\frac{1}{\sqrt{\rho-(2\rho-1)\sin^2 x}} - \frac{1}{\sqrt{\rho-(2\rho-1)\cos^2 x}}\right)dx \\
&< 0.
\end{aligned}$$

Since $\phi(1) = 1$ the proof is finished. $\square$

The elastic energy over a fundamental period of a wavelike solution has already been estimated in Lemma 5.16

Let us now summarize our findings to obtain the proof of Lemma 9.5:

Proof. Let u be a non-even solution of (1.8) and K the geodesic curvature parameterised by hyperbolic arclength with fundamental period $P > 0$. According to Lemma 9.4 the fundamental period is contained in the hyperbolic arclength of u. Equation (2.12) in combination with the Lemmas 9.6 and 5.16 yield

$$W_e(S(u)) = \frac{\pi}{2} W_h(u) \geq \frac{\pi}{2}\int_0^P K^2(s)\,ds$$
$$\left\{ \begin{array}{cccc} \geq & \frac{\pi}{2}\cdot 4\pi & > & 4\pi \\ > & \frac{\pi}{2}\cdot 8 & = & 4\pi. \end{array} \right.$$

$\square$

Let us now summarize the important steps of the proof of Theorem 1.5:
Existence and regularity of an energy minimising solution $u : [-1,1] \to (0,\infty)$ of (1.8)

is given by Theorem 1.3, which also yields

$$W_e(S(u)) < 4\pi.$$

If we combine this with our energy estimate Lemma 9.5, we obtain Theorem 1.5.

A. A numerical scheme

In this chapter a numerical algorithm to solve the Dirichlet problem (1.4) is presented. This procedure only works in a reliable way, if numerical results of [18] for the symmetric problem (1.8) are used. This algorithm is explained in Section A.1 and resulting plots are given in Section A.2.

A.1. A shooting/perturbation method

The numerical method to obtain the results shown in Section A.2 is a shooting method for ordinary differential equations, taylored to our situation. Let $\alpha_-, \alpha_+ \in (0,\infty)$ and let $\gamma : \mathbb{R}\times\mathbb{R}\times\mathbb{R} \to \mathbb{H}^2$ be a smooth solution of (see also (4.8))

$$\begin{cases} \nabla_{\dot\gamma}\dot\gamma = KN,\ \nabla_{\dot\gamma}N = -K\dot\gamma, & \ddot K = K - \frac{1}{2}K^3 \\ \gamma(0,K_0,\dot K_0) = (-1,\alpha_-)\,,\ \dot\gamma(0,K_0,\dot K_0) = (\alpha_-,0)\,, & K(0)=K_0,\ \dot K(0) = \dot K_0. \end{cases} \tag{A.1}$$

Here $N = (-\dot\gamma^2, \dot\gamma^1)$ denotes a unit normal, which is possible since $\gamma(\cdot, K_0, \dot K_0)$ is parameterised by hyperbolic arclength. Hence $\gamma(\cdot, K_0, \dot K_0)$ is the profile curve of a Willmore surface of revolution. We now look for a triple $(L, K_0, \dot K_0) \in \mathbb{R}_+ \times \mathbb{R}^2$, such that

$$\gamma(L,K_0,\dot K_0) = (1,\alpha_+), \quad \dot\gamma(L,K_0,\dot K_0) = (\alpha_+,0). \tag{A.2}$$

Then $\gamma(\cdot, K_0, \dot K_0)\big|_{[0,L]}$ solves (1.4). This initial value problem was solved in matlab$^{\text{TM}}$ by a Runge-Kutta method.

We solved (A.2) by Newton's method. For convergence we used a perturbation approach and solved the symmetrical case first. This case was already solved numerically in [18], which gave us K_0. $\dot K_0$ was then obtained by (9.4) and (9.6). Since we are treating the symmetrical case, we have $b = 0$ in these formulae. Hence we only had to guess a suitable starting value for the arclength L.

After we solved the symmetrical case, we perturbed α_+ in small steps and used the already obtained solutions as starting points for Newton's method.

Unfortunately the shooting method alone seems to be very difficult to implement, if we want to show existence of a solution of (1.4). In Theorem 8.1 solutions with arbitrary big hyperbolic arclength were found. Hence the differential equation is not enough to derive a priori bounds on the arclength, which in turn means the Brouwer

fixed-point theorem cannot be applied.
On the other hand a perturbation method via the inverse function theorem is also very difficult to implement, since we do not have an explicit formula for a solution in the symmetric case. The present author was not able to overcome these obstacles directly and chose a variational approach instead (See Section 3 and Theorem 1.1).
This variational approach needs smallness conditions on the boundary data. A shooting method restricted to wavelike elastica (cf. Lemma 4.4) may overcome this problem as indicated by the Sections 6.1 and B.

A.2. A set of solutions of the Dirichlet problem

This section collects a few numerical solutions of (1.4). The applied method is described in Section A.1. The caption of the figures give some parameters. α_- is the height at the left border and α_+ is the height at the right border respectively. K_0 is the initial geodesic curvature and $\dot{K}_0$ is the initial derivative of that curvature (cf. (A.1)). L is the hyperbolic arclength and W_e the Willmore energy of the respective surface of revolution.

We start with solutions, where the left height α_- is fixated and the right height α_+ grows: If α_- and α_+ are very close to each other, Figure A.1 shows a hill near

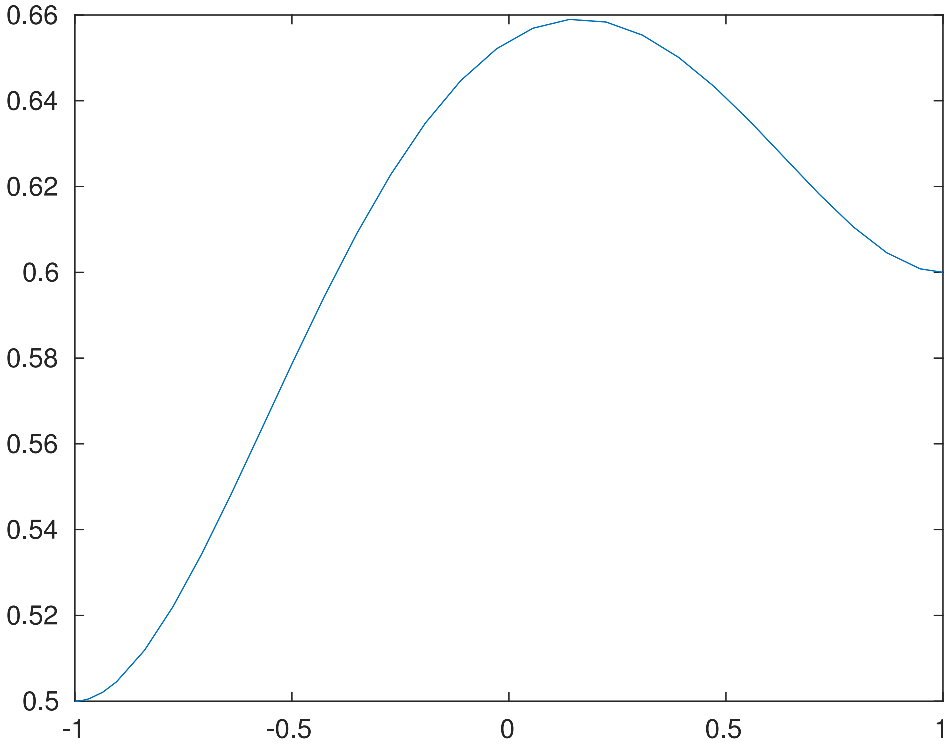

Figure A.1.: $\alpha_- = 0.5$, $\alpha_+ = 0.6$, $K_0 = 1.535312$, $\dot{K}_0 = -0.702980$, $L = 3.350976$, $W_e = 5.396793$.

the middle of the solution. This kind of hill was already observed for symmetric data in [17].

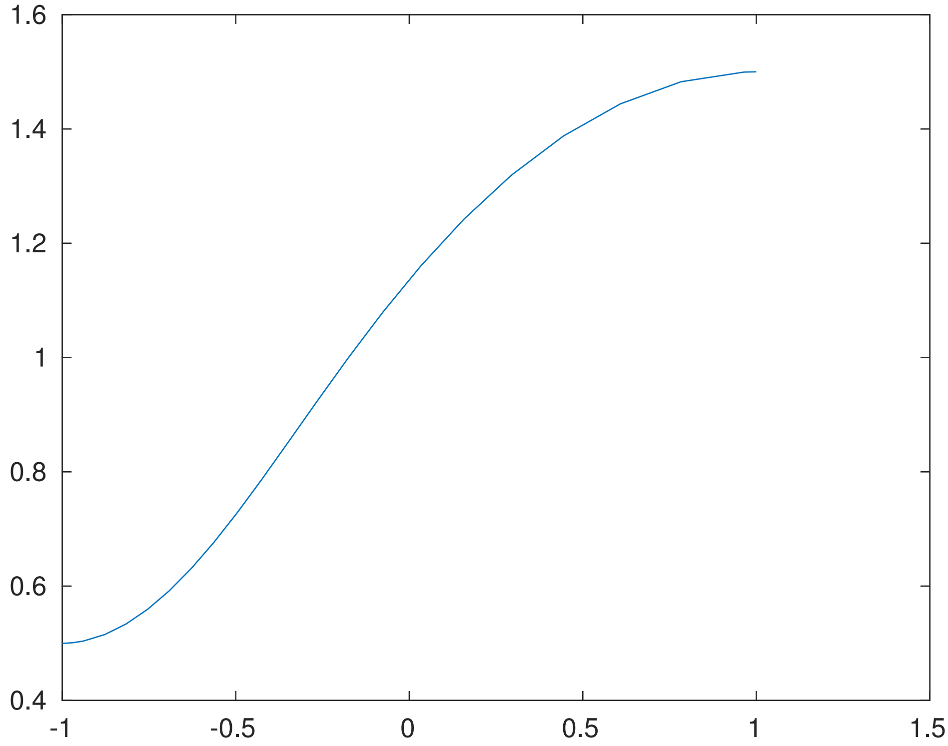

Figure A.2.: $\alpha_- = 0.5$, $\alpha_+ = 1.5$, $K_0 = 2.045919$, $\dot{K}_0 = -0.469671$, $L = 2.470591$, $W_e = 4.865637$.

When α_- and α_+ are a bit further apart, the hill seen in Figure A.1 seems to vanish as exhibited by Figure A.2. This indicates, that the solution is strictly monotone.

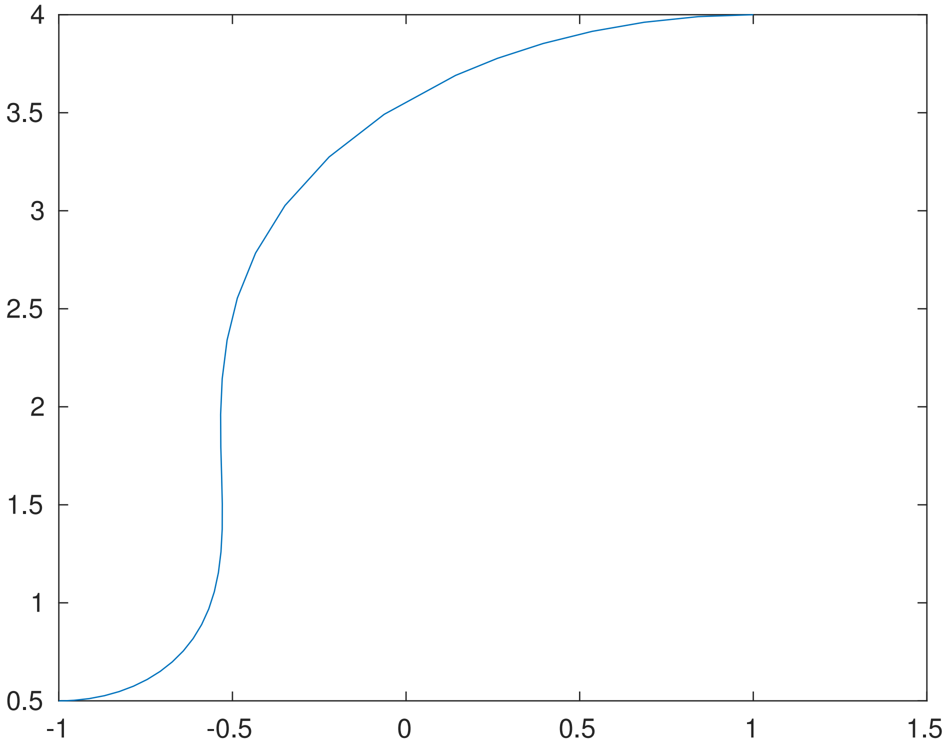

Figure A.3.: $\alpha_- = 0.5$, $\alpha_+ = 4.0$, $K_0 = 2.446962$, $\dot{K}_0 = 0.543533$, $L = 2.697657$, $W_e = 9.564734$.

The projectivity of the solution seems to start breaking down at about $x = -0.5$, if the distance of α_- and α_+ is moderate.

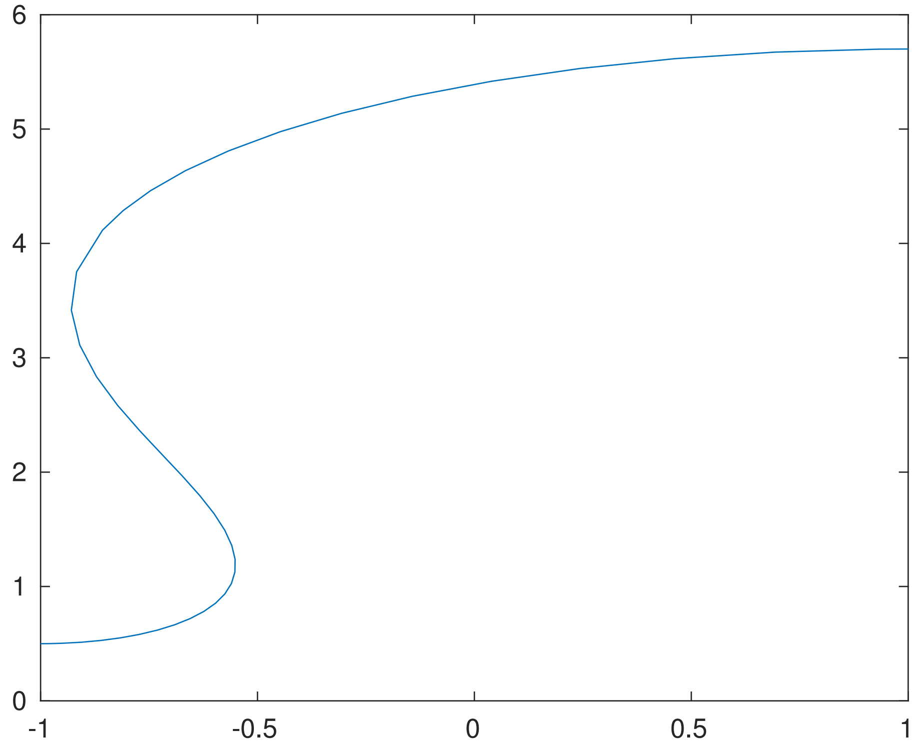

Figure A.4.: $\alpha_- = 0.5$, $\alpha_+ = 5.7$, $K_0 = 2.362879$, $\dot{K}_0 = 0.672563$, $L = 3.054481$, $W_e = 10.984159$.

Figure A.4 illustrates, that the non-projectivity issue grows worse, if the distance of α_- and α_+ becomes bigger. On the other hand, the monotony of the second coordinate γ^2 seems to stay.

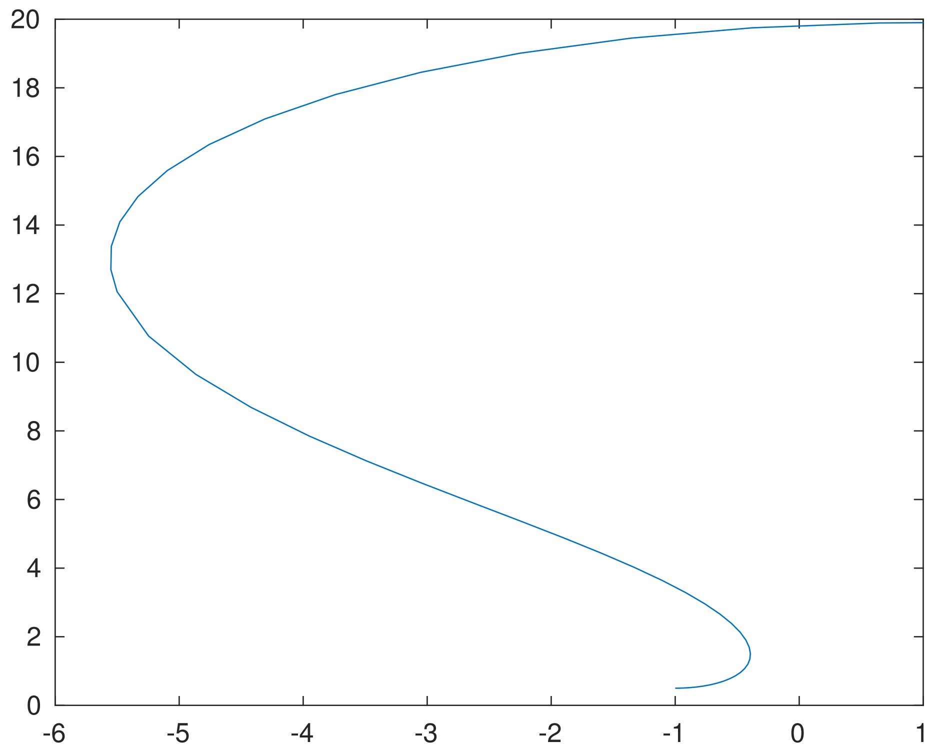

Figure A.5.: $\alpha_- = 0.5$, $\alpha_+ = 19.9$, $K_0 = 2.105029$, $\dot{K}_0 = 0.372020$, $L = 4.633284$, $W_e = 12.568947$.

Figure A.5 shows the behaviour of a solution, when α_- and α_+ are very far away from each other. The upper part seems to grow like an inflating balloon. It probably behaves asymptotically like a Möbius inverted catenoid around α_+ (cf. Lemma 4.11 or Figure 6.3).
The lower part around α_- probably converges to a part of an asymptotically geodesic solution as well, which would not be symmetric (see Figure B.2).

The next set of solutions features a fixated $\alpha_- = 1$ and a falling α_+: As seen in

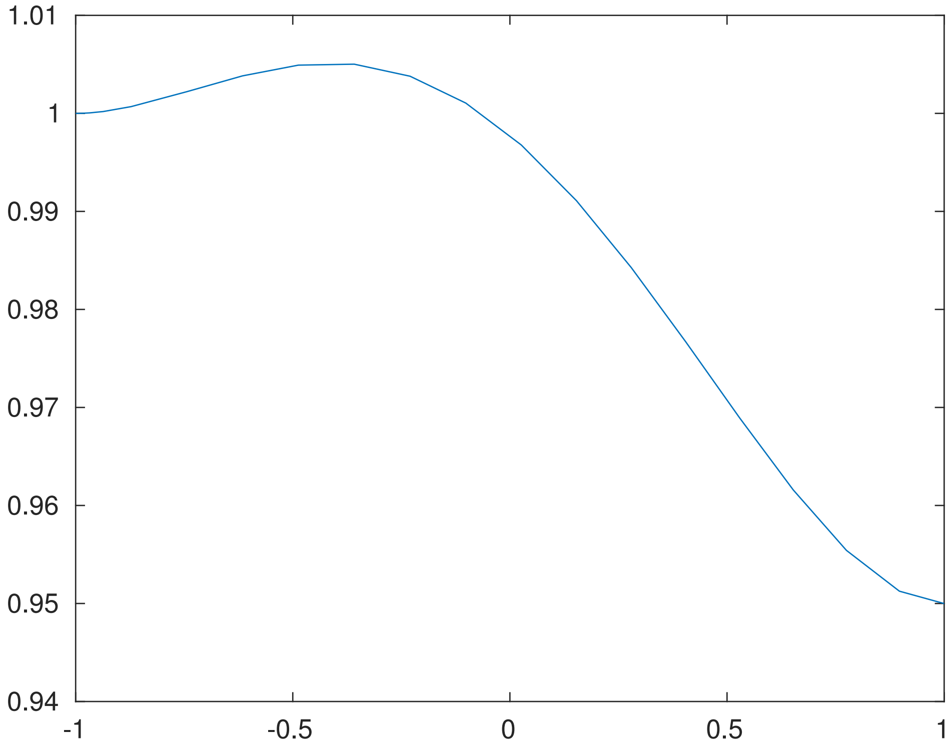

Figure A.6.: $\alpha_- = 1.0$, $\alpha_+ = 0.95$, $K_0 = 1.102888$, $\dot{K}_0 = -0.442682$, $L = 2.028232$, $W_e = 3.176068$.

Figure A.1 we observe a hill near the middle in Figure A.6, if α_- and α_+ are very close to each other.

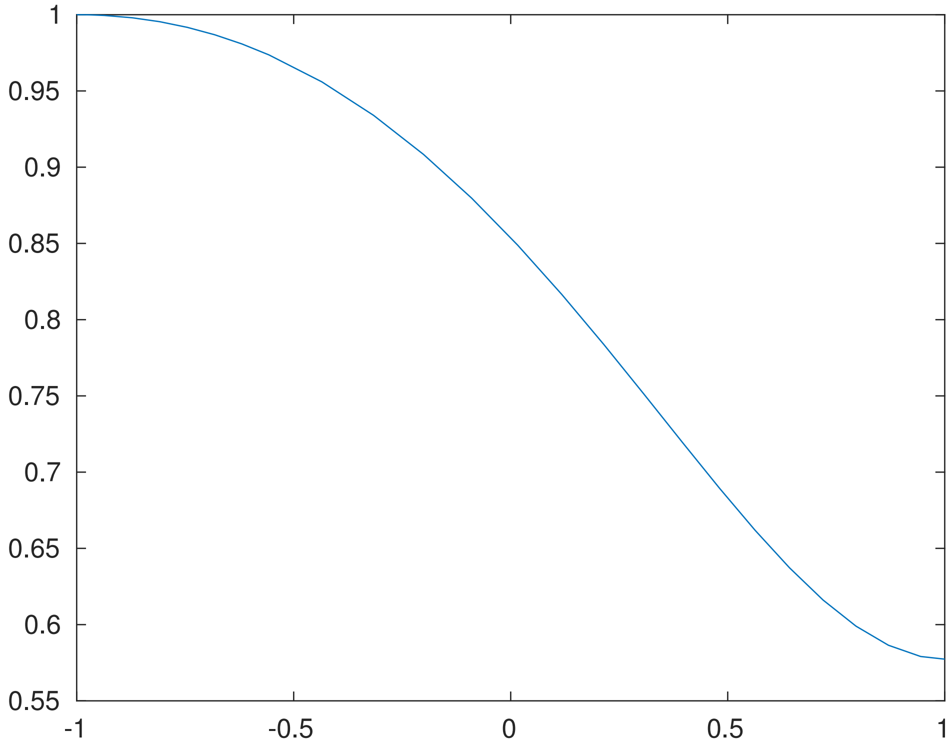

Figure A.7.: $\alpha_- = 1.0$, $\alpha_+ = 0.577350$, $K_0 = 0.767184$, $\dot{K}_0 = -0.294503$, $L = 2.591920$, $W_e = 4.070799$.

Figure A.7 features the disappearence of the hill of Figure A.6. The solution seems to become monotone again.

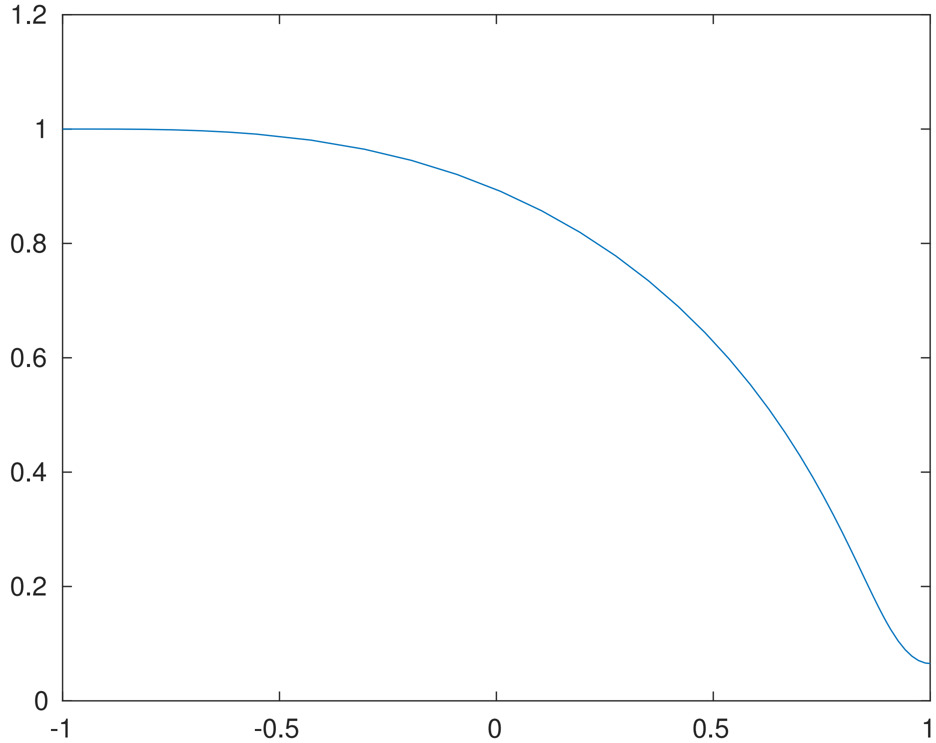

Figure A.8.: $\alpha_- = 1.0$, $\alpha_+ = 0.065233$, $K_0 = 1.025679$, $\dot{K}_0 = -0.823972$, $L = 5.145433$, $W_e = 6.592535$.

In contrast to Figure A.3 the projectivity of the solution does not seem to break down easily, if α_+ tends to 0 (see Figure A.8).

B. Future research

The biggest problem left open in this thesis is existence of solutions of (1.4) for arbitrary $\alpha_-, \alpha_+ > 0$. The present author likes to present an idea on how to possibly proceed:
First a numerical observation is needed to underline the following method. Here we utilised the same numerical scheme as in Section A.1. Lemma 5.15 shows that a non-projectable solution of (1.4) under energy constraints is wavelike (cf. Lemma 4.4). In the symmetrical case, i.e. $\alpha_- = \alpha_+$, the solution is most likely orbitlike (cf. Theorem 8.6). Hence the type of solution changes, if α_- is fixed and α_+ grows (cf. Figures A.1, A.2 and A.3). Equation (4.2) gives us the possibility to distinguish the type of solutions found in Section A.2 by their extremal curvature in terms of their initial data. Shortly before the change a solution looks like Figure B.1. It being orbitlike is not obvious from the solution itself, but their extension gives a better clue (cf. Lemma 5.19). The dashed lines represent these extensions, while the solid line is the solution of the Dirichlet problem itself. Even before projectability is lost, the type of solution changes to wavelike (see Figure B.3). The intermediate solution between these two seems to be an asymptotically geodesic one (cf. Lemma 4.3) as shown in Figure B.2. These can be obtained by e.g. reflecting a catenoid at an upper half circle, in such a way that the result is not symmetric to some straight line parallel to the y-axis.

The roadmap to show existence for every $\alpha_-, \alpha_+ > 0$ would be as follows:
First $\alpha_- > 0$ has to be fixed. Afterwards an $\alpha_+^* > \alpha_-$ has to be found, for which the solution of (1.4) is of the asymptotically geodesic type. Then for every $\alpha_+ \in (\alpha_-, \alpha_+^*)$ one needs to show, that $W^h_{\alpha_-,\alpha_+} < 8$ to obtain solutions by Theorem 1.1 in this regime. This conjecture is supported by Lemma 7.2, which shows that the hyperbolic energy of such a solution of asymptotically geodesic type is at most 8.
The next step consists in finding solutions for $\alpha_+ > \alpha_+^*$ in the wavelike class. For this a shooting method seems appropriate as seen in Section 6.1. But instead of fixing the initial derivative of the geodesic curvature to be zero, it needs to be varied as well.

This α_+^* may also yield a better smallness condition for projectivity than Assumption 1.2, since every solution with right boundary value between α_- and α_+^* seems to be orbitlike.

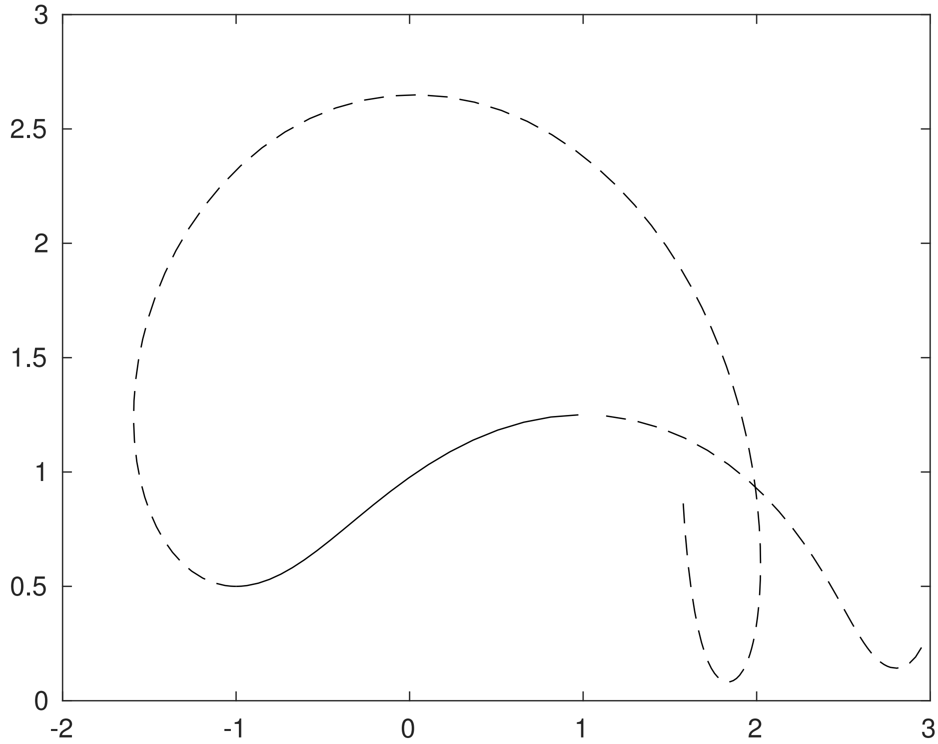

Figure B.1.: Orbitlike solution: $\alpha_- = 0.5$, $\alpha_+ = 1.25$, $K_0 = 1.892309$, $\dot{K}_0 = -0.556467$, $L = 2.581276$.

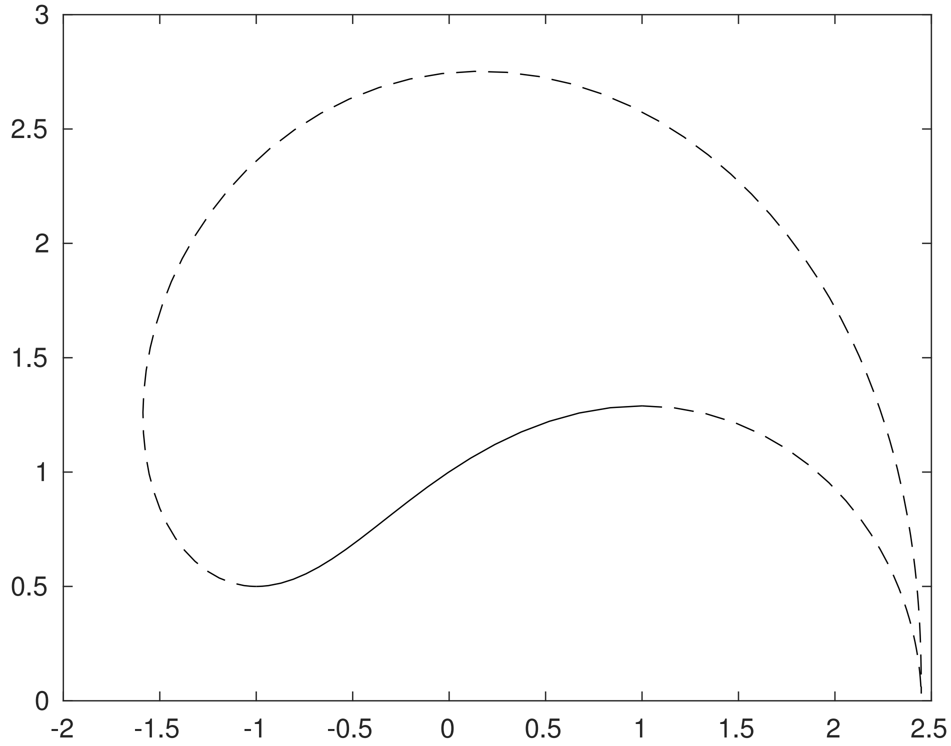

Figure B.2.: Asymptotically geodesic solution: $\alpha_- = 0.5$, $\alpha_+ = 1.2894$, $K_0 = 1.9176$, $\dot{K}_0 = -0.5448$, $L = 2.5594$.

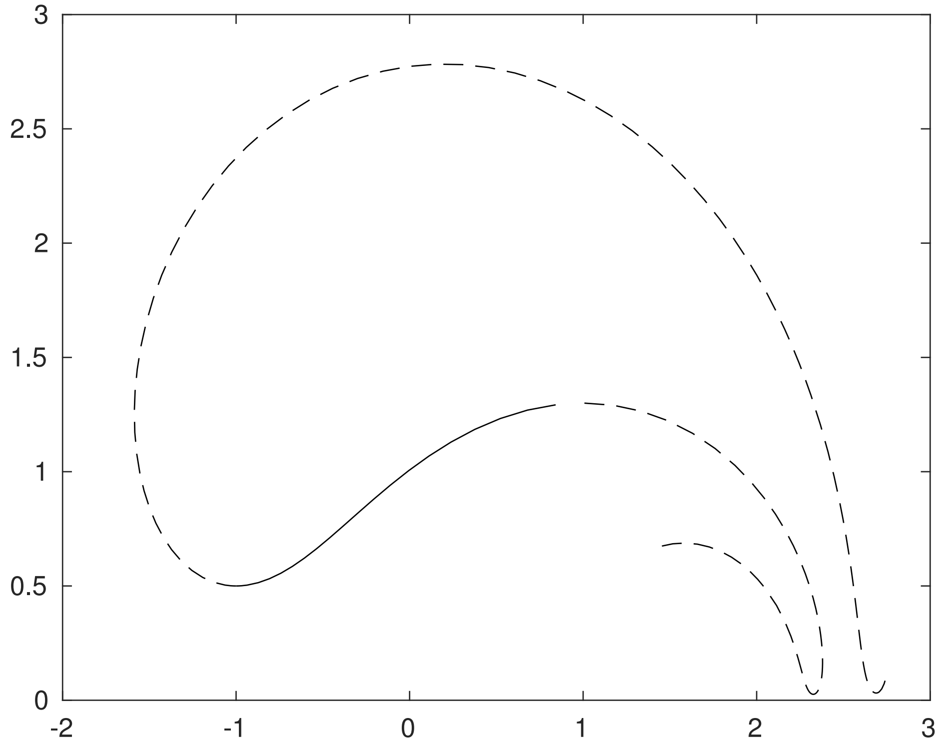

Figure B.3.: Wavelike solution: $\alpha_- = 0.5$, $\alpha_+ = 1.3$, $K_0 = 1.924355$, $\dot{K}_0 = -0.541498$, $L = 2.553789$.

Bibliography

[1] M. Abramowitz and I.A. Stegun. *Handbook of mathematical functions.* United States Department of Commerce, National Bureau of Standards, U.S. Government Printing Office Washington, D.C. 20402, 10th edition, 1972.

[2] R. Alessandroni and E. Kuwert. Local solutions to a free boundary problem for the Willmore functional. *Calc. Var. Partial Differential Equations*, 2016. DOI 10.1007/s00526-016-0961-3.

[3] S. Alexakis and R. Mazzeo. Complete Willmore surfaces in $\mathbb{H}^3$ with bounded energy: Boundary regularity and bubbling. *J. Differential Geom.*, 101:369–422, 2015.

[4] C. Bär. *Elementare Differentialgeometrie.* De Gruyter Berlin, 2nd edition, 2010.

[5] M. Bauer and E. Kuwert. Existence of minimizing Willmore surfaces of prescribed genus. *Int. Math. Res. Notices*, 10:553–576, 2003.

[6] M. Bergner, A. Dall'Acqua, and S. Fröhlich. Symmetric Willmore Surfaces of revolution satisfying natural boundary conditions. *Calc. Var. Partial Differential Equations*, 39:553–576, 2010.

[7] M. Bergner, A. Dall'Acqua, and S. Fröhlich. Willmore Surfaces of revolution with two prescribed boundary circles. *J. Geom. Anal.*, 23:283–302, 2013.

[8] M. Bergner and R. Jakob. Sufficient conditions for Willmore immersions in $\mathbb{R}^3$ to be minimal surfaces. *Ann. Glob. Anal. Geom.*, 45:129–146, 2014.

[9] Y. Bernard and T. Rivière. Energy quantization for Willmore surfaces and applications. *Ann. of Math.*, 180:87–136, 2014.

[10] J.P. Bowman. 612 Class Lecture: Hyperbolic Geometry. `http://www.math.cornell.edu/~bowman/metrics.pdf`, date of download 21st September 2013.

[11] R. Bryant. A duality theorem for Willmore surfaces. *J. Differential Geom.*, 20:23–53, 1984.

[12] R. Bryant and P. Griffiths. Reduction for constrained variational problems and $\int k^2/2\, ds$. *Am. J. Math.*, 108:525–570, 1986.

[13] D. Bucur and G. Buttazzo. *Variational Methods in Shape Optimization Problems.* Birkhäuser, 1st edition, 2005.

[14] M. Burger, S.-Y. Chu, P. Markowich, and C.-B. Schönlieb. Cahn-Hilliard inpainting and the Willmore functional. *Proc. Appl. Math. Mech.*, 7:1011209–1011210, 2007.

[15] J. Chen and T. Lamm. A Bernstein type theorem for entire Willmore graphs. *J. Geom. Anal.*, 23:456–469, 2013.

[16] A. Dall'Acqua. Uniqueness for the homogeneous Dirichlet Willmore boundary value problem. *Ann. Glob. Anal. Geom.*, 42:411–420, 2012.

[17] A. Dall'Acqua, K. Deckelnick, and H.-Ch. Grunau. Classical solutions to the Dirichlet problem for Willmore surfaces of revolution. *Adv. Calc. Var.*, 1:379–397, 2008.

[18] A. Dall'Acqua, S. Fröhlich, H.-Ch. Grunau, and F. Schieweck. Symmetric Willmore surfaces of revolution satisfying arbitrary Dirichlet boundary data. *Adv. Calc. Var.*, 4:1–81, 2011.

[19] K. Deckelnick and H.-Ch. Grunau. Boundary value problems for the one-dimensional Willmore equation. *Calc. Var. Partial Differential Equations*, 30:293–314, 2007.

[20] K. Deckelnick and H.-Ch. Grunau. A Navier boundary value problem for Willmore surfaces of revolution. *Analysis (Munich)*, 29:229–258, 2009.

[21] K. Deckelnick and H.-Ch. Grunau. Stability and symmetry in the Navier problem for the one-dimensional Willmore equation. *SIAM J. Math. Anal.*, 40:2055–2076, 2009.

[22] K. Deckelnick, H.-Ch. Grunau, and M. Röger. Minimising a relaxed Willmore functional for graphs subject to boundary conditions. *I.F.B.*, 19:109–140, 2017.

[23] S. Eichmann. Nichtperiodische Fortsetzbarkeit von Willmore-Flächen unter Axialsymmetrie. 2014. Diploma thesis: `http://www-ian.math.uni-magdeburg.de/home/grunau/papers/EichmannDiplomarbeit.pdf`.

[24] S. Eichmann. Nonuniqueness for Willmore surfaces of revolution satisfying Dirichlet boundary data. *J. Geom. Anal.*, 26:2563–2590, 2016. DOI 10.1007/s12220-015-9639-x.

[25] S. Eichmann and H.-Ch. Grunau. Existence for Willmore surfaces of revolution satisfying non-symmetric Dirichlet boundary conditions. 2016. Preprint: `http://www-ian.math.uni-magdeburg.de/home/grunau/papers/Eichmann_Grunau.pdf`.

[26] S. Eichmann and A. Koeller. Symmetry for Willmore Surfaces of Revolution. *J. Geom. Anal.*, 2016. DOI 10.1007/s12220-016-9692-0.

[27] P.M. Galbo and M.C. Barg. Approximate Formulae for Willmore Surfaces via Support Functions and Matlab. *Am. J. Undergrad. Res.*, 13:41–49, 2016.

[28] F. Gazzola, H.-Ch. Grunau, and G. Sweers. *Polyharmonic Boundary Value Problems.* Springer-Verlag Berlin Heidelberg, 1st edition, 2010.

[29] H.-Ch. Grunau. The Asymptotic Shape of a Boundary Layer of Symmetric Willmore Surfaces of Revolution. *In: C. Bandle et al. (eds.), Inequalities and Applications 2010. International Series of Numerical Mathematics*, 161:19–29, 2010.

[30] W. Helfrich. Elastic properties of lipid bilayers: Theory and possible experiments. *Z. Naturforsch. C*, 28:693–703, 1973.

[31] L. Heller. Constrained Willmore tori and elastic curves in 2-dimensional space forms. *Comm. Anal. Geom.*, 22:343–369, 2014.

[32] U. Hertrich-Jeromin and U. Pinkall. Ein Beweis der Willmoreschen Vermutung für Kanaltori. *J. Reine Angew. Math.*, 430:21–34, 1992.

[33] J. Jost. *Riemannian Geometry and Geometric Analysis.* Springer Berlin, 1st edition, 1995.

[34] L.G.A. Keller, A. Mondino, and T. Rivière. Embedded surfaces of arbitrary genus minimizing the Willmore energy under isoperimetric constraint. *Arch. Ration. Mech. Anal.*, 212:645–682, 2014.

[35] E. Kuwert and R. Schätzle. Removability of isolated singularities of Willmore surfaces. *Ann. Math.*, 160:315–357, 2004.

[36] E. Kuwert and R. Schätzle. Branch points for Willmore surfaces. *Duke Math. J.*, 138:179–201, 2007.

[37] J. Langer and D. Singer. The total squared curvature of closed curves. *J. Differ. Geom.*, 20:1–22, 1984.

[38] J. Langer and D. Singer. Curve-Straightening in Riemannian manifolds. *Ann. Global Anal. Geom.*, 5:133–150, 1987.

[39] J.M. Lee. *Introduction to Smooth Manifolds.* Springer New York, 2nd edition, 2012.

[40] Y. Luo and G. Wang. On geometrically constrained variational problems of the Willmore functional I. The Lagrangian-Willmore problem. *Comm. Anal. Geom.*, 23:191–223, 2015.

[41] R. Mandel. Boundary value problems for Willmore curves in $\mathbb{R}^2$. *Calc. Var. Partial Differential Equations*, 54:3905–3925, 2015.

[42] F.C. Marques and A. Neves. Min-Max theory and the Willmore conjecture. *Ann. of Math.*, 149:683–782, 2014.

[43] S. Müller and M. Röger. Confined structures of least bending energy. *J. Differential Geom.*, 97:103–139, 2014.

[44] J.C.C. Nitsche. Boundary value problems for variational integrals involving surface curvatures. *Quart. Appl. Math.*, 51:363–387, 1993.

[45] Z. Ou-Yang. Elasticity theory of biomembranes. *Thin Solid Films*, 393:19–23, 2001.

[46] B. Palmer. Uniqueness theorems for Willmore surfaces with fixed and free boundaries. *Indiana Univ. Math. J.*, 49:1581–1601, 2000.

[47] S.D. Poisson. Mémoire sur les surfaces élastiques. *Cl. Sci. Mathém. Phys. Inst. de France*, pages 167–225, 1812.

[48] J.G. Ratcliffe. *Foundations of Hyperbolic Manifolds.* Springer New York, 1st edition, 1994.

[49] T. Rivière. Variational principles for immersed surfaces with L^2-bounded second fundamental form. *J. Reine. Angew. Math.*, 695:41–98, 2014.

[50] R. Schätzle. The Willmore boundary problem. *Calc. Var. Partial Differential Equations*, 37:275–302, 2010.

[51] R. Schätzle. Conformally constrained Willmore immersions. *Adv. Calc. Var.*, 6:375–390, 2013.

[52] L. Simon. Existence of surfaces minimizing the Willmore functional. *Comm. Anal. Geom.*, 1:281–326, 1993.

[53] G. Thomsen. Über Konforme Geometrie I: Grundlagen der konformen Flächentheorie. *Hamb. Math. Abh.*, 3:31–56, 1924.

[54] D. Werner. *Funktionalanalysis.* Springer Berlin, 2nd edition, 1997.

[55] T.J. Willmore. Note on embedded surfaces. *An. Ştiinţ. Univ. Al. I. Cuza Iaşi Seçt. I a Mat*, 11:493–496, 1965.

List of Symbols

a, b, c	Parameters for Killing field on $\mathbb{H}^2$.
α_+	Positive real number. Height for boundary value problem on the right side.
α_-	Positive real number. Height for boundary value problem on the left side.
α	Positive real number. Height for boundary value problem, if $\alpha_- = \alpha_+$.
B_+	Bounding circle for wavelike γ, i.e. γ touches B_+, iff the geodesic curvature is maximal.
B_-	Bounding circle for wavelike γ, i.e. γ touches B_-, iff the geodesic curvature is minimal.
c	Regular curve in $\mathbb{H}^2$.
C	Constant varying from line to line.
dist_g	Distance w.r.t. hyperbolic metric.
F	Flow coordinates of $\mathbb{H}^2$.
G	Gauss curvature.
$g(\cdot, \cdot)$	First fundamental form of $\mathbb{H}^2$.
γ	Elastic curve parameterised by hyperbolic arclength.
H	Mean curvature.
$\mathbb{H}^2$	$= \{(x, y) \in \mathbb{R}^2 : \ y > 0\}$ with hyperbolic metric $ds^2 = \frac{dx^2+dy^2}{y^2}$.
J	Killing field on $\mathbb{H}^2$. Extension of J_γ to $\mathbb{H}^2$.
J_γ	$= K^2\dot{\gamma} + 2\dot{K}N$ along γ.
K	Geodesic curvature of γ, satisfying $\ddot{K} = K - \frac{1}{2}K^3$.
$\kappa[c]$	Geodesic curvature of c w.r.t. the hyperbolic metric.
K_0	Initial geodesic curvature for initial value problem for elastic curve.

$\dot{K}_0$	Initial derivative of geodesic curvature for initial value problem for elastic curve.
L	Hyperbolic arclength of a curve.
$\lvert\cdot\rvert$	Euclidean length.
$\lvert\cdot\rvert_g$	Length of vector w.r.t. hyperbolic metric.
Δ_S	Laplace-Beltrami operator for a regular immersion S.
M_{α_-,α_+}	$= \{c \in H^2([0,1], \mathbb{R} \times (0,\infty)) : c(0) = (-1,\alpha_-),\ c(1) = (1,\alpha_+),\ \dot{c}^2(0) = \dot{c}^2(1) = 0, \dot{c}^1(0), \dot{c}^1(1) > 0,\ \lvert\dot{c}\rvert \neq 0\}$.
N	Unit normal of a curve c, such that the tangent of c and N are positively oriented.
$\mathbb{N}$	Natural numbers without 0.
$p_{x_0,r}$	Upper half circle with centre $(x_0, 0)$ and radius r.
Φ_J	Flow of J.
$\mathbb{R}$	Real numbers.
$\nabla_W V$	Covariant derivative of V in direction W w.r.t. hyperbolic metric.
$S(\cdot)$	Surface of revolution, generated by a profile curve.
Σ	Geodesic crossing wavelike γ perpendicularly. Integral curve of J.
Σ_+	Subset of $\mathbb{H}^2$, in which a wavelike elastica has positive geodesic curvature.
Σ_-	Subset of $\mathbb{H}^2$, in which a wavelike elastica has negative geodesic curvature.
t_γ	Second coordinate of γ in flow coordinates.
u	Positive function.
W_e	Willmore energy.
$W^e_{\alpha_-,\alpha_+}$	$= \inf\{W_e(S(c)) : c \in M_{\alpha_-,\alpha_+}\}$.
W_h	Elastic energy.
$W^h_{\alpha_-,\alpha_+}$	$= \inf\{W_h(v) : v \in M_{\alpha_-,\alpha_+}\}$.
x_s	Zero of J on x-axis. Point in which Σ crosses x-axis.
Y_γ	First coordinate of γ in flow coordinates.

Index

Ehrenerklärung

Ich versichere hiermit, dass ich die vorliegende Arbeit ohne unzulässige Hilfe Dritter und ohne Benutzung anderer als der angegebenen Hilfsmittel angefertigt habe; verwendete fremde und eigene Quellen sind als solche kenntlich gemacht.
Ich habe insbesondere nicht wissentlich:

- Ergebnisse erfunden oder widersprüchliche Ergebnisse verschwiegen,
- statistische Verfahren absichtlich missbraucht, um Daten in ungerechtfertigter Weise zu interpretieren,
- fremde Ergebnisse oder Veröffentlichungen plagiiert oder verzerrt wiedergegeben.

Mir ist bekannt, dass Verstöße gegen das Urheberrecht Unterlassungs -und Schadenersatzansprüche des Urhebers sowie eine strafrechtliche Ahndung durch die Strafverfolgungsbehörden begründen kann.
Die Arbeit wurde bisher weder im Inland noch im Ausland in gleicher oder ähnlicher Form als Dissertation eingereicht und ist als Ganzes auch noch nicht veröffentlicht.

____

(Ort, Datum)

____

(Unterschrift)